UNIVERSITY OF CAPE COAST

DETERMINATION OF LIVER VOLUME MODEL OF AN ADULT GHANAIAN FROM SOME SELECTED HEALTH CENTERS FOR CLINICAL APPLICATIONS AND DOSE OPTIMIZATION

ERNEST KOJO EDUFUL

2021

UNIVERSITY OF CAPE COAST

DETERMINATION OF LIVER VOLUME MODEL OF AN ADULT GHANAIAN FROM SOME SELECTED HEALTH CENTERS FOR CLINICAL APPLICATIONS AND DOSE OPTIMIZATION

BY

ERNEST KOJO EDUFUL

Thesis submitted to the Department of Physics of the School of Physical Sciences of the College of Agriculture and Natural Sciences, University of Cape Coast, in partial fulfillment of the requirements for the award of Doctor of Philosophy degree in Physics

JULY 2021

DECLARATION

Candidate's Declaration

I hereby declare that this thesis is the result of my own original research and that no part of it has been presented for another degree in this university or elsewhere.

Candidate's Signature:..... Date:.....

Name: Ernest Kojo Eduful

Supervisors' Declaration

We hereby declare that the preparation and presentation of the thesis were supervised in accordance with the guidelines on supervision of thesis laid down by the University of Cape Coast.

Principal Supervisor's Signature:..... Date:.....

Name: Professor Moses Jojo Eghan

Co-Supervisor's Signature: ..... Date:.....

Name: Dr. Yaw Boateng Mensah

ABSTRACT

Despite refinements in surgical techniques for liver transplantation, liver size disparity remains one of the most common problems in patients. The aim of this study was to establish a relationship between patient liver volume and their body parameters such as Body Mass Index (BMI), Body Surface Area (BSA) and Body Surface Index (BSI), measure the length of the liver in the midclavicular line and also perform dose optimization. The height and weight of patients undergoing for abdominal Computed Tomography (CT) scan were measured. The BSA, BSI and BMI were calculated using their respectively formulas. Using MeVisLab software and CT abdominal images each patient's liver volume and the length of the liver in the midclavicular line were measured. Using the SPSS and gender variation, statistical analysis was performed using the null hypothesis to ascertain if there exists a relationship between the calculated body parameters and their respective liver volume. Dose optimization was performed by predicting the effective dose (ED) to the patients even before they are scanned. This was achieved using the peak kilo voltage (kVp) and milli amperes seconds (mAs) to predict signal-to-noise ratio (SNR) and ED to the patient. The average male and female liver volumes measured were 1.356 L and 1.363 L, respectively. The length of the liver in the midclavicular line for male and female were 15.70 ± 2.31 cm and 15.90 ± 2.53 cm, respectively. A model equation, $\text{Effective Dose} = 36.1 - 0.325 \times \text{kVp} + 0.2522 \times \text{mAs}$ was achieved and a C# code was written with a Graphic User Interface (GUI) for easy clinical application.

KEY WORDS

Effective Dose

Dose Optimization

Liver volume

MeVisLab

Size Specific Dose Estimate

Voxel

ACKNOWLEDGEMENTS

I take this opportunity to express my sincere and heartfelt appreciation to God Almighty for strength, wisdom and understanding to complete this studies.

My second appreciation goes to my supervisors: Professor Moses Jojo Eghan, Department of Physics, University of Cape Coast and Dr. Yaw Boateng Mensah of the Department of Radiology, Korle Bu Teaching Hospital. They gave me excellent advice, thoughtful correction, research materials for reference and encouragement throughout this work.

. In addition, my sincere gratitude goes to Prof. Mary Boadu of Ghana Atomic Energy Commission and School of Nuclear and Allied Sciences, University of Ghana, Atomic Campus and Dr. Hewlett of Supreme Specialist Centre for their support and encouragement.

Furthermore, my sincere thanks also goes to the entire staff of the Medical Radiation Physics Centre, Radiological and Medical Sciences Research Institute of Ghana Atomic Energy Commission, Department of Radiology, Korle-Bu Teaching Hospital, Cape Coast Teaching Hospital and Supreme Specialist center for their support and cooperation during the data collection process.

Finally, I wish to thank my family, especially, my wife Mrs. Brigitte Naa Kooko Eduful and my mother Mrs. Mary Batsa for their guidance and encouragement.

DEDICATION

To my wife Brigitte Naa Kooko Eduful for her love and support.

TABLE OF CONTENTS

LIST OF TABLES

LIST OF FIGURES

LIST OF ABBREVIATIONS

2D	2 dimension
3D	3 Dimensions
AAPM	American Association of Physicists in Medicine
AP	Anterior-Posterior
BMI	Body Mass Index
BSA	Body Surface Area
BSI	Body Surface Index
CAD	Computed Assisted Design
CCTH	Cape Coast Teaching hospital
CNR	Contrast to Noise ratio
CT	Computed Tomography
$CTDI_w$	Weighted Computed Tomography Dose Index
$CTDI_{vol}$	Volume Computed Tomography Dose Index
DICOM	Digital Imaging and Communications in Medicine
DVD	Digital Versatile Disc
EC	European Commission
ED	Effective Dose
Eff-D	Effective Diameter
GUI	Graphic User Interface
IAEA	International Atomic Energy Agency
ICRP	International Commission on Radiological Protection
IDE	Integrated Development Environment
KBTH	Korle Bu Teaching hospital
Lat	Lateral
MDCT	Multidetector computed tomography

MRI	Magnetic Resonance Imaging
NDE	Non-destructive examination
PET	Positron Emission Tomography
Pixels	Picture elements
ROI	Region of Interest
SLV	Standard liver volume
SPECT	Single Photon Emission Tomography
SSC	Supreme Medical Center
SNR	Signal-to-noise ratio
SSDE	Size-Specific Dose Estimate
SPSS	Statistical Package for the Social Sciences
TLV	Total liver volume
Voxels	Volume elements

k	Normalized effective dose coefficient
h	Planck's constant
v	X-ray frequency
I	X-ray Intensity
μ	linear attenuation coefficient.
μ_{H_2O}	Attenuation coefficient of water
ρ_ε	Tissue electron density
Z	Atomic number
A	Atomic mass
μ_0	Gray value
σ_0	Standard deviation

CHAPTER ONE

INTRODUCTION

Background to the Study

The production of human voxel models has increased dramatically in recent years with models appearing in literature since 2001 with all these models being specific to North American, European and Asian populations (Caon, 2004). Patrizio et al, 2013, stated that it is uncommon to find models formulated for Africans (Patrizio et al, 2013). Clinicians working in Africa have had to rely on these existing models for their clinical work even though there is a chance that the shape and volume derived from an African voxel model may be different from the existing voxel models from other races. This assumption is based on the fact that the existing research models have some amount of differences between them, for instance the American, European and the Asian models are different from each other, so would the African model be expected to be. Hence, the need to develop a voxel model to represent Ghanaian setting which could be used by our clinicians.

This study is to measure the dimensions of Ghanaian adult liver from abdominal Computed Tomography (CT) scans, estimate the dose to the abdominal section and also to the liver as an organ.

The study is a liver volume model that has been developed using abdominal CT images of Ghanaians to obtain the volume of the liver and estimate its relationship with parameters like the BSA, BSI, BMI, height, and weight of a normal Ghanaian within a specific age group. Graphic User Interface (GUI) and Computed Assisted Design (CAD) models have also been designed to adequately reflect the comfortable working process of all the mathematical modelled equations (Shiraz, 2018). The fundamental principles, theories, methodology and

available literature on these parameters have been discussed under a broad area of medical imaging in terms of organ measurement and dose optimization procedure.

Liver volume, can reflect liver function, and serve as an important indicator of the severity of liver disease. Research has shown that changes in liver volume correlate with the prognosis and severity of liver diseases (Saygili et al., 2005; Chen et al., 2014**;** Caldwell et al., 1996**;** Schindl et al., 2005). Liver graft volume is a good indicator and a major factor that determines outcome in liver transplant. A graft that is too large for a recipient will lead to poor perfusion while a graft that is too small may cause postoperative small-for-size syndrome, primary non-function, and even severe liver failure (Kawasaki et al., 1993**;** Kokudo et al., 2015). It is therefore very important to have an accurate estimation of total liver volume (TLV) which is essential for clinical condition assessment and some pharmacological applications.

Liver volume can be measured by the Achimedes principle or calculated indirectly from its weight, (Yu et al., 2004). However, these methods are limited to autopsy. Other non-invasive methods have been developed to noninvasive measurement of liver volume based on different imaging modalities, including ultrasonography (Zoli et al., 1990) CT, and magnetic resonance imaging (MRI) (Henderson et al., 1981; Saygili et al., 2005; Shimamoto et al., 2015) but CT volumetric analysis is the most frequently used among these methods (Urata et al., 1995; Shiraz, 2018)

Statement of the Problem

Despite the new and accurate procedures in surgical techniques for liver transplant, liver size disparity still remains one of the most commonly problems

in patients. An accurate liver graft size remains unknown and the size of diseased liver in the recipient is not indicative of the optimal volume liver for the recipient's metabolic demands (Urata et al., 1995)

The liver is classed as a gland and associated with many different functions. It is difficult to an accurate or precise number, as scientists are still exploring it, but it is believed that the liver carries out about 500 distinct roles (Gao et al., 1996) .

It is a complex organ so the liver as the liver can experience a range of problems. A healthy liver functions very efficiently. However, with a diseased or malfunctioning liver, the consequences could be dangerous or even fatal. Estimation the size of the liver could be used as an index to monitor various aspects of liver diseases and response to treatment (Gao et al., 1996; Strunk et al., 2003)

Dose received by a patient from a CT scan is dependent on the patient scanned and the scanner radiation output. Volume Computed Tomography Dose Index ($CTDI_{vol}$) provides information regarding only the scanner output. It does not address patient size, hence patient dose (McCollough et al., 2011).

Dosimetry is an essential requirement for optimization of patient protection in CT. There is a need not only to estimate typical organ doses and risks to patients from CT procedures, but also to conduct periodic monitoring to evaluate the effectiveness of patient protection as part of routine quality assurance (Shrimpton, 2004).

Research Objectives

The general aim of this study was to collect abdominal CT images of normal sized livers, analyze them with respect to body size and gender to establish a local based standard reference volume value for the liver and other body parameters and also calculate the doses to the abdominal section from a CT abdominal scan.

This would specifically lead to:

i. Determination of the length of the liver in the craniocaudal direction in the midclavicular line for clinical application.
ii. Prediction of liver volume of an average Ghanaian adult with standard reference body parameters like, BMI, BSI and BSA using graphic user interface (GUI) for clinical application.
iii. Review and compare measured dose parameters with international reference values and to make appropriate recommendations.
iv. Measure the doses to the abdominal section using the Size-Specific Dose Estimate (SSDE) and effective dose (E) method and compare to the recommended values.

Scope of Work

Subjects were patients of the Korle Bu Teaching Hospital (KBTH), Cape Coast Teaching Hospital (CCTH) and Supreme Specialist Center (SSC). These patients were 18 years and above and of Ghanaian descent. These subjects have no history of liver illness or any other illness that could affect the liver anatomy in anyway. The radiation dosage elements measured in this study are SSDE and effective dose using CT images.

A population size for this study was ninety two (92) patients from the various health facilities using equation a sampling equation.

Relevance and Justification

(Chen et al., 2014) and (Caldwell et al., 1996) have indicated that the state of health of the liver correlates with its size (Chen et al., 2014; Caldwell et al., 1996). Knowing the liver size or volume of healthy patients can help Ghanaian or African medical practitioners diagnose diseased livers.

There exists strong evidence that connects liver cancer deaths and exposure to ionizing radiation. This evidence is based upon studies conducted at Los Alamos National Laboratory, studies of nuclear workers at other sites, and others exposed to ionizing radiation (Board et al., 2012). These findings are consistent with the National Research Council's determination that the liver is sensitive to ionizing radiation (Board et al., 2012) .

Estimating the doses received by patients undergoing CT examinations in the various centers will help to determine if these patients are being protected and to give the correct recommendations if that is not the case (Board et al., 2012).

Organization of the Study

This write-up is presented in five chapters.

It begins with Chapter One which gives a vivid background information about the study, problem statement and objectives. It also describes the scope of the study in relation to its relevance and justification, its clinical application in Ghana and ends with the summary of the study organization.

Chapter Two reviews the literature on existing publications on exposure and patients dose optimization procedures, organ measurements and modelling. It also includes further discussions on the quantity that relates dose to the risk associated with radiation exposure and thus the correlation with stochastic effects, as a result of various dose estimates. Furthermore, the review also includes basic practical and clinical reference information from European

Commission (EC) and International Commission on Radiological Protection (ICRP) recommendations. The review also covers estimates of liver and other related body parameters, including BMI, BSI and BSA related to liver volume.

Chapter Three provides relevant information about the materials and the methodology used to achieve the desired goal of the study. The chapter also describes the various measuring procedures that were used to measure and process the primary data in order to successfully establish relationship between them. The chapter also talks about the various statistical tools used such as: Minitab, SPSS application software used to analyze the data.

In chapter four, the findings of the study are presented in the form of tables and various graphical representations. The chapter also presents the data that facilitates the implementation process in the pictorial format. The relationship between the various measurable quantities were used to calculate the derived quantities and to draw conclusions.

Chapter Five presents a comprehensive summary of the major findings in relation to the measured liver volume, body indices, exposure and effective dose optimization procedures during the abdominal CT examinations. The chapter also provides the concluding summary of this study and recommendations to relevant stakeholders.

Chapter Summary

Chapter One presents a comprehensive summary of what the research is all about. This includes a background of the study, the statement of the problem to be solved. The entire scope of the research is also presented. The relevance and justification are also presented, and finally the organization of the study.

CHAPTER TWO

LITERATURE REVIEW

Introduction

Reviewed in this chapter, are some of the important information based on literature pertaining to the estimation of standard liver measurements history, already established liver volume, exposure and dose optimization procedures. Dose models were used in this study to discuss and access risk associated with the examinations performed by the patients.

History of CT

The X-radiation was discovered by Röntgen in 1895, when investigating radiance of electric discharges inside an evacuated glass tube. His findings revolutionized the diagnosis of several diseases including cancer (Cierniak, 2011; Röntgen, 2006). After 1895, X-ray research saw a quantum jump in its findings as the first picture of a whole skeleton was obtained by X-rays in 1897 (Cierniak, 2011). X-ray equipment design over the years has improved from was improved massively from high quality two-dimensional images of the inside of the human body to 3-dimensional images. Through research, Edison and others made a significant contribution to the development of medical imaging techniques (Cierniak, 2011). Von Helmholtz also investigated and formulated mathematical equations that described X-ray properties and their penetration effect through different objects (Cierniak, 2011). Thompson also researched on the possibility of obtaining a three-dimensional X-ray image (Cierniak, 2011). These studies coupled with others led to the development of some techniques, these include patents by Baese in 1915 and Bocage in 1922 (Thomson, 1996). Later on more research led to contemporary scanners. These studies used gamma radiation to obtain a layered image of tissues, proposed in 1963 by Kuhn (Thomson, 1996).

The first new commercial fan-beam CT scanner was introduced in 1973 onto the market, with 30 detectors and an acquisition time of 20 seconds (Thomson, 1996). Six (6) years later, through research Cormack and Hounsfield both won the Nobel Prize and were credited with the invention of the modern CT. Since then, the CT has seen a lot of progress in its structural design and manufacture. In comparison with the old scan, the modern ones scan in few contemporary ones can scan in a few milliseconds, and reconstructs images of 2,048×2,048 pixels from spiral slices (Cierniak, 2011; Hounsfield, 1973). Figure 1 shows the old and new CT machines after several technical evolutions

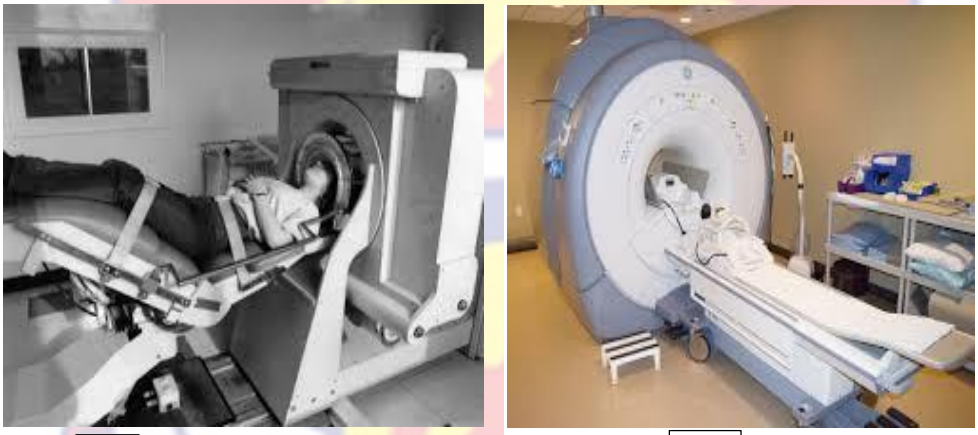

A B

Figure 1: Old (A) and modern (B) CT scanner systems. Source: isct.org, 2018

Principles of Operation in CT

The operation of CT is based on the principle that the density of the exposed object to an X-ray beam can be measured by calculating the attenuation coefficient. The X-ray emitter discharges monochromatic photons that produce a high kV X-ray beam with an average energy of 75 keV. X-rays are generated by physical processes that take place within matter at the atomic level (Bushberg et al., 2003). This is a result of two mechanics; the transition of electrons between the inner shells of an atom, and the deceleration of electrons by the electromagnetic fields within the nuclei of atoms. The resultant X-ray spectrum

obtained is the sum of the energies of both the above-mentioned processes, resulting in discrete characteristic X-rays and continuous X-ray emission, respectively**.** After a beam of X-rays (I_o) pass through a biological material, an attenuated X-ray intensity (I) is measured by the detector. The intensity of the X-ray beam, I_0, is also measured by the CT scanner (Bushberg et al., 2003). X-ray monochromatic intensity, I, is defined as the amount of photon energy ($N \cdot hv$) passing through a unit area (S) in unit time (t) as indicated in equation 2.1:

$$I = \frac{N \,.\, hv}{S \,.t} \qquad (2.1)$$

where

h is Planck's constant

v is the frequency of the photon emitted.

Using Lambert-Beer's law, the relationship between the two intensities I_t and I_0 can be expressed as:

$$\ln(I_t/I_0) = \mu \,.\, x \qquad (2.2)$$

where

x represents the thickness of the biological tissue and μ is the linear attenuation coefficient of the tissue.

CT images are normalized to integer values comprising the Hounsfield unit. This unit defines the degree of attenuation of radiation by various substances before the images are stored and displayed. The number CT(x,y) in each image pixel (x,y) is expressed as (Bushberg et al., 2003):

$$CT\,(x,y) = 1000\,\frac{\mu(x,y) - \mu_{H_2O}}{\mu_{H_2O}} \qquad (2.3)$$

where μ_{H_2O} is the attenuation coefficient of water. This normalization results in Hounsfield unit ranging from approximately −1,000 to +3,000.

Contrast in CT scan images is obtained from the physical properties of tissue that influence incoherent scattering. This depends on tissue electron density (ρ_ε),

$$\rho_\varepsilon = NZ/A \quad (2.4)$$

where;

Z and *A* are the atomic number and atomic mass, respectively.

As such any tissue containing a relative higher number of hydrogen atoms is well visualized by CT (Glover, 1982). The CT number helps in accurate and improved diagnosis in some clinical settings, and accurate estimation of some tissue parameters like volume and diameter.

Clinical Application of Computed Tomography

In 1917, Radon postulated a principle in which he was able to obtain an image from of an object with an infinite number of projections through the object ("History of computed tomography - Wikipedia," 2021.).

Unlike conventional radiography, CT scan enables the differentiation of soft tissue structures from hard tissue, such as liver, lung, and fat. CT scan is useful in searching for both malignant and benign diseases. It can provide information on their location, size, extent of the tumor, its constituents, its extents among others. ("Applications and Clinical Benefits of CT Imaging ," 2020.) The first application of CT scan dates back to a period between 1957 and 1963 when Cormack applied this newly invented technology to improve radiotherapy planning (Cormack, 1973). The first successful use of CT scan was achieved a few years later by Hounsfield, who surprised the entire medical community with his findings (Hounsfield, 1973). From the introduction of the CT technology in the early 1970s, its advantages in clinical imaging has exceeded

the expectation of most researchers. The increasing number of CT scans and their new procedures have encouraged a lot of clinical research. Nowadays, CT has a wide application in both therapeutic and diagnostic procedures. Some of the clinical applications of CT include the following;

1. CT polytrauma is used to diagnose patients with multiple injuries sustained after significant trauma.
2. CT is also used in the diagnosis and staging of diseases such as cancer.

CT use in Nuclear Medicine / Positron Emission Tomography (PET)/Single Photon Emission Computed Tomography (SPECT)

CT is also used in Nuclear Medicine for in many area such as; supplementing gamma camera images as seen in SPECT/CT with anatomical information to help in diagnosing of certain diseases.

Vascular studies

The use of CT intravenous contrast agents injected into the patient allows "non-invasive" visualization of blood vessels. CT is readily available and quick to perform. Faster tube rotation times in cardiac CT have enabled a much higher visualization of the coronary (Generation cardiac CT scanners, 2020)

Intervention

CT guided intervention helps in sampling of diseased tissue. It is used as a source of guidance during treatment of certain conditions. It is also used in fluoroscopy for treatment guidance.

Paediatrics

CT is also used as an imaging modality to investigate disease such as cancer in children.

CT in Radiotherapy

In Radiotherapy, Radiographers use CT simulators to plan patient treatment.

Imaging Principles in Computed Tomography

In Radiography, 3-D body part is reduced into a 2D body image. These 2-D images have reduced contrast because structures that lie on top of each another are projected onto a single image. Certain agents are used to improve the contrast of CT so that certain structures can be observed well. One advantage of CT is the massive improvement it brings in image contrast, using a 2D image to show an almost-2D section of the patient without any overlapping effects of structures ("Imaging Principles in Computed Tomography | Radiology Key," 2021).

Figure 2 shows a cross-section view of a patient being scanned by the CT machine. It is not an X-ray shadow of the beam passing through the body part. An X-ray beam collects information about anatomical and physiological tissue, the resultant image is then a cross-sectional chart of the X-ray attenuation of different tissues within the patient. A typical CT scan generates a trans-axial image oriented in the anatomic plane of the transverse dimension of the anatomy. This image is then reconstructed into a final image which can be reformatted to provide sagittal or coronal images depending on the medical need. These images are viewed as thin slices of tissue rather than superimposed tissues and structures. The pixel values denote how strongly the tissue attenuates the scanner's X-ray beam compared to the attenuation of the same X-ray beam by water ("Imaging Principles in Computed Tomography | Radiology Key," 2021).

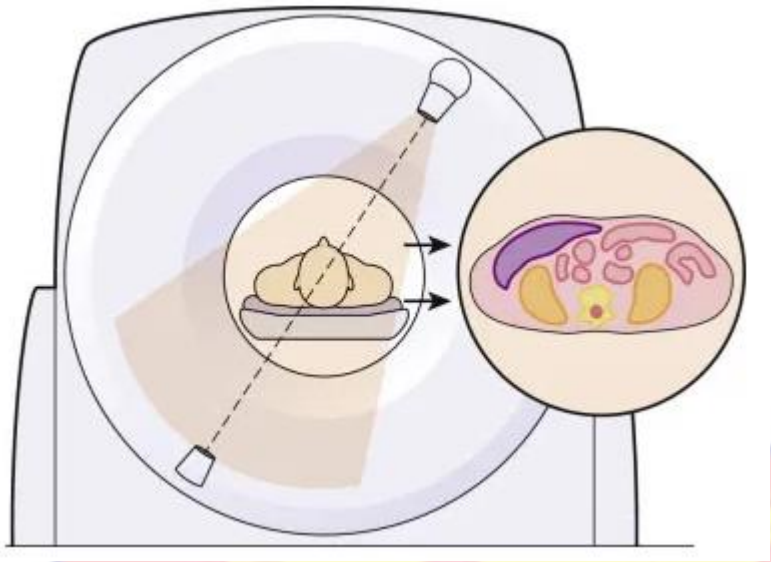

Figure 2: A CT image represents a cross section of the imaged subject rather than the X-ray shadow of the anatomy, as in a conventional radiograph. Source: radiologykey.com, 2019.

Each image is made up of a group of Picture elements (pixels). Each pixel has a grayscale value that is displayed to the radiographer or Radiologist. The image is two-dimensional (2D), but it represents a three-dimensional (3D) volume of physical tissue with a finite thickness, called slice thickness (for this study, it was 5 mm and 10 mm). The size of the pixels and the thickness of the voxels correlate to some important image quality features, such as detail, noise, contrast, accuracy of the attenuation measurement (CT number value) and artifacts("Imaging Principles in Computed Tomography | Radiology Key," 2020).

CT Acquisition Overview

The basic process of collecting data in CT is shown in figure 3. In a CT of a single section of tissue using a single detector, the X-ray beam is collimated to the desired image thickness "Imaging Principles in Computed Tomography | Radiology Key," 18/01/2020). The detector array has a number of individual detector elements that each record the intensity of the beam passing through the

tissue along the path from the X-ray tube to the element. The system captures a simple projection x-ray through the patient, consisting of a thin strip or row of pixels. It can be thought of as a 1D radiograph. The source and detector are then rotated by the scanner to capture additional 1D "strip X-rays" through the same section of the patient, viewed from a number of angles. Each projection is stored in the computer memory for later reconstruction ("Imaging Principles in Computed Tomography | Radiology Key," 18/01/2020).

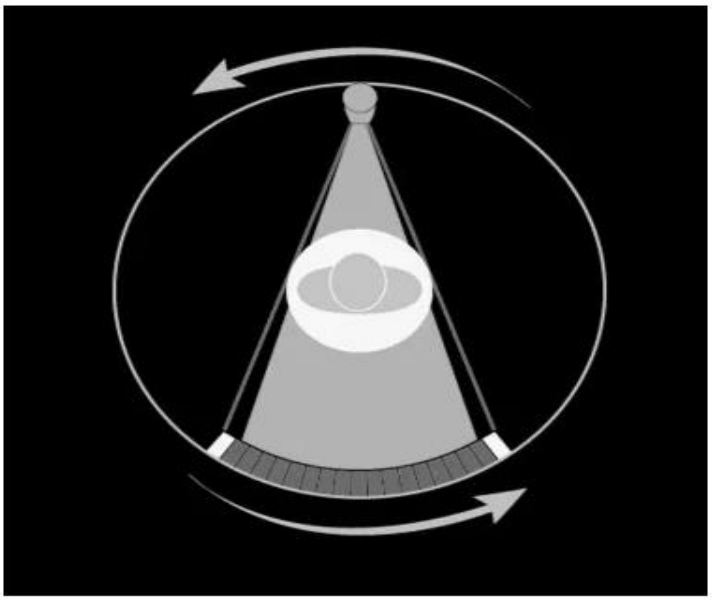

Figure 3: A simple CT scan produces a one-dimensional strip radiograph for each projection through the patient.
Source: https://radiologykey.com/, 2017

In multislice CT as shown in Figure 4, its operation is performed simultaneously for many arrays of detectors stacked side by side along the z-axis which is the long axis of the patient. The X-ray beam collimators are opened according to the size of the patent so that a wider section of the patient is irradiated. Each row of detectors measures a separate transmission signal for the tissue section that lies between the detector row and the tube. The width of tissue that is sampled by each detector row is then determined by the physical width of

the detector elements which is along the z-axis ("Imaging Principles in Computed Tomography | Radiology Key," 18/01/2020).

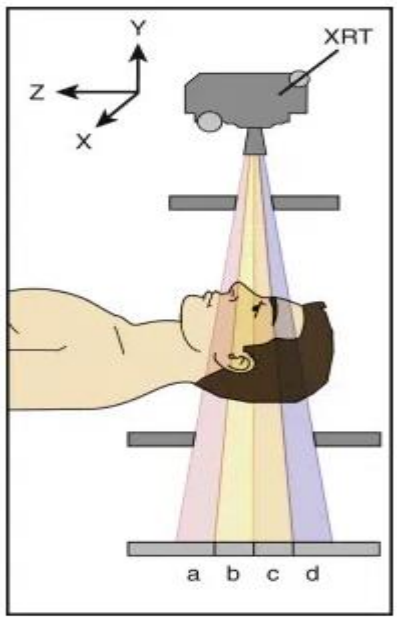

Figure 4: In multislice CT, several independent detectors arranged side by side sample data from unique locations within the x-ray beam. Source: https://radiologykey.com/, 18/01/2020

CT images produced from the scanner gantry are often called slices. The tissue displayed in the image represents the same tissue in the form of a thin slice. Older CT scanners collimate the width of the X-ray beam to the width of a slice (e.g., 5 mm or 10 mm). Multislice scanners mostly use a wider beam to cover more tissue with each pass of the tube, and the detectors contain arrays that are arranged to collect data for multiple individual adjacent slices at the same time.

When a CT scanner is called a "16-slice" model, it normally means that the scanner can acquire up to 16 individual detector data sets at each rotation. Data is normally acquired in thicknesses of 0.5 to 0.7 mm in multi detector-row scanner and reconstructed to image thicknesses of 3 to 10 mm. ("Imaging Principles in Computed Tomography | Radiology Key," 18/01/2020.).

Radiation Dose in Computed Tomography (CT)

Multidetector computed tomography (MDCT) scanners have revolutionarised the clinical application of CT scan. Simultaneous imaging of up to multiple sections and advancement in the CT technology has improved the volume coverage, z resolution, and scanning speed of CT scanners. This has led to an increase in the number of CT examinations performed and also a higher scanned volume obtained per examination. Consequently, CT studies have increased tremendously in the past two (2) decades (Leitz et al., 1995; "Imaging Principles in Computed Tomography | Radiology Key," 2021)

Radiation doses from CT examinations vary substantially across patients, facilities, and countries. (Smith-Bindman et al., 2009) Ionizing radiation from CT scan is a known cause of cancer, (De González & Darby, 2004), which is associated with many cancer incidences world-wide (Task Group on Control of Radiation Dose in Computed Tomography, 2000) , as such it is very important to minimize radiation exposure to patients by optimizing examination protocols.

Choice of Computed Tomography over other Modalities in Liver Volumetry

There are several modalities for body organ volumetric measurement and analysis such as Magnetic Resonance Imaging (MRI), Ultrasound and CT etc. but CT organ volumetric measurement and analysis is the most frequently used among these modalities. Studies show that with the development of CT imaging technology, which involves a refined imaging techniques, and the availability of sophisticated software, for three-dimensional reconstruction has improved organ volume estimation within a 5% deviation (Heymsfield et al., 1979; Urata et al., 1995). Hence, CT volumetry is considered the gold standard for the measurement

of liver volume. It is also used in liver resection (Pulitano et al., 2018; Schindl et al., 2005) and transplantation.

Review of Existing Publications on Liver Measurements

There are several studies which have established different standard liver volume models for different countries (Kokudo et al., 2015). Over the years, three (3) types of liver volumetry have been used to estimate the volume of the liver; these are autopsy, CT, and graft measurement. These volumetry methods have been established using anthropometric variables such as gender, age, height, weight, BSA, BMI, BSI, waist circumference and thoracic width. Currently, Ghana has no such model and which is the first of its kind. Several research works on liver have been done all over the world.

In 2018, Yang developed three formulas to estimate SLV with high accuracy (in terms of correlation co-efficient) for the Korean population.

$$SLV = 331 - 4.1 \times age + 41.6 \times gender + 15.3 \times BW \ (adj\ R^2 = 0.56) \quad (2.5)$$

$$SLV = 161 - 3.6 \times age - 182 \times gender + 27.4 \times SMM \ (adj\ R^2 = 0.60) \quad (2.6)$$

$$SLV = 45 - 4.3 \times age - 152 \times gender + 24.3 \times SMM + 3.36 \times WC \ (adj\ R^2 = 0.60) \quad (2.7)$$

(Yang et al., 2018)

In 2015 Kokudo et al used the parameters of 180 Japanese adult donor candidates and 160 adult Swiss patients with healthy livers to develop another formula. Their data was later divided into two subsets, the test and validation samples which were stratified by race that is Japanese and Swiss. They used age, thoracic width as measured on a CT scan image, and race to independently predict the total liver volume (TLV);

$$\text{TLV} = 203.3 - (3.61 \times \text{age}) + (58.7 \times \text{thoracic width}) - (463.7 \times \text{race}) \quad (2.8)$$

(Kokudo et al., 2015).

Existing Liver Volume

Liver volume estimates have been established from various research. Table 1 provides a summary of this data.

Table 1: Various Standard Liver Volume Established from researches

Studies	SLV regression formulas	Data Source	Population	Sample size
Urata, et al	SLV=2.4+706.2×BSA	CT Volumetry	Japanese	96
Heineman n, et al	SLV=345+1072×BSA	Autopsy	German	1332
Vauthey, et al	SLV=794+1267×BSA	CT Volumetry	North America	292
Hashimoto , et al	SLV=404.8+961.3×BSA	CT Volumetry	Japanese	301
Yu, et al	SLV=21.585×$BW^{0.732}$×H	Autopsy	Korean	652

Source: (Yang et al., 2018)

Image Quality and Dose Optimization

CT among others is one of the most effective imaging methods used by medical officers for medical diagnosis and some guiding therapeutic procedures. With the continuing advances in technology there is the capability to produce images with characteristics that can be optimized for a wide range of clinical purposes. With this, there is the need to also manage the radiation dose for each patient and balance it with respect to the image quality requirements.

In current CT images, the quality of images is discussed in terms of either SNR or the contrast to noise ratio (CNR). However, according to an American Association of Physicists in Medicine (AAPM) publication, there is incoherent limitation regarding the use of CNR, mainly because it does not take into account background noise correlations (Surujpaul et al., 2019).

Principles of SNR Estimate

The SNR is a measure for the detectability of an object in a noisy image (Mahesh, 2013). The SNR of an object is also described as the ratio between the mean gray value μ_0 of the image to the noise in that image, this is associated with standard deviation σ_0 of the image gray values as in equation 2.9:

$$\text{SNR} = \frac{\mu_0}{\sigma_0} \qquad (2.9)$$

SNR is calculated using the level of the desired signal and that of the background deviation. In general, the larger the number of photons transmitted, the greater the SNR.

In CT the signal-to-noise ratio is determined by (Murphy et al., 2020):

i. mAs - greater mAs increases SNR
ii. slice thickness - thicker slices increase SNR
iii. patient size - larger patients reduce SNR

Principles of Exposure and Dose Parameters Estimate

There has been a tremendous increase in the speed and z-axis coverage of CT scanning since MDCT was introduced (Goo, 2010). As a result, the clinical utility have increased considerably in our practice not only in general applications, but also in newer applications such as cardiac CT (Goo, 2010; Mahnken et al., 2007) and dual energy CT (Johnson et al., 2007). As CT utilization increases, the concern about radiation hazards from CT also increases (Brenner & Hall, 2007). In fact, the worldwide average annual per-capita effective dose from medical procedures has approximately doubled in the past 10-15 years (Mettler et al., 2009; Shiraz, 2018). A study (Mettler et al., 2009) has also found an uneven distribution of medical radiation exposure, which is greater in highly developed countries. For example, the 2006 United States data showed

that medical imaging contributed to approximately half (3.0 mSv) of the total radiation dose (5.6 mSv) (Hricak et al., 2011; Mettler et al., 2009) and a similar study can be done here in Ghana. CT is known to be the greatest contributor to medical radiation exposure (Hricak et al., 2011; Mettler et al., 2009).

In view of trying to reduce the potential of radiation hazards, various CT dose-saving strategies have been established (Kalra et al., 2004). This helps with the minimizing of dose to the younger population because they have the benefit-risk ratio of CT examinations can be maximized with optimized unequivocally higher radio sensitivity and longer life expectancy than the older population. In this research some dose parameters that can be considered during scanning that could help determine the dose to patients would be explored. These include; volume computed tomography dose index ($CTDI_{vol}$), dose length product (DLP), etc.

Volume Computed Tomography Dose Index

The $CTDI_{vol}$ is a single CT dose parameter. It is based on a quantity that is easily and directly measured. It represents the average dose received within the scan volume for a standardized (CTDI) phantom (European Commission, 2010). The SI units are milligray (mGy). The values of $CTDI_{vol}$ may be displayed on the console of newer CT scanners, although it may be mislabeled on some systems as $CTDI_w$ (AAPM, 2008).

$CTDI_{vol}$ estimates the average radiation dose within an irradiated volume for an object of similar attenuation to the CTDI phantom, but it does not take into account the size, shape of the object being scanned (AAPM, 2008). Furthermore, it does not indicate the total energy deposited into the scan object or because it is

independent of the length of the scan. Thus, $CTDI_{vol}$ values remain unchanged whether the scan coverage is 10 or 100 cm.

Dose Length Product (DLP)

Dose length product (DLP) is another important dose parameter. It is associated with the $CTDI_{vol}$. DLP is measured in $mGy \times cm$ as a measure of CT tube radiation output/exposure (Huda et al., 2008; Murphy & Morgan, 2016). DLP accounts for the length of radiation output along the z-axis (the long axis of the patient). DLP and $CTDI_{vol}$ are related by equation 2.10

$$DLP = (CTDI_{vol}) \times (length\ of\ scan, cm) \quad (2.10)$$

DLP does not take the size of the patient into account and is not a measure of absorbed dose.

Effective Dose (ED)

Effective dose (ED), is a dose descriptor that reflects this difference in biologic sensitivity. This dose parameter reflects the risk of a non-uniform exposure in terms of its equivalent whole-body exposure. Usually, millisieverts (mSv) is used in diagnostic radiology (McCollough & Schueler, 2000). The use of ED facilitates communication with patients regarding the potential harm of a medical exam that uses ionizing radiation. It is calculated by

$$\mathrm{ED} = \mathrm{DLP} \times \mathrm{K} \quad (2.11)$$

where K is the normalized effective dose coefficient. It varies depending on the area of scan, for abdominal scan K is 0.0153 for adults,

DLP is the dose length product.

The main uses of effective dose are the prospective dose assessment for planning and optimization in radiological protection, and demonstration of compliance with dose limits for regulatory purposes. It is not recommended for

epidemiological evaluations, or for individual specific dose risk or estimate for patients.

Table 2 (Shiraz, 2018) shows the mean effective doses range to patients, standard DLP, standard $CTDI_{vol}$ and coefficients constants. These are used as references that other measurements could be compared with. It also shows the mean DLP and volume CTDI for various CT body examinations.

Table 2: Region Specific Normalized Effective Doses for CT scan

CT Examination	Effective Dose	DLP mGy	$CTDI_{vol}$ mGy	E_{DLP} (coefficients) mSv mGy cm^{-1}
Head	1-2	1050	73.80	0.0023
Chest	5-7	650	36.90	0.0170
Pelvis	3-4	570	43.05	0.0190
Abdomen	5-7	780	43.05	0.0153
Abdomen-Pelvis	8-14	780	43.05	0.0150

Source: (Shiraz, 2018)

Table 3: Typical effective dose in various European countries

EU COUNTRIES	ABDOMINAL E. Dose (mSv)
Austria	14.7
Belgium	8.6
Bulgaria	11.2
Croatia	11.3
Cyprus	10.4
Czech	6.7
Denmark	12.2
Estonia	10.0
Finland	6.7
France	9.4
Hungary	12.1
Iceland	14.1
Ireland	8.4
Italy	8.6
Liechtenstein	28.7
Luxembourg	10.5
Macedonia	17.2

Table 3 continued

Malta	12.4
Monaco	13.5
Montenegro	20.1
Netherland	10.6
Norway	10.0
Poland	17.0
Portugal	6.7
Romania	2.6
Russia	8.2
Serbia	9.7
Slovakia	12.6
Slovenia	15.3
Ukraine	13.5
UK	5.5
Mean	11.3
Maximum	28.7
Minimum	2.6
Max/Min	11.0

Source: (Shiraz, 2018)

Size Specific Dose Estimate (SSDE)

Recent research proposed a new dose index which takes into account the dose received by an individual patient during a scan, by considering the patient's size in terms of the lateral (Lat) (left to right dimensions of the body part being scanned) anterior-posterior (AP) (thickness of the body part being scanned) dimensions of the patient and the $CTDI_{vol}$ (AAPM, 2011; Angeles et al., 2011). Another body parameter that is calculated is the product and sum of the lateral and anterior-posterior dimensions. Measurement of patient size can be obtained from the mid-slice location on the transverse CT image series (Pourjabbar, 2014)

The scan conversion factors used are; head scans (based on the 16 cm diameter head dosimetry phantom) or body scans (based on the 32 cm diameter body dosimetry phantom) (AAPM, 2008). The dimensions are shown in figure 5. It shows the image of the diameter phantom (left) and how it depicts the image of the abdomen (right) and how the dimensions are measured.

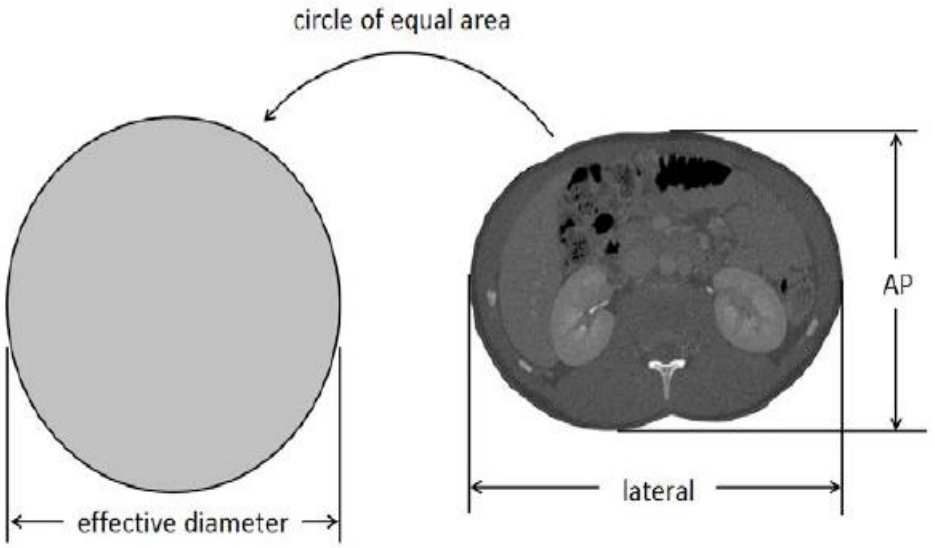

Figure 5: Illustration of AP and lateral parameters discussed.

Effective Diameter (EffD)

The effective diameter represents the diameter of the patient at a given location along the z−axis of the patient (in the cranialcaudal dimension), assuming that the patient has a circular cross section as shown in Figure 5. The patient is assumed to be elliptical in cross section, with the radii r_1 and r_2 being:

$$r_1 = \frac{LAT}{2} \quad (2.12)$$

$$r_2 = \frac{AP}{2} \quad (2.13)$$

The area, A, of the ellipse is computed using:

$$A = \pi r_1 r_2 \quad (2.14)$$

From the area of the patient's cross section, A, the effective diameter is computed as:

$$EffD = 2\sqrt{\frac{A}{\pi}} \quad (2.15)$$

Combining equations 2.13 through 2.16, it can be calculated that (AAPM, 2011);

$$EffD = (AP \times LAT)^{1/2} \quad (2.16)$$

Using the reference phantom of either 16 cm or 32 cm diameter and the patient's EffD, the appropriate conversion factor was derived from the AAPM 204. Multiplying this factor with the displayed $CTDI_{vol,}$ the SSDE (in mGy) of a certain CT scan for a particular patient was calculated.

The general form of the conversion is the following equations 2.17 and 2.18:

$$SSDE = f_B \times CTDI^{Bv} \quad (2.17)$$

$$SSDE = f_H \times CTDI^{H_{vol}} \quad (2.18)$$

The f_B and f_H factors were calculated based on the effective diameters. For example, when a tube of 120 kV is used, they are calculated as shown in equation 2.19 and 2.20:

$$f_B = 3.704369 \times \exp(-0.03671937 \times EffD) \quad (2.19)$$

$$f_H = 1.874799 \times \exp(-0.03871313 \times EffD) \quad (2.20)$$

for the 32 cm and the 16 cm reference body phantoms respectively.

For the purposes of this study the 32 cm reference body phantom was used hence equation 2.19 was used since the study focused on adults.

Liver Anatomy

The liver is the second largest organ in the human body after the skin and the largest gland. It is seemingly coned shaped, dark reddish-brown in colour and weighs an average of 1360 g and located in the upper right quadrant of the abdominal cavity. It is beneath the diaphragm, and anterior to the stomach, right kidney, and intestines. (Kapoor, 2017). Figure 6 shows an image of the liver.

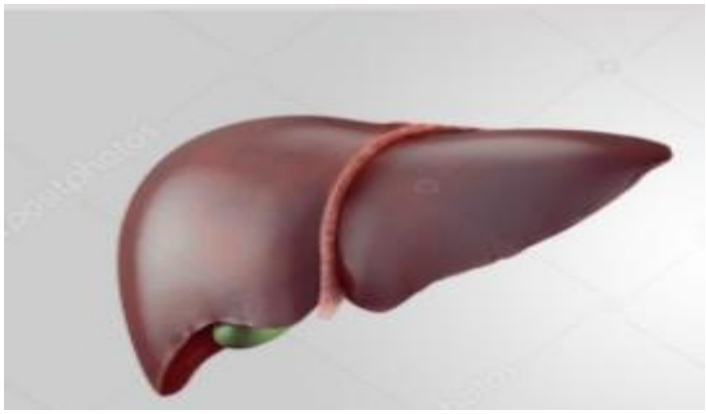

Figure 6: Diagram of the liver source: (https://depositphotos.com/75463987/stock-photo-realistic-illustration-of healthy-and.html, 20/03/2019)

The liver is divided into two parts when viewed from above; a right and a left lobe and four parts when viewed from below; left, right, caudate, and quadrate lobes (Karanjia, 2020). The falciform ligament divides the liver into a left and right lobe. Another imaginary line called the "Cantlie's' line also runs from the left of the vena cava and all the way forward to divide the liver and gallbladder into two halves (Gurakar & Dogan, 2015; Cantlie, 1897).

Basic Liver Morphology

The size of the liver increases with age, from an average span of 5 cm at the age of five years, to an average span of 15 cm when fully an adulthood (Wolf, 1990). Normal liver also varies with sex and body size (Naylor, 1994; Walker et al, 1990; Kratzer et al, 2003). The normal liver weighs 1.4 to 1.5 kg in men and 1.2 to 1.4 kg in women (Wolf, 1990).

Application Software

One important visual programming and application software language is the MeVisLab (MVL). MeVisLab is a software application for medical image processing and scientific visualization. As part of the package, it comes with advanced algorithms for various image processing such as image registration, segmentation, and quantitative morphological and functional image

analysis. It is written in C++ and uses the Qt framework for graphical user interfaces. It is available on all operating systems ("MeVisLab - Wikipedia," 18/01/2020)

Its application also ranges from software neuro-imaging, dynamic image analysis, surgery planning, and cardiovascular analysis. (Image Processing Research and Development, 2020). It is readily available in different versions, for this study the free open-source version was used.

MeVisLab contributes significantly to DICOM as a standard software protocol for distributing as well as viewing all kinds of medical images, regardless of the origin of the images (MeVisLab Medical Solutions, 2015). These are used to accurately carry out the measurement of the various organ dimensions. In lieu of this it is currently used to measure radiological and other non-radiological organ parameters like renal parameters and the implementation of the CAD modeling during image analysis and visual indicators in clinical reporting and research (MeVisLab Medical Solutions, 2015). The MeVisLab application software has application features that are used to extract basic data from the real, raw tomographic images to fulfil research study requirements. The application software features help users to identify and define complex organ shape. MeVisLab application software is distinguished as a rapid prototype and development program for medical image processing and visualization (Heckel et al., 2009; MeVis Medical Solutions, 2015).

MeVisLab software is capable to manage large volume of data and can process all dimensional images (x, y, z, color, time or user-delimited), including those in this study. MeVisLa offers easy and fast-breaking ways to customize any application on medical images by developing novel algorithms or improve existing ones in a modular C++ or VB interface, which is the fundamental bases

of this study for the development of GUI. MVL offers easy ways of combining algorithms to algorithm pipelines and networks which is required in this study.

MVL platform (Heckel et al., 2009) enables integration with digital networks.

Basic Principles of Body Parameters

This section discusses the relationship between various body parameters, including; height, weight, waist circumference, BMI, BSI and BSA. It also includes discussions that relate these parameters with renal volume of individuals, in addition to various publications regarding the use of these parameters in clinical applications.

Body Height and Weight

There exists various relationships between body height and body weight. These relationships include; BMI, BSA and BSI. In addition, there is a positive correlation between body height and weight as published (Sargent, 1963). She devised a relationship between weight and height in the American population, which she stated as equations 20.20 and 20.21:

$$W = 12.1e^{0.01H} \quad \text{For men} \quad (2.20)$$

$$W = 9.5e^{0.0108H} \quad \text{For women} \quad (2.21)$$

where W is the weight in kg and H is the height in cm.

Figure 7 shows the normal human growth curve. The growth period for the human body is unusually long among mammalian species, usually requiring more than a quarter of the normal life span. This is due to the delay in nearly all aspects of bodily development, especially skeletal and endocrine maturation (Watts, 1986).

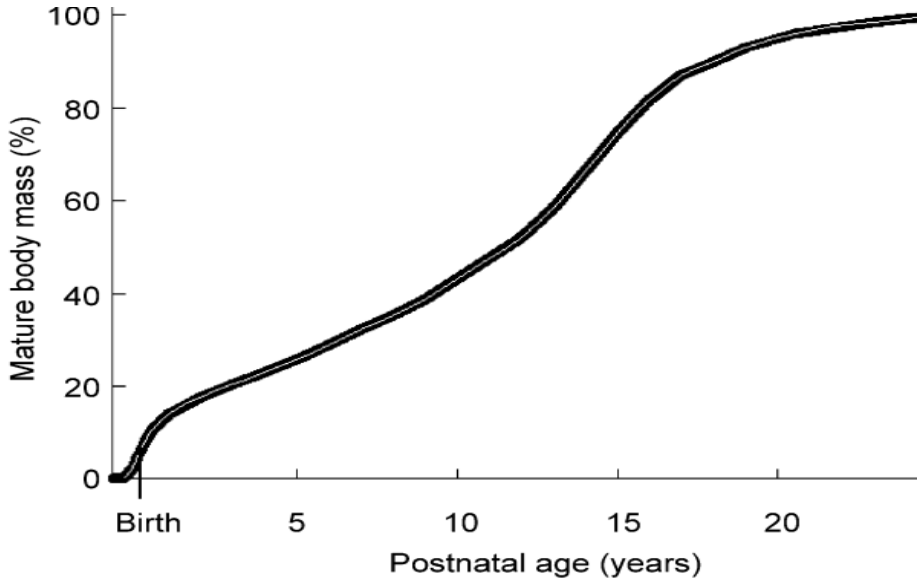

Figure 7: Increase of body mass during growth as a percentage of mass at age 25 years. Source: (Shiraz, 2018)

In humans, the total body mass continues to increase after maturity, but in males this rate of increase slows down considerably after the age of 18 years and about 16 years in females. This is illustrated in Figure 8, which summarizes measurements of body mass made in the extensive NHANES II survey of nutritional status in the USA during the period 1976–1980 (NCHS, 1987; Burmaster and Crouch, 1997).

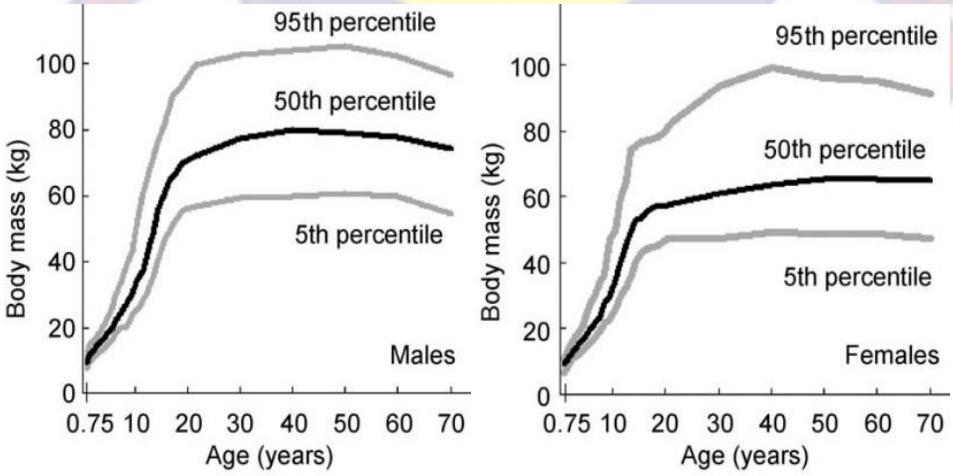

Figure 8: Body mass as a function of age and gender in the USA population, as determined in a crosssectional study conducted during the period 1976–1980. Source: Shiraz, 2018.

Body Mass Index (BMI)

A BMI scale provides information about body weight and height. This explains whether a person's body weight is appropriate with the person's body height. This idea was first estimated by Adolphe Quetelet (1796-1874) who formulated a method to evaluate the body index (Eknoyan, 2008). It was then known as the Quetelet Index until it in 1972 it was changed to BMI by Ancel Keys (Shuter & Aslani, 2000; Du Bois & Du Bois, 1989). The standard unit for BMI is the kg/m^2. Basically, it represents the human body fat between ages 18 and 65 years. Studies by Frempong shows that the average Ghanaian adult BMI is 25.7 kg/m^2 for male and 21.65 kg/m^2 for female (Frempong, 2013).

Body Surface Area (BSA) and Body Surface Index (BSI)

Other studies in body weight and height resulted in two body parameters namely; BSA and BSI. The term body surface area was invented to show the relationship between surface region of a human body and its weight and height (Du Bois & Du Bois, 1989; Ferreira & Ja, 2014).

The mean body surface area varied based on age and gender. Studies done by the European communities estimates the average BSA value for an adult male to be 1.9 m^2, while that for an adult female is 1.6 m^2 (IAEA, 1993). For the purpose of this study the Du Bois formula was used to estimate the BSA.

Furthermore, BSA in relation to the body weight describes a new parameter called BSI. This parameter is a more precise indicator than both the BMI and the BSA. It is estimated by dividing the body weight by the calculated square root of its BSA, mathematically expressed in equation 2.22 as:

$$\text{BSI} = \frac{\text{WEIGHT}}{\sqrt{\text{BSA}}} \quad (2.22)$$

Studies indicates that these parameters increase with increasing age (Ferreira et al., 2014).

Liver Volume Related to Body Parameters

Determination of the correlation between the BMI and BSA in relation to liver volume and other measurable parameters has been developed by various researchers. However, a much precise, measurable parameter has been developed in relation to body weight and body surface area and described as the body surface index (BSI) (Ferreira et al., 2014).

This unique parameter is also related to other body and internal organ measurements and described as BSI-related body parameters without direct measurement. For instance, the determination of the correlation between the BSI in relation to liver dimensions and other measurable parameters has been developed by various researchers to arrive at BSI related body parameters without direct measurement.

In conclusion, several reference organ models and body parameters are reported in literature, this has led to the understanding of human anatomy through medical imaging and therapeutic procedures. Table 4 represents a summary of the ICRP and 'Asian reference man' designed from data taken over a period to support individual states in clinical practice (WHO, 2004; IAEA, 1993)

Table 4: Asian and ICRP Reference Male/Female Models

Parameter	Asian (1998)	ICRP (1975)	ICRP (1995)	ICRP (2015)
Male				
Age	35 (20-50)	35(20-50)	35(20-50)	42(20-80)
Race	Mongoloid and South Caucasoid	Caucasoid	Caucasoid	Caucasoid
Sex	Male	Male	Male	Male
Body weight (kg)	60	70	73	76
Body Height (cm)	170	170	176	179
BMI (kg/m^2)	22	24	24	24.6
BSA (m^2)	1.78	1.8	1.9	2.05
BSI (kg/m)	33.71	38.25	38.42	38.95
Female				
Age	35(20-50)	20-30	35(20-50)	42(20-50)
Race	Mongoloid and South Caucasoid	Caucasoid	Caucasoid	Caucasoid
Body weight (kg)	51	60	60	63
Body height (cm)	160	161	163	165
BMI (kg/m^2)	22	22	23	24.1
BSA (m^2)	1.55	1.60	1.69	1.70

(Source: Shiraz, 2018)

Chapter Summary

In summary, a comprehensive review of the literature on exposure and patients dose optimization procedures, organ measurements and modelling was done in this chapter. It also includes further discussions on dose associated with radiation exposure in relation to CTDI, DLP, SSDE and effective dose parameters as related to EC and ICRP recommendations. The final discussions were based on estimates of body parameters (BMI, BSA and BSI).

CHAPTER THREE

MATERIALS AND METHODS

Introduction

This chapter provides relevant information on the experimental framework of this study. The health facilities, materials and methods used to measure, analyse and model the relationship between the volume and body parameters are described. The chapter also describes the calibration of the equipment and software used in this study. It also shows a flowchart of the study. Also this chapter presents how dose assessment in terms of SNR, ED and SSDE for each patient was calculated.

Health Facilities

The study was carried out at three (3) health facilities in Ghana, namely; the Korle Bu Teaching Hospital (KBTH) located in Accra, Cape Coast Teaching Hospital (CCTH) located in Cape Coast and Supreme Specialist Centre (SSC) located in Accra. All the three (3) health facilities were used for the dose assessment whiles CCTH and SSC were used in the liver volume study. Table 5 shows the equipment specification for the three facilities.

For liver volume analysis, Sixty-four (64) patients from the SSC and twenty-eight (28) patients from the CCTH were used. The lesser numbers from CCTH was due to the breakdown of the DVD burner drive. For the dose optimization analysis, fifty (50) patients from both KBTH and SSC were used with thirty-seven (37) patients from CCTH.

Ethical clearance was sought from the University of Cape Coast Institutional Review Board (UCCIRB) (see Appendix A)

Table 5: Specifications of CT Scanners from the various Health Facilities

	Health facilities		
Specifications	KBTH	CCTH	SSC
Manufacturer	Toshiba	Toshiba	Toshiba
Model	Aquilion one TSX-301A	Aquilion TSX-101A	Asteion TSX-021B
Year of manufacture	2012	2013	2009
Number of slice	16	16	4
Input	3~200 V 50/60 Hz	3~200 V 50/60 Hz	3~200 V 50/60 Hz
Max input power	90 kVA	90 kVA	75 kVA
Output	120 kV 580 mA	120 kV 580 mA	120 kV 300 mA
	135 kV 510 mA	135 kV 510 mA	135 kV 260 mA
Country of origin	Japan	Japan	Japan
Couch length	2.64 m	2.64 m	2.92 m

Source: Field work, 2017

Equipment

The equipment used for this research include the following;

- Computed Tomography machine
- Digital weighing scale

The materials that were used include;

- Tape measure
- MeVisLab software (version 2.7.1)
- RadiAnt Software (version4.6.8.18460 64 bits)

Computed Tomography Machine

The three (3) CT machines used were all made by Toshiba Corporation (Figures 9, 10 and 11) with varied slice numbers from 4 to 16. The KBTH health facility uses the Toshiba Aquilion one TSX 301A CT machine with a 16 slice capacity, the CCTH uses a Toshiba Aquilion TSX 101A with a slice capacity of

16, whille the SSC uses a Toshiba Asteion TSX 021B with a slice capacity of 4 (Specifications shown in Table 5).

These CT scan machines were used to obtain images in the axial and coronary series.

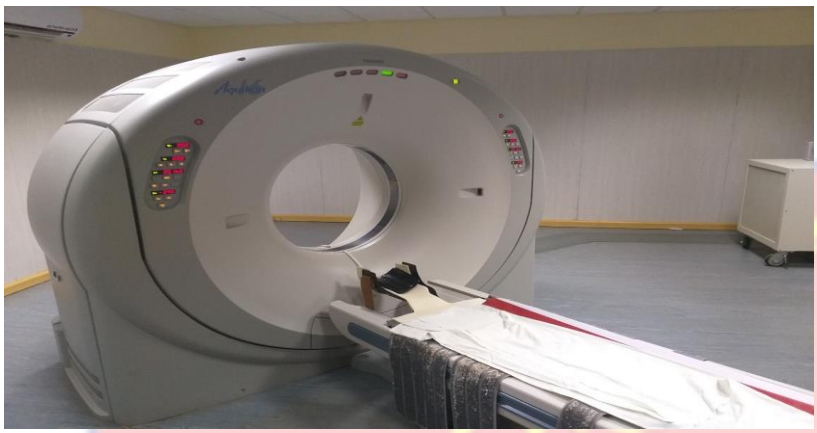

Figure 9: Toshiba Aquilion CT machine of the Cape Coast Teaching Hospital (CCTH)

Figure 10: Toshiba Asteion CT machine of the Supreme Specialist Centre (SSC)

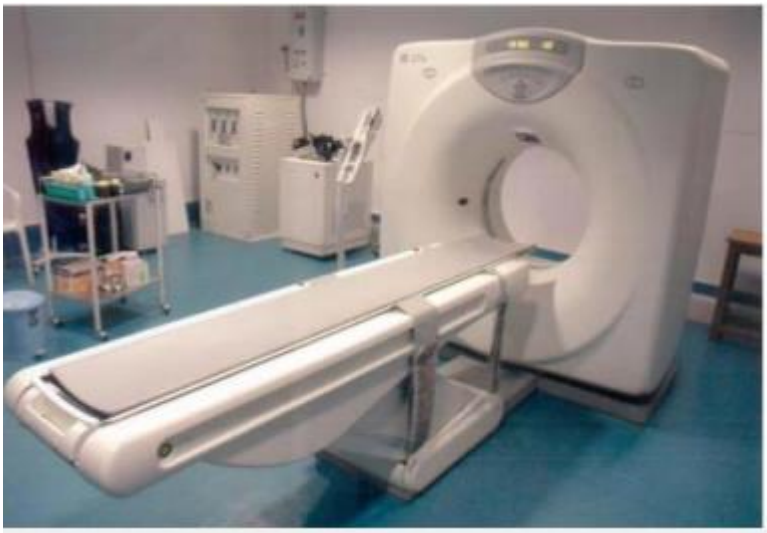

Figure 11: Toshiba Aquilion one CT machine of the Korle Bu Teaching Hospital (KBTH)

MeVisLab software (version 2.7.1)

The MeVisLab software enabled various measurements in axial and coronary planes to be undertaken, in addition to this it also shows patient dose information. The measurements made include; length of the liver in the midclavicular line, the number of voxels in the liver region, the lateral and anterior – Posterior axial CT dimensions of a patient. Figure 12 shows the interface of the MeVisLab software.

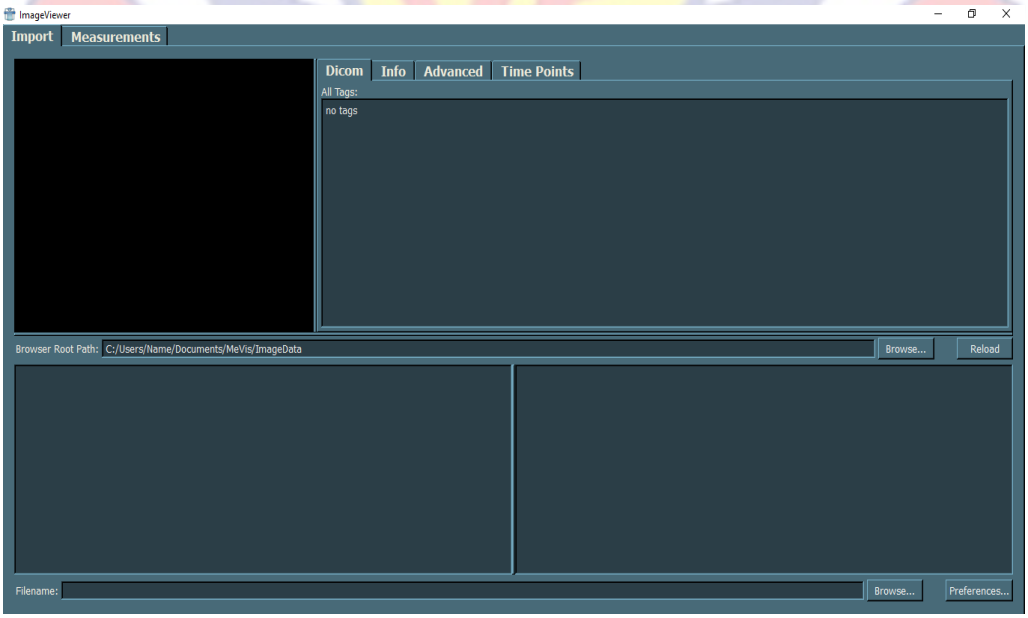

Figure 12: Showing MeVisLab Software Interface. Source: Field data

RadiAnt DICOM viewer Software (version 4.6.8.18460 64 bits)

The RadiAnt software was used to convert the images into DICOM format to be used on the MeVisLab software. Figure 13 shows the user interface of RadiAnt software.

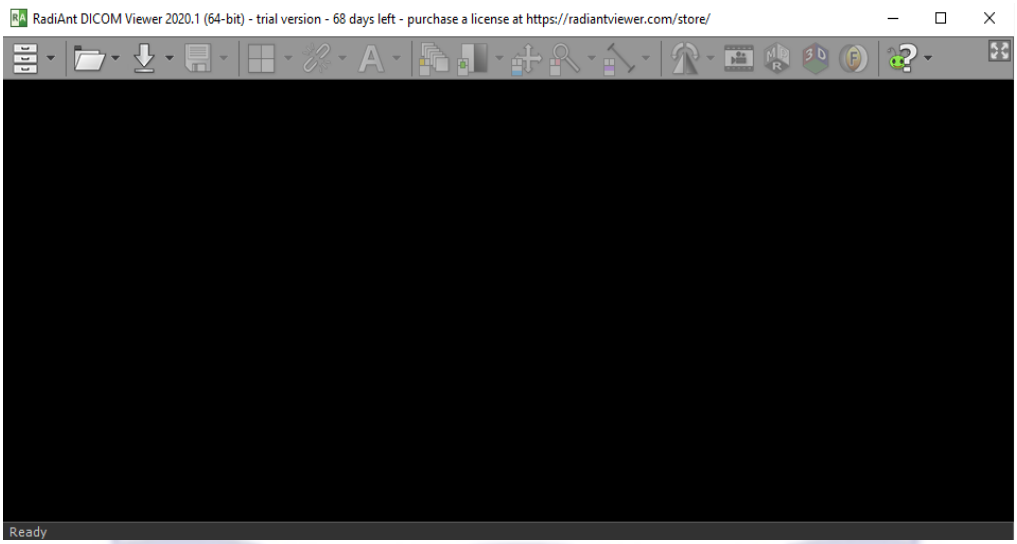

Figure 13: Showing RadiAnt Software Interface Source: Field data

Digital Personal Weight Scale

The digital personal weight scale machine was used to measure the weight of patients. The model used was LOT-2011A2, produced by the Yongkang Lot Electronics Company Limited in China. It could measure in both kilograms (kgs) and pounds (Ibs). For this study the kilogram was used as the measuring unit. The scale has a measuring range from 7.00–180.00 kg with a graduation of 0.1 kg. It has four (4) digits display screen and powered by a 3.0 volts CR2032 lithium battery. Its operating temperature is between 5.0 – 35.0 °C. It has three (3) error displays which includes; 'Lo' – for Low voltage display, 'Err'- for Error display, 'O-Ld' – for overweight display. For the purpose of this study two (2) weight scales of the same model were used, one (1) for each health facility KBTH and SSC. Figure 14 shows one of the weight scales used for this study.

Figure 14: One of the weight scales (LOT-2011A2 model) used for this study

Tape Measure

The health facilities for this study did not have stadiometers at the CT scan buildings so a tailor's tape measure was used in taking the height of the patient. The tape measure is made from fiber glass with linear-measurement markings on both sides. One side has measurement in centimeters and the other side has readings in inches. For the purpose of this study the centimeter units were used. The tape measure has a measuring range of 0 – 150 cm with a graduation of 0.1 cm. To ensure accurate and steady measurements, the tape measures were fixed to walls in the CT scan buildings as indicated in figure 15. The average height of a Ghanaian adult is more than the 150 cm length of the tape measure (Shiraz, 2018), so to ensure a continuous and accurate measurement, the tape measure used at CCTH and SSC were fixed 58.0 cm and 70.0 cm above the ground respectively. So 58.0 cm and 70.0 cm were added to measurements taken at CCTH and KBTH, respectively.

Figure 15: Tape measures fixed on wall for patient height measurement

CT Abdominal Images

The section of abdominal CT images used were the axial and coronary. The axial CT images were used to measure the volume of the liver and estimate SSDE. The coronary CT images were used to measure the length of the liver in the mid clavicular line.

Methodology

Flowchart of study

The flowchart as shown in figure 16 explains and gives a step to step account of how the measurements and calculations were performed in this study. The flowchart shows the design for this study.

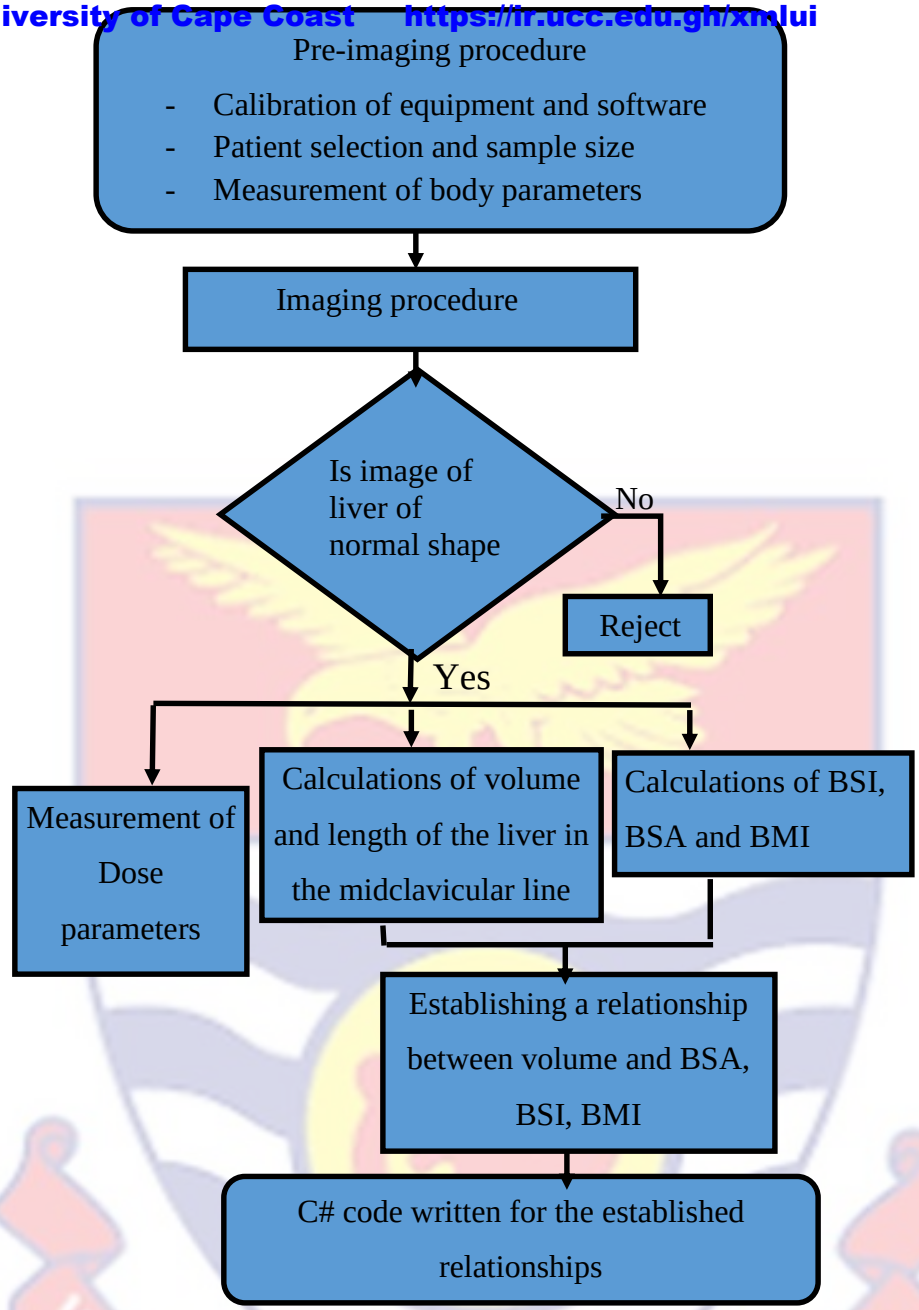

Figure 16: Flowchart for this study

Pre-Imaging Procedure

Calibration of Instruments

Calibrating Weight Scale

The weight scale was calibrated at the Balance Calibration Laboratory of the Ghana Standards Authority (GSA).

Calibration of MeVisLab (MVL) Software

To ensure that the functionality and accuracy of the measurement taken with the MeVisLab software, a calibration test was performed to ascertain the

accuracy of measurement with the MeVisLab software. To achieve this a Wilke Phantom was used. In the center of the phantom are two (2) holes (marked 1 and 2), 5.5 cm apart as shown in Figure 17.

Figure 17: Wilke phantom with defined length dimension

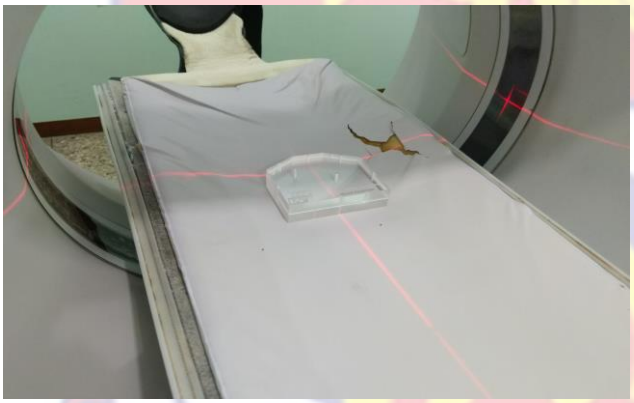

Figure 18: Setup of Wilke phantom for calibration scan

The Wilke Phantom was placed on the couch of the CT machine, scanned with the setup and protocol for CT abdominal scan as shown in figure 18. The image was processed and copied onto an encrypted drive. The image was loaded into the MeVisLab software and the length between these two (2) holes (figure 19) measured three (3) times and the average recorded.

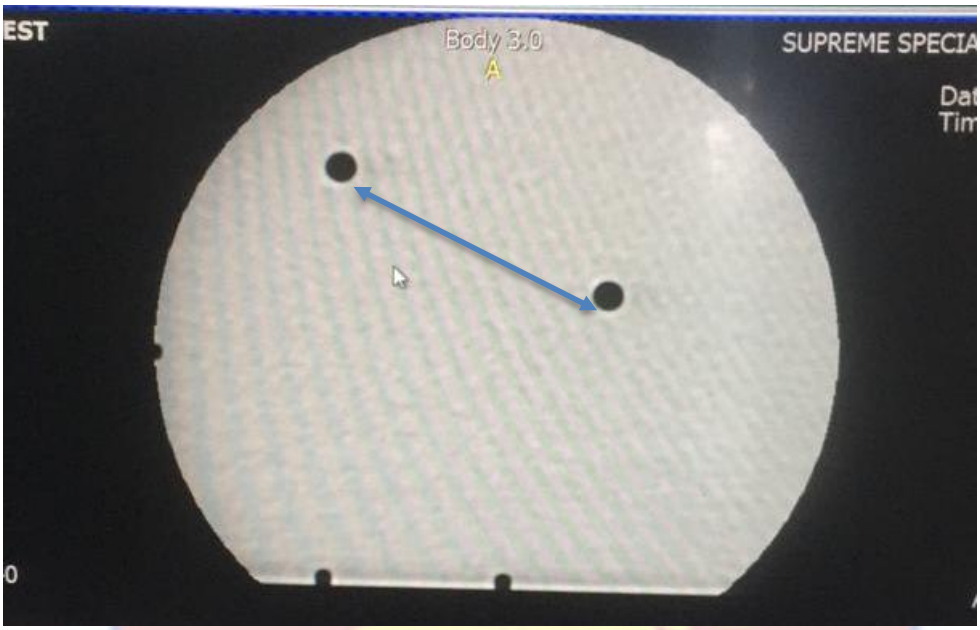

Figure 19: Image of Wilke phantom captured with the MeVisLab software

The correction factor was calculated using equation 3.1 and multiplied to all measurements obtained from the MeVisLab. This calibration was performed at CCTH and SSC.

$$\text{Correction factor} = \frac{\text{Actual value}}{\text{Average measured length}} \quad (3.1)$$

Patient Selection and Sample Size

This process starts with the patient coming for an abdominal CT scan. The patient should be 18 years of age or above and of Ghanaian decent, and not coming for CT scan due to any liver related disease, this was verified from the patient health records.

The targeted group for this study were patients coming for CT abdominal scan. In order to obtain a sample size for this study, equation 3.2 was used with a confidence level of 90 %. This is the same equation used by UNICEF for their sampling method for their studies.

$$n = \frac{N}{1+N(\alpha^2)} \quad (3.2)$$

where N is the total population of the targeted group (patients coming for CT abdominal Scan) for a year, n is the sample size for this study and α is margin of error, for this study, 10 % was used.

Measurement of Body Parameters (Height and Weight)

After a patient qualifies to be a subject for this study, the patient was spoken to and taken through the ethical clearance. If the patient agreed to be part of this study, the age was taken followed by the measurement of the body weight and height using the scale meter and the tape measure respectively.

Measurement of Height

Each patient stood upright on the scale with the head perpendicular to the body (Figure 20a). The height measurement was taken from the top of the head as shown in Figure 20b. The measurement was taken three (3) times and the average calculated and recorded with Microsoft Excel software 2013 version.

(a) *(b)*

Figure 20: a: A patient standing b: Height of a patient being measured

Measurement of Patient Weight

In measuring the weight of the patient, the patient was asked to remove their footwear and stood on the weight scale with the body upright and the head

perpendicular to the body as shown in Figure 21a and the displayed weight (Figure 21b) value on the scale was recorded. The patient stepped down and the process was repeated three (3) times and the weight values recorded. The correction factor from the calibration was multiplied with the values, the average was calculated and recorded. This process was repeated on each patient to obtain his or her weight.

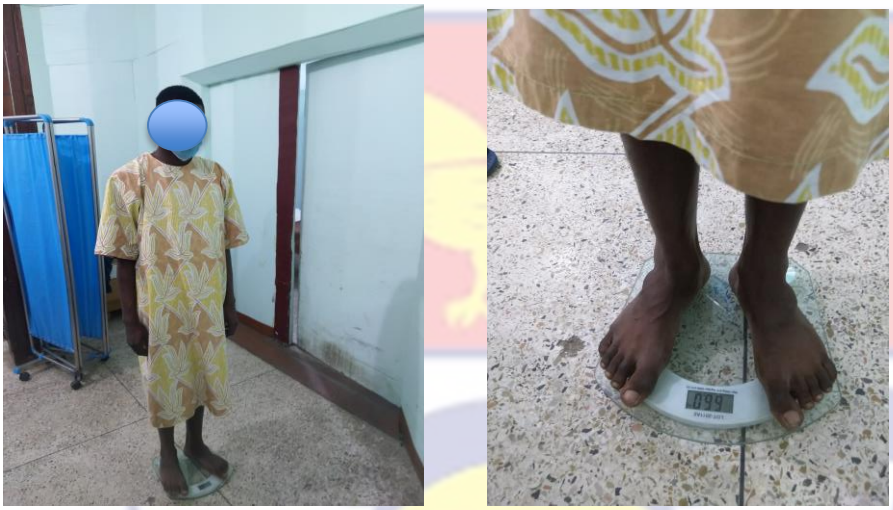

(a) *(b)*

Figure 21: 21a showing the Patient Standing up right on the scale

(b) Patient on the Weighing Scale.

CT scan of Patient

After the primary body parameters were recorded the patient underwent CT scan.

The patient was placed on the couch of the CT machine in a supine position as shown in Figure 22. Table 6 shows the technical scan parameters used for this study.

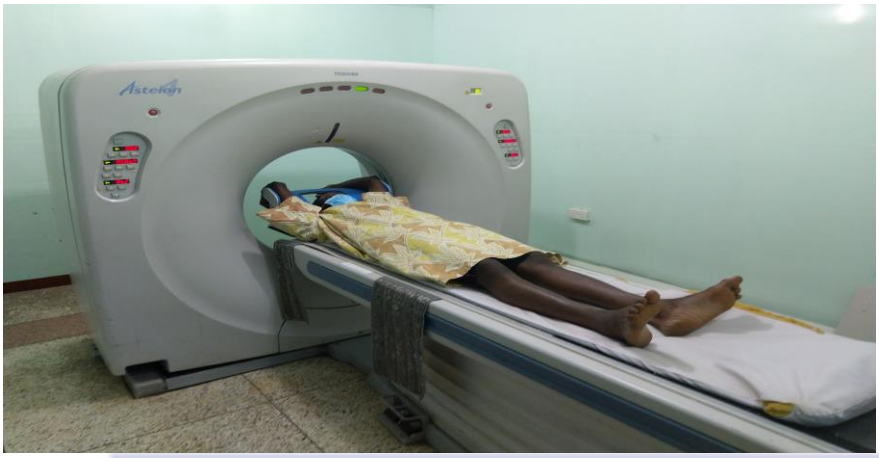

Figure 22: A Patient lying on the Couch in a Supine Position to undergo a CT Abdominal Scan

Table 6: Technical Scan Parameters used for this Study

Scan parameters	Values
Collimation	0.625-7.00 mm
Table Speed	50.5-60.5 mm/rotation
Rotation Time	0.5-0.8 s
Voltage	100 - 120 kV (peak).
Body Part Examined	ABDOMEN
Scan Options	HELICAL_CT
Slice Thickness	5.0 – 10 mm
Exposure Time	500 s
X-Ray Tube Current	80-253 A
Exposure	25-126
Filter Type	LARGE
Generator Power	9
Focal Spots	0.8-1.6
Estimated Dose Saving:	0-55.51
Spiral Pitch Factor	0.813
Exposure Modulation Type	3D
Pixel Spacing	0.500 - 0.999
Window Center	40
Window Width	400

Source: Field Data, 2018

The first session of scanning involves scanning the entire abdomen of the patient without a contrast. The scan process was paused after the first complete scan and the patient injected with a 50 – 80 mL of nonionic contrast material. Depending on the indication of the study, images were obtained between 30-60 s; 60-90 s, 180 s after contrast medium has been administered.

Axial and coronary section images were reconstructed with a 5.0 mm slice thickness at the SSC and 10.0 mm slice thickness at CCTH.

After the scan the images are reconstructed and copied onto an encrypted external hard disk and viewed using the MeVisLab software.

Healthy Liver and Unhealthy Liver

The images were loaded into the MeVisLab software and viewed. A healthy liver is one with a normal shape, homogeneous density, smooth outline which is without focal lesions like masses or abnormal density.

Any liver without the above features was considered unhealthy, thus the parameters enumerated above were not evaluated.

Measurement of Signal to Noise Ratio

In order to ascertain the quality of the images used, a signal to noise ratio test was performed on the images. The items used were; axial images and MeVisLab software.

Using the MeVisLab software, the cursor was placed in a homogeneous area within the axial CT image and a region of interest (ROI) was drawn and labelled A as shown in figure 23. The average (signal) and (noise) standard deviation (Std.Dev) values (labelled B&C) as shown in figure 23 were recorded. This process was repeated at five (5) different portions of the image. The mean of the ‘average’ and ‘Std.Dev’ values were calculated and recorded using

Microsoft Excel 2013. To obtain the SNR, the mean average values was divided by their corresponding mean standard deviation (Std.Dev) values.

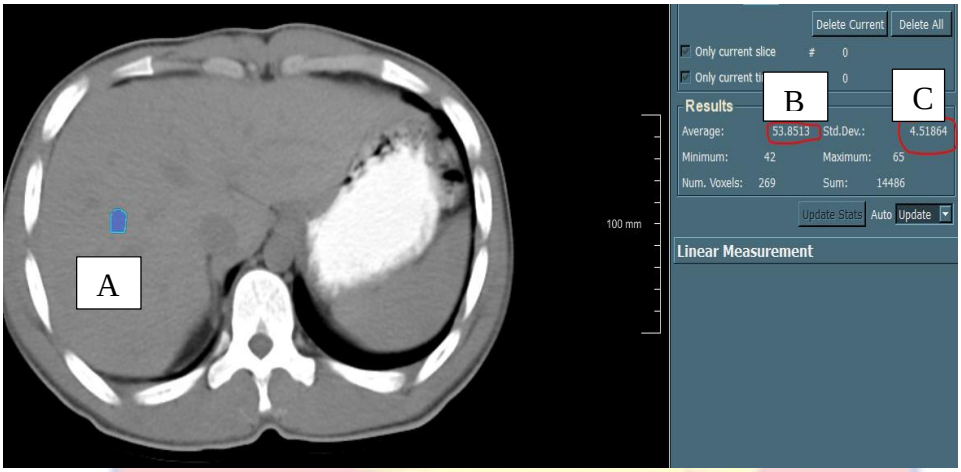

Figure 23: Region of Interest (ROI) selected to aid in calculating Average and Standard Deviation of Image

Calculation of Volume

In determining the volume of a liver from a patient, three parameters were used; the number of volume elements (voxels), pixel area of the voxels and slice thickness of the voxels.

In calculating the number of the voxels in the liver image, the axial CT scan images and the MeVisLab software were employed.

The axial CT images were loaded into the MeVisLab software. Mostly the first organ that appears on the first axial slice was not the liver so the images was scrolled down until the first liver image slice appeared. The 'Enable ROI' box as shown in Figure 24 and labelled A was checked or ticked, and the computer cursor changed to a drawing tool.

The computer cursor was placed at the edge of the liver at any point and manually traced carefully along the boundaries of the liver in a cross-wise direction until the initial starting point was met again. The MeVisLab software automatically colours the region within the trace area blue as shown in Figure 24

labelled B. The numerical value for number of voxels as shown in Figure 24 labelled C was recorded. For the image shown in Figure 24, the number of voxels for that particular slice was 25240.

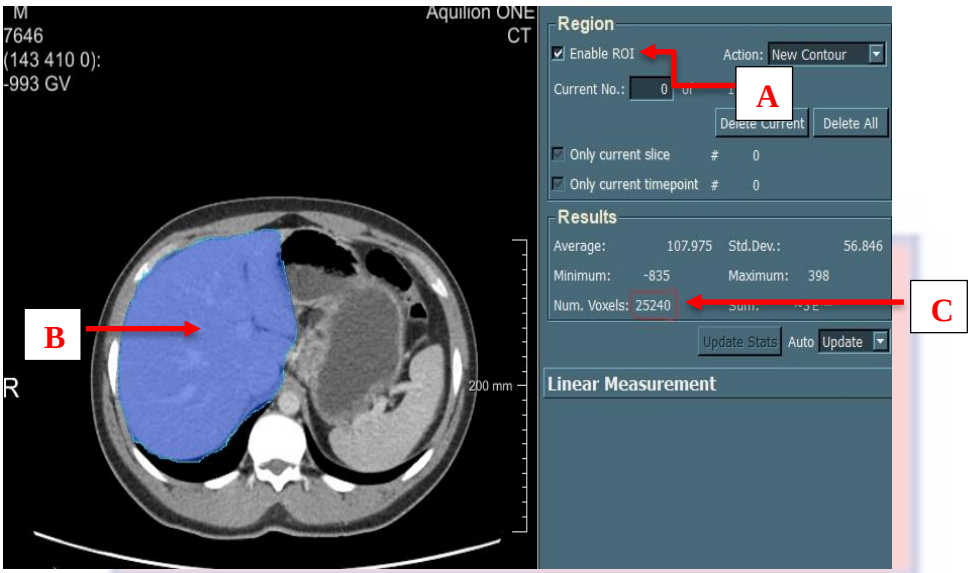

Figure 24: ROI for Measurement of Volume with MeVisLab

This process was repeated for all the axial slices that contain liver image until the last liver was seen. The number of voxels values obtained (as shown in Figure 24) for a patient was recorded and summed up using Microsoft Excel.

The pixel area was obtained by finding the square of the pixel spacing. The pixel spacing was obtained by scrolling to the patient and image section of the CT images which were the first two (2) slices from abdomen CT images as shown in figure 25 labelled A. From Figure 25, the pixel area for the patient was ($0.604 \times 0.604 = 0.365$ mm^2)

The slice thickness (height of the voxel) was obtained by also scrolling to the patient and image section of the CT images which were the first two (2) slices as shown in Figure 25 B. The slice thickness for this patient was 5.0 mm.

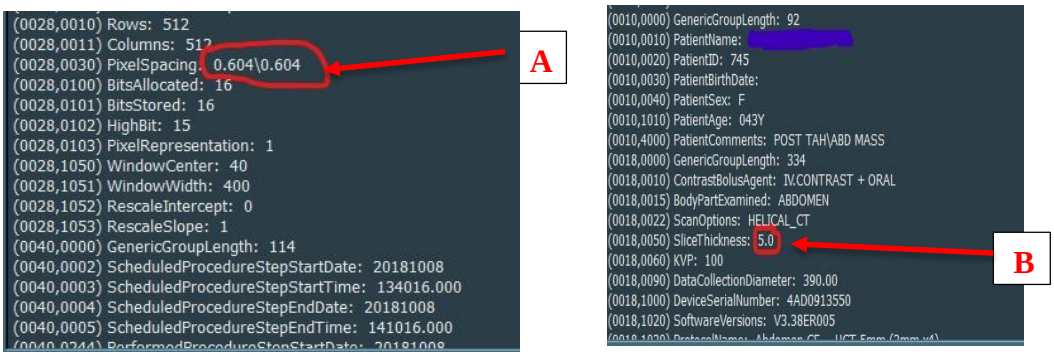

Figure 25: Pixel Spacing and Slice thickness values circled in Red (A&B) from Image Information

In determining the volume of the liver, the pixel area (the product of pixel spacing) was multiplied by the slice thickness (the height of the voxel) to obtain the volume of a single voxel, which was multiplied by the total number of voxels, and expressed mathematically in equation 3.3 as:

$$V_l = \underbrace{(Pixel\ area \times slice\ thickness)}_{\text{Volume of a single voxel}} \times total\ number\ of\ voxels \qquad (3.3)$$

where V_l is the volume of liver.

Measurement of the Length of the Liver in the Mid clavicular Line

In determining the length of liver in the midclavicular line, the MeVisLab software and coronary CT images were employed. The coronary section was loaded into the MeVisLab software. The slices were scrolled through until the largest liver size was observed since the length of the liver was normally measured from the largest coronary liver image. The cursor was placed at the left side of the image and a lateral line was drawn on the top (marked 1) and bottom (marked 2) of the liver to the right side of the image using the MeVisLab software as shown in figure 26.

The two parallel lines were further divided into two equal parts by a perpendicular line (marked 3). The left side portion was further divided into two

(2) equal halves by another perpendicular line (marked 4). MeVisLab automatically generates the length of a line drawn as shown in Figure 26 marked 5.

The length of the line marked 4 was recorded as the length of the liver in the midclavicular line. This procedure was repeated three (3) times and the average length calculated and recorded with Excel software 2013 version. This was measured in millimeter (mm).

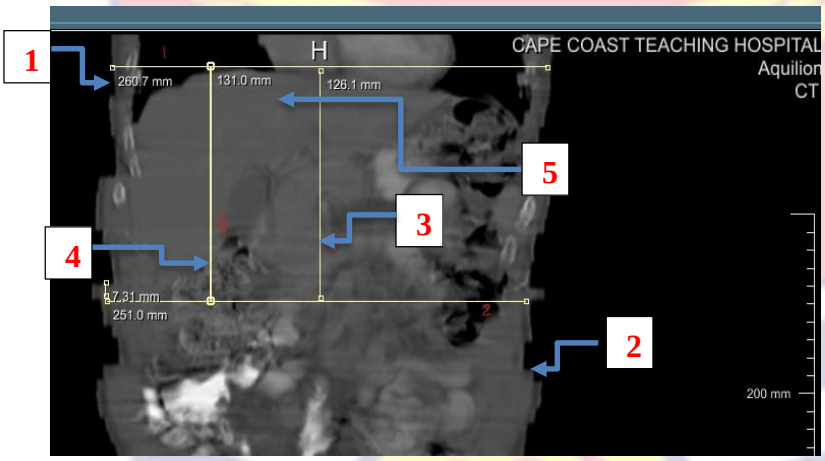

Figure 26: Determining the length of a scanned image of liver from the mid clavicular line by drawing two parallel lines (Lines 1 and 2) and then dividing these lines into two equal half.

Calculations of BMI, BSA and BSI

In calculating the BMI for each patient, the patient height initially measured in centimeters (cm) was converted to meters (m) and the patient weight in kilogram (kg) were used. The patient weight was divided by the square of the patient height as shown by equation 3.4

$$\text{BMI} = \frac{Weight}{(Height)^2}\left(\frac{\text{kg}}{m^2}\right) \qquad (3.4)$$

The results were tabulated and recorded with Microsoft Excel software 2013 version using a HP Elite Book core i5 laptop.

In calculating the BSA for each patient, Du Bois formula was used (equation 3.5). The data was fed into the computer and with the help of Microsoft excel, equation 3.5 was formulated and used in calculation

$$BSA = Weight^{0.425}(kg) \times Height^{0.725}(cm) \times 0.007184 \quad (3.5)$$

The results were tabulated and recorded in another Excel sheet for further analysis.

In calculating the BSI for each patient, the patient weight in kilograms (kg) was divided by the square root of the BSA as shown by equation 2.19

$$BSI = \frac{Weight}{\sqrt{BSA}} \left(\frac{kg}{m}\right) \quad (2.19)$$

The results were tabulated and recorded in another Excel sheet for further analysis.

Measurement of Dose Parameters

SSDE Measurements

In determining SSDE of each patient the materials used were axial CT images and MeVisLab software, since SSDE takes into consideration the size of the patient which is the lateral dimension and the anterior-posterior dimension.

In measuring the Lat dimension of the patient, the computer cursor was placed at left side of the axial image and an horizontal line was drawn to the right side of the image so that it divides the image into two equal halves as shown in Figure 27 labelled B. This was repeated three (3) times and data was fed into the computer and an excel code was developed and used in calculating the average measured value. The results were then tabulated.

In measuring the anterior-posterior (AP) dimension of the axial image, the cursor was placed at the anterior part of the image and a vertical line was drawn in such a way that it divides the image into left and right equal halves as shown in Figure 27 labelled C. This was repeated three (3) times. The measured values

were fed into the computer and an excel code was developed to calculate the average length. The results were tabulated.

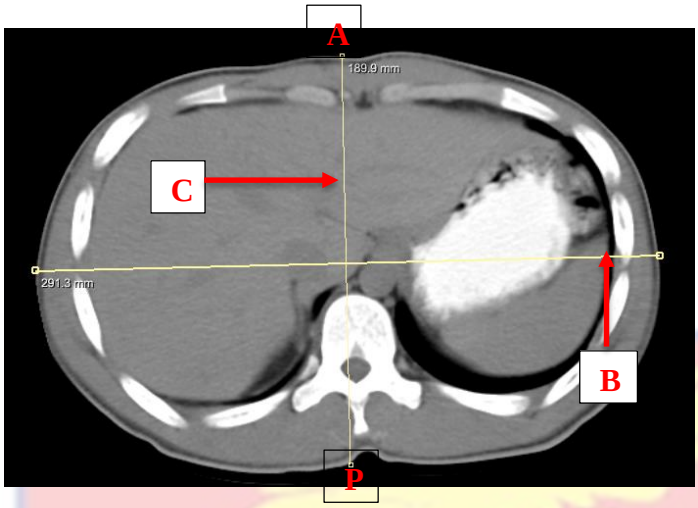

Figure 27: AP and Lat Measurements from Axial Images

The square root of the product of the Lat and AP lengths was calculated to obtain the effective diameter (EffD) as shown in equation 2.12

$$\text{EffD} = \sqrt{AP \times Lat} \tag{2.12}$$

The effective Diameter (EffD) obtained for each patient was used to calculate the size-dependent conversion factor f_B the patient from the equation 2.15

$$f_B = 3.704369 \times exp^{(-0.03671937 \times \text{EffD})} \tag{2.15}$$

The value of f_B obtained was used to calculate the SSDE using the equation 2.13

$$SSDE\ (mGy) = f_B \times CTDI_{vol} \tag{2.13}$$

where $CTDI_{vol}$ was obtained from patient and image information section of the CT images which were the first two (2) slices as shown in Figure 28

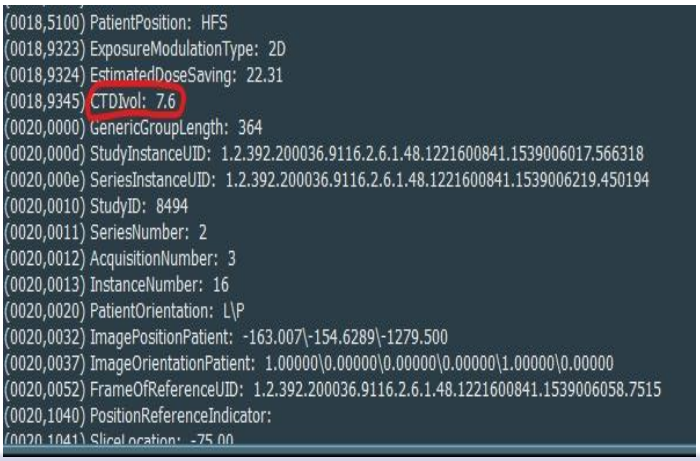

Figure 28: Image Information containing $CTDI_{vol}$ circled in Red.

Effective Dose (ED) Measurements

In calculating the ED to each patient, the DLP was multiplied to the estimated abdominal conversion factor as shown in equation 3.5. The abdominal conversion factor from ICRP publication 103 was 0.0153 (Shiraz, 2018).

$$\text{Hence the Effective Dose, } (\text{mSv}) = DLP \times 0.0153 \qquad (3.5)$$

The DLP was obtained from the patient and image information section of the CT images as circled in Figure 29. Using equation 3.5 an Excel formula was written to calculate ED, the results were recorded and tabulated using a different Excel sheet.

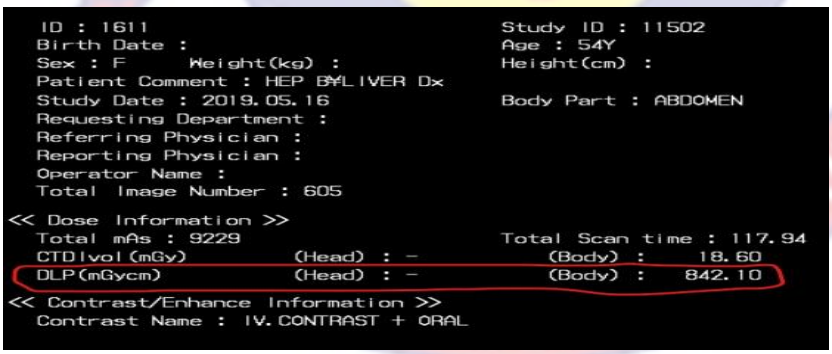

Figure 29: DLP for a Patient circled in Red.

Establishing a relationship between Liver Volume and Body Parameters (BSA, BSI, BMI)

In order to establish a relationship between the liver volume and body parameters, Statistical Package for the Social Sciences (SPSS) software version 26 was used. All measured and calculated parameters were categorized into gender variation (male and female). A graph of liver volume against BMI, liver volume against BSA, liver volume against BSI were plotted with the aid of the SPSS, a statistical linear regression analysis was performed with a confidence interval of 95 % to determine the mathematical relationship between the two variables (Dependable and Predictors).

Establishing a relationship between SNR, Exposure (mAs) and Peak Voltage (kVp)

In order to help Radiographers and also protect patient during CT examination, a graph of SNR against exposure (mAs) and peak voltage (kVp) was plotted using the Minitab software to obtain a regressional (model) equation. This equation would have the potential to help Radiographers to know the quality of the images for each patient before scanning.

Establishing a relationship between Effective Dose (ED), Exposure and Peak Voltage

In order to help Radiographers and also protect patient during CT examination, a graph of ED against mAs and kVp was plotted using the Minitab software to obtain a regressional (model) equation. This equation would have the potential to help Radiographers to know the dose to a patient before scanning.

Decision and Principle rule

In order to make a decision based on the analysis of the data for the various models, the decision rule and the conclusion hypothesis were used, that is, the null hypothesis was used. The null hypothesis simply states that there exists no relationship between the dependent and independent variables. To accept a model, the null hypothesis must be rejected, that is if the p-value is less than 5% significance level ($p < 0.05$) or fail to accept if otherwise. This means that when the p-value is less than 0.05, the model should be accepted.

Graphic User Interface (GUI)

In order to make the modelled equations user friendly, it would be written in C# code with a Graphic User Interface (GUI) for immediate visual feedback. GUI is a computer interface that makes a computer code easy to use by developing buttons, input and output interface.

Chapter Summary

In summary this chapter discussed relevant information about the materials and the methodology used to achieve the study objectives. The chapter also gave a vivid information about the various measuring procedures that were used to measure and process the primary data in order to successfully design the modelled equations.

CHAPTER FOUR

RESULTS AND DISCUSSION

This chapter presents results of experiment, analyses and discusses the graphs, tables with relevant scientific information. The results from this research is also discussed. It also establishes a relationship between the various calculated parameters to model equations. These equations were used to establish a computer code with a graphic user interface (GUI).

Presentation of Results

Calibration of MeVisLab Software

Table 7 shows the results from calibration of the MeVisLab software using the Wilke phantom. Using equation 3.1, the correction factor was calculated to be 1.00 for the two health facilities (SSC and CCTH). The AP, Lat lengths and the length of the liver in the midclavicular line measurements were all multiplied by the correction factor. This means the measured lengths were exactly the same as the actual lengths.

Table 7: Results of MeVisLab Software calibration using the Wilke Phantom

Centre	Actual length (cm)	Measured length (cm)			Mean Value	Correction factor
SSC	5.50	5.49	5.49	5.50	5.49 ± 0.01	1.00
CCTH	5.50	5.50	5.49	5.49	5.49 ± 0.01	1.00

Source: Field data

Results of calibration of Weight Scale

The weight scale was calibrated at the Balance Calibration Laboratory of the Ghana Standards Authority (GSA). The calibration certificate is presented in Appendices B and C. From the calibration, the maximum errors for both weight scales were 0.01 kg so this was used in all the weight measurements as the uncertainty.

Results of measured Body Parameters and Liver Volume

Appendix D shows all the primary body parameters recorded from the SSC and CCTH for liver volume analyses. The ages for each patient was recorded from the patient X-ray scan request forms. The height and weight parameters were measured using a digital weight scale and tape measure respectively. In all ninety-two (92) patients comprising of male and female were measured.

Table 8 shows the calculated body parameters from the measured primary body parameters; weight and height. Values from the measured parameters were used to evaluate the BSA, BMI and BSI of each patient.

It also shows the measured liver length in the mid clavicular line and the liver volume of each patient. These calculated body parameters were obtained from equations 2.19, 3.4 and 3.5.

The number of male and female patients used for this study were 39 and 53 respectively. From table 8, the median ages for male and female were 44 and 52 years respectively. The median heights for male and female was 1.69 and 1.61 cm respectively. The median weights for male and female was 71.4 and 73.3 kg respectively. The median BMIs for male and female was 24.78 and 28.29 kg/m^2 respectively. The median BSAs for male and female was 1.77 and 1.76 m^2 respectively. The median BSIs for male and female was 53.14 and 55.03 kg/m respectively. The median liver volumes for male and female was 1.252 and 1.329 L respectively.

Table 8: Calculated Body Parameters from the Measured Primary Body Parameters of Each Patient

Patient	Age (years)	Height (m)	Weight (kg)	BMI (kg/m^2)	BSA (m^2)	BSI (kg/m)	Mid clavicular line	Volume (l)
1	44	1.62	50.5	19.24	1.52	40.95	0.17	2.86
2	44	1.68	93.5	33.13	2.03	65.64	0.16	1.54
3	64	1.59	52.3	20.69	1.52	42.38	0.14	1.59
4	45	1.76	77.8	25.12	1.94	55.84	0.14	1.83
5	41	1.66	63.7	23.12	1.71	48.73	0.13	1.38
6	49	1.64	109.2	40.60	2.13	74.82	0.12	0.58
7	56	1.60	64.2	25.08	1.67	49.69	0.18	0.76
8	69	1.56	77.2	31.72	1.77	57.98	0.14	1.54
9	42	1.72	61.4	20.75	1.73	46.73	0.15	2.37
10	81	1.55	64.9	27.01	1.64	50.69	0.17	1.19
11	48	1.66	99.5	36.11	2.07	69.23	0.19	2.34
12	62	1.79	82.9	25.87	2.02	58.35	0.22	1.66
13	65	1.30	68.4	40.47	1.46	56.31	0.16	1.59
14	49	1.58	46.2	18.51	1.44	38.52	0.20	0.81
15	49	1.56	88.6	36.41	1.88	64.63	0.16	1.07
16	32	1.39	71.4	36.95	1.58	56.85	0.17	1.50
17	55	1.65	86.8	31.88	1.94	62.31	0.18	1.11
18	66	1.59	89.3	35.32	1.91	64.58	0.20	1.09
19	50	1.72	72.3	24.44	1.85	53.15	0.14	1.07
20	55	1.74	51.5	17.01	1.62	40.52	0.14	1.44
21	85	1.74	71.9	23.75	1.86	52.70	0.14	1.52
22	37	1.05	81.7	74.10	1.36	69.99	0.17	0.85
23	60	1.46	84.5	39.64	1.76	63.77	0.14	1.15
24	58	1.67	54.5	19.54	1.61	43.00	0.17	1.41
25	57	1.61	69.9	26.97	1.74	53.01	0.15	0.82
26	29	1.76	110.9	35.80	2.26	73.82	0.15	1.11
27	43	1.62	84.9	32.35	1.90	61.64	0.16	1.26
28	50	1.61	58.2	22.45	1.61	45.89	0.13	0.93
29	55	1.70	58.5	20.24	1.68	45.18	0.16	1.10

Table 8 continued

30	66	1.71	62.4	21.34	1.73	47.43	0.12	2.07
31	44	1.62	93.8	35.74	1.98	66.68	0.17	1.12
32	49	1.62	68.0	25.91	1.73	51.76	0.16	1.97
33	35	1.56	41.7	17.14	1.36	35.70	0.14	0.84
34	56	1.61	58.0	22.38	1.61	45.77	0.16	1.14
35	38	1.63	95.0	35.76	2.00	67.20	0.17	1.54
37	42	1.70	52.4	18.13	1.60	41.42	0.13	0.88
38	53	1.60	93.4	36.48	1.96	66.75	0.15	1.53
39	61	1.69	56.1	19.64	1.64	43.80	0.13	1.18
40	60	1.61	73.3	28.28	1.77	55.03	0.17	1.52
41	56	1.58	90.0	36.05	1.91	65.13	0.17	1.47
42	68	1.67	68.5	24.56	1.77	51.49	0.13	1.07
43	45	1.63	82.0	30.86	1.88	59.84	0.13	1.29
44	45	1.63	72.1	27.14	1.78	54.08	0.20	2.27
45	73	1.63	74.9	28.19	1.81	55.73	0.13	0.92
46	52	1.50	80.9	35.96	1.76	61.02	0.17	1.39
47	49	1.69	98.6	34.52	2.08	68.29	0.18	1.96
48	72	1.62	98.3	37.46	2.02	69.18	0.16	1.46
49	53	1.74	93.9	31.01	2.09	65.03	0.15	1.63
50	34	1.69	76.9	26.92	1.86	56.15	0.14	1.16
51	33	1.61	72.1	27.82	1.76	54.32	0.15	1.21
52	85	1.59	55.0	21.76	1.56	44.09	0.12	1.04
53	51	1.54	79.0	33.31	1.77	59.32	0.16	1.87
54	42	1.62	55.1	21.00	1.58	43.86	0.20	1.98
55	18	1.41	37.7	18.96	1.21	34.21	0.22	1.41
56	45	1.70	71.2	24.64	1.82	52.74	0.11	1.11
57	73	1.74	81.8	27.02	1.97	58.33	0.16	1.04
58	42	1.75	86.5	28.24	2.02	60.83	0.18	1.49
59	55	1.31	49.0	28.55	1.29	43.19	0.23	0.99
60	67	1.32	79.3	45.51	1.59	62.92	0.15	1.06
61	75	1.33	94.5	53.42	1.72	72.04	0.16	1.57

Table 8 continued

62	79	1.63	75.1	28.27	1.81	55.84	0.14	1.33
63	27	1.57	43.7	17.73	1.40	36.96	0.15	1.29
64	24	1.74	59.9	19.78	1.72	45.64	0.15	1.22
65	79	1.60	50.8	19.97	1.51	41.37	0.13	0.77
66	73	1.56	64.9	26.67	1.65	50.58	0.16	1.23
67	43	1.61	64.6	25.08	1.68	49.88	0.20	2.15
68	40	1.67	66.4	23.95	1.74	50.29	0.17	1.18
69	24	1.46	78.5	37.08	1.70	60.25	0.16	1.16
70	38	1.65	70.3	25.98	1.77	52.84	0.17	1.33
71	56	1.54	58.4	24.62	1.56	46.76	0.17	1.88
72	22	1.67	73.8	26.62	1.82	54.66	0.15	1.00
73	78	1.60	71.7	28.18	1.75	54.27	0.17	1.34
74	54	1.62	60.2	23.08	1.64	47.07	0.14	2.20
75	39	1.72	73.3	24.78	1.86	53.73	0.19	1.28
76	19	1.71	60.7	20.88	1.71	46.46	0.14	1.04
77	25	1.81	80.7	24.77	2.01	56.95	0.15	1.86
78	39	1.60	61.9	24.33	1.64	48.34	0.15	1.31
79	34	1.74	71.2	23.52	1.85	52.29	0.14	1.30
80	48	1.61	58.2	22.59	1.60	45.94	0.19	1.30
81	42	1.64	65.0	24.32	1.70	49.78	0.14	1.34
82	44	1.93	85.4	23.05	2.16	58.17	0.14	1.21
83	40	1.68	82.4	29.37	1.92	59.48	0.16	1.17
84	44	1.77	79.9	25.65	1.97	56.97	0.15	1.20
85	70	1.59	39.1	15.56	1.34	33.74	0.12	1.11
86	67	1.65	76.2	28.16	1.83	56.30	0.15	1.38
87	62	1.66	86.3	31.51	1.94	61.96	0.22	1.48
88	36	1.83	73.4	22.04	1.94	52.64	0.16	1.32
89	37	1.74	77.2	25.65	1.91	55.79	0.18	1.21
90	74	1.67	71.3	25.57	1.80	53.14	0.13	1.25
91	35	1.54	76.5	32.38	1.75	57.88	0.13	1.36
92	32	1.35	89.3	48.93	1.70	68.51	0.17	1.26

Source: Field data, 2018

Table 9 shows a summary of the measured body parameters of males and females in terms of mean, maximum and minimum variations.

Table 9: Summary of Measured and Calculated Body Parameters

Sex	measure	Age (yrs)	Weight (kg)	Height (m)	BMI (kg/m^2)	BSA (m^2)	BSI (kg/m)
Male	Max	79.00	110.90	1.93	74.10	2.26	73.82
	Min	19.00	50.80	1.05	17.01	1.36	40.52
	Mean	47.92	72.43	1.66	27.18	1.80	53.88
Female	Max	85.00	109.20	1.74	53.42	2.13	74.82
	Min	18.00	37.70	1.30	15.56	1.21	33.74
	Mean	52.83	72.61	1.59	29.10	1.74	54.67

Source: Field Data, 2018

The average ages for this study was 47.92 ± 30.29 and 52.83 ± 32.15 years for male and female, respectively. The maximum and minimum age for the males was 79 and 19 years with 85 and 18 years being the maximum and minimum age for the females. This indicates that females used for this study were must older than that of the males.

The average heights for this study for males and females was 1.66 ± 0.29 and 1.59 ± 0.20 m respectively. The maximum heights for male and female was 1.93 and 1.74 m respectively whereas the minimum height for male and female was also 1.05 and 1.30 m, respectively. This indicates that the males used for this study had higher height than that of the females.

The average weights for this study for male and female was 72.43 ± 27.05 and 72.61 ± 34.12 kg respectively. The maximum weights for this study for male and female are 110.90 and 109.20 kg respectively. The minimum weights for this study for male and female was 50.80 and 37.70 kg, respectively. This indicates that the females, for this study were slightly heavier than the males.

For the male patients, 2 % were underweight, 49 % were within the normal weight range 28 % were overweight and about 21 % were obese. For the female patients 7 % were underweight, 26 % were within the normal weight range, 25 % were overweight and 42 % were obese.

The average BMIs for this study for male and female was 27.18 ± 19.64 and 29.10 ± 15.56 kg/m^2. The maximum BMI for this study for male and female are. 74.10 kg/m^2 and 53.42 kg/m^2 respectively. The minimum BMIs for this study for male and female are 17.01 and 15.56 kg/m^2, respectively. This indicates that that average both sexes were obese but the female patients were more obese.

The mean BSAs for this study for male and female was 1.80 ± 0.38 and 1.74 ± 0.42 m^2, respectively. This means the body surface of the male patients used for this study were broader than the female patients. The maximum BSA for this study for male and female are 2.26 and 2.13 m^2, respectively. The minimum BSAs for male and female are 1.36 and 1.21 m^2, respectively.

The mean BSIs for this study for male and female are 53.88 ± 16.38 and 54.67 ± 20.45 kg/m as shown in Figure 35, respectively. This means the female patients were heavier in weight than the males when you compare their weight to their body surface area. The maximum BSIs for this study for male and female are 73.82 and 74.82 kg/m respectively. The minimum BSI for this study for male and female are 40.52 and 33.74 kg/m, respectively.

Table 10 compares the mean measured and calculated body parameters with that of other studies. It indicates that the calculated values for this study, that is; BMI, BSA and BSI were different from the studies by International Commission on Radiological Protection (ICRP). Studies done by International Atomic Energy Agency (IAEA) and International Commission Radiological Protection (IAEA**,** 1993; ICRP, 2012) on basic human body parameters for Asian

and European study population respectively showed that these two different races produced two completely different body parameters, so it is expected that this study (Ghanaian Adults-African race) would also produce different body parameters.

The age range for the men in this study and that of the ICRP – European population were similar but that of the ICRP was very short (ie from 20-50), but for the female, the age range for the ICRP-Asian and European were similar (20-50 years) but that of this study was larger.

For the weight, the ICRP- European males were heavier than that of the males for this study and the ICRP- Asian males. The females for this study were heavier than that of the ICRP –Asian and ICRP-European study.

For the height, the males for this study were shorter than the two other studies, the Asian study were the tallest. For the females, those of this study were also the shortest with that of the European study been the tallest.

With the BMI, the males for this study were obese while that of the other two studies were in the normal range. The female population for this study were also obese compared to the other two studies. This means that for this study both sexes had a lot of fat in their body.

With the BSA, the male population for the European population had the highest body area, which means that the males were broader than that of the other two populations. With the female populations, the females from this study had the highest BSA value, this means they were much broader than that of the other two study populations.

The male population for this study had the highest BSI compared to the other two populations which means that they were heavier when you compare their weight to their body surface area. The female for this study also had the

highest BSI compared to the other two study. Which also indicates that they were heavier when you compare their weight to their body surface area.

Table 10: A Comparison of the Average Measured Ghanaian Adult body Parameters from this Study with Asian and Caucasian Adult

Parameter	This study (2019)	ICRP-Asian (1998)	ICRP-European (2015)
Male			
Age (years)	47.92(19-79)	35(20-50)	42(20-80)
Race	African	Mongoloid	Caucasoid
Weight (kg)	72.43	60.00	76.00
Height (m)	1.66	1.70	1.79
BMI (kg/m^2)	27.18	22.00	24.00
BSA (m^2)	1.80	1.78	1.95
BSI (kg/m)	53. 88	33.71	38.95
Female			
Age (years)	52.83(18-85)	35.00(20-50)	42.00(20-50)
Race	African	Mongoloid	Caucasoid
Weight (kg)	72.61	51.00	63.00
Height (m)	1.59	1.60	1.65
BMI (kg/m^2)	29.10	22.00	23.00
BSA (m^2)	1.74	1.55	1.67
BSI (kg/m)	54.67	32.90	35.20

Source: Field Data 2020; Shiraz, 2018

Table 11 shows the summary of the calculated values for the volume and length of liver in the mid-clavicular line in terms of gender. The mean liver volumes for this study for male and female was 1.356 ± 0.744 and 1.363 ± 0.845 L respectively. The maximum liver volumes for this study for male and female was 2.371 and 2.864 L, respectively. The minimum liver volumes for this study for male and female are 0.763 and 0.584 L respectively. The female liver was slightly larger than that of the male by 0.007 L.

Table 11: Results of Liver Volume and Length of Liver in the Midclavicular line

Sex	measure	V_L (L)	Midclavicular line (cm)
Male	Min	0.763	11.0
	Max	2.371	22.0
	Mean	1.356	15.7
Female	Min	0.584	12.0
	Max	2.864	23.0
	Mean	1.363	15.9

Source: Field Data, 2020

It also indicates that the length of liver in the midclavicular line (or as commonly known as the span of the liver) for females was slightly higher by 0.2 cm than that of males. This was also expected as the mean female liver volume was larger than that of the males.

Table 12 compares the calculated liver volume to the study performed by ICRP. The population used for the ICRP study were of European decent (ICRP, 2002).

Table 12: Comparison of Liver Volume from this Study with International values

Gender	This study (L)	ICRP (2002) (L)
Male	1.356	1.714
Female	1.363	1.333

Source: ICRP (2002)

Research studies performed by Chouker et al and Wolf (Choukèr et al., 2004; Wolf, 1990) show that the female liver size is normally smaller in size than that of males but results from this study indicates otherwise. This abnormally was

explained by the fact that 49 % of the female patients used were obese and studies by Grante et al (Grant et al., 2020) indicates that obese persons tend to have liver sizes about 50 - 100 % larger than persons with normal BMI. This means that the volume of the liver for females if they were of normal BMI was expected to be smaller than 1.356 L (male liver volume). This also explains why the length of the liver in the midclavicular line was longer in females than in males.

Table 12 also indicates that the results from this study was not similar from that of (ICRP, 2002). Studies by Govender and his colleagues explain this findings (Govender et al., 2017). Their study indicates that organ mass is influenced by several demographic parameters and environmental conditions such as food, altitude and they differ among populations. Since volume is a function of mass, it presupposes that it is also influenced by these same factors.

Establishing a relationship between Liver Volume and Body Parameters

In order to establish a relationship between the volume and the body parameters. IBM SPSS statistical tool was used. The SPSS parameter used to explain the models was the correlation coefficient R between the dependent and independent (predictors) variables. It indicates whether there was a good relationship between the two (2) variables. The second parameter used was the coefficient of determination, which was the adjusted R square, it indicated the total variation in the dependent variable as explained by predictors (independent variable). The third parameter used was the p-value, which was the probability of obtaining test results at least as extreme as the results actually observed, under the assumption that the null hypothesis was correct.

Model relationship between Liver Volume and BMI

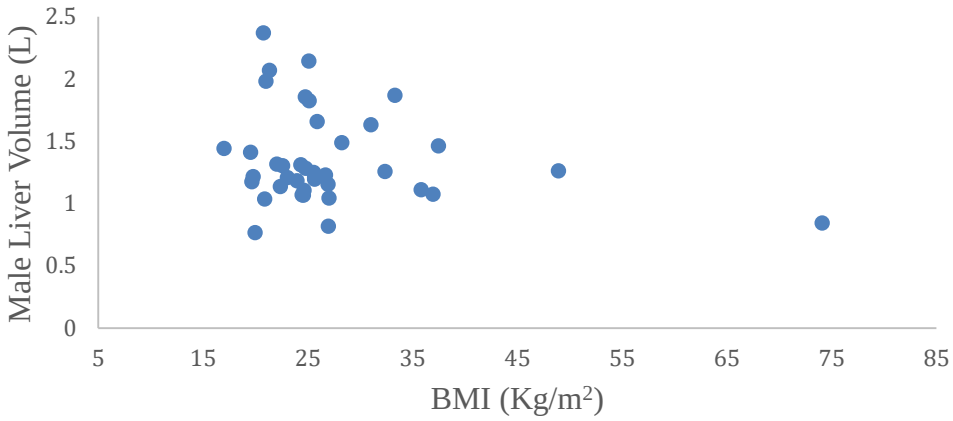

Figure 30: Male Liver Volume against BMI

Table 13: Model Summary of Graph of Male Liver Volume against BMI using SPSS

Model	R	R Square	Adjusted R Square	P-value
1	0.226[a]	0.051	0.025	0.167

Model equation

Liver volume (male) = 1.589 - 0.009 × BMI

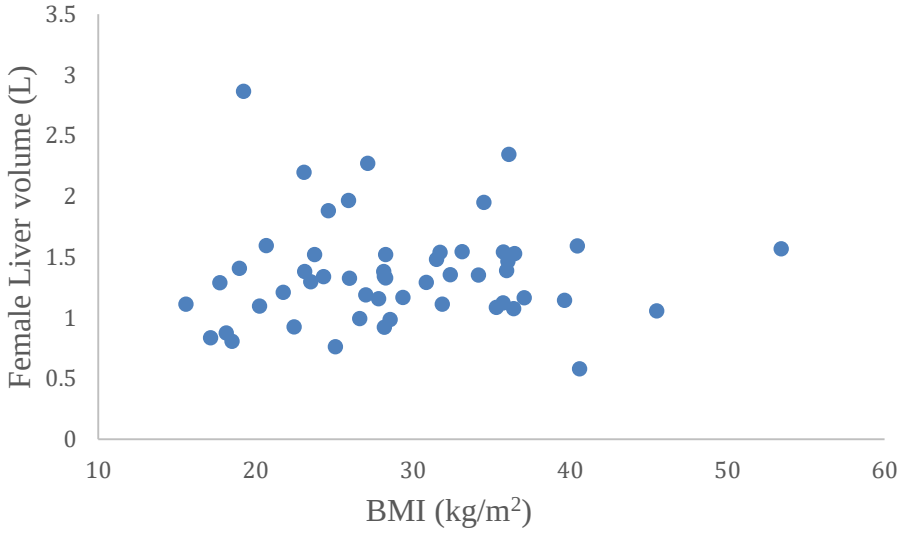

Figure 31: Female liver volume against BMI

Table 14: Model Summary of Graph of Female Liver Volume against BMI using SPSS

Model	R	R Square	Adjusted R Square	P-value
1	0.013[a]	.000	0.019	0.928

Model equation
Liver volume (female) = 1.343 + 0.001 × BMI

Model relationship between Liver Volume and BSA

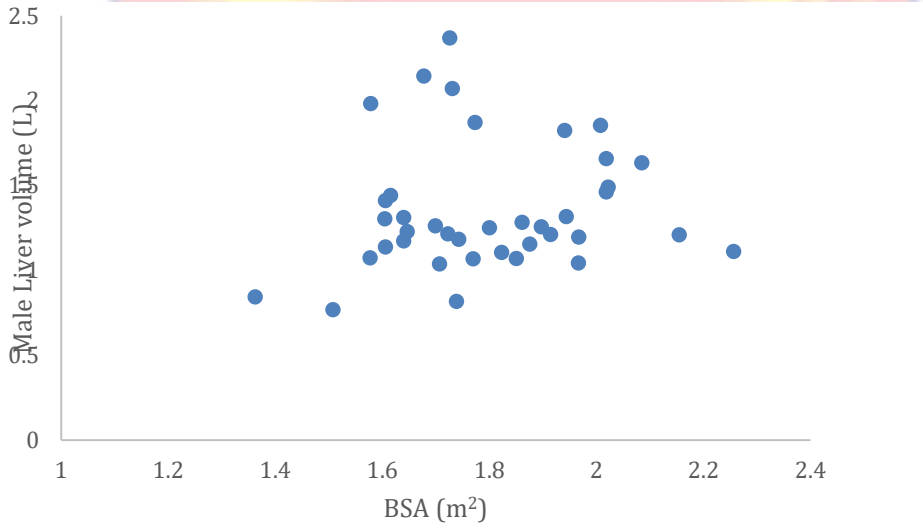

Figure 32: Male Liver Volume against BSA

Table 15: Model Summary of Graph of Male Liver Volume against BSA using SPSS

Model	R	R Square	Adjusted R Square	P-values
1	0.119[a]	0.014	0.012	0.470

Model equation
Liver volume (male) = 0.940 + 0.232 × BSA

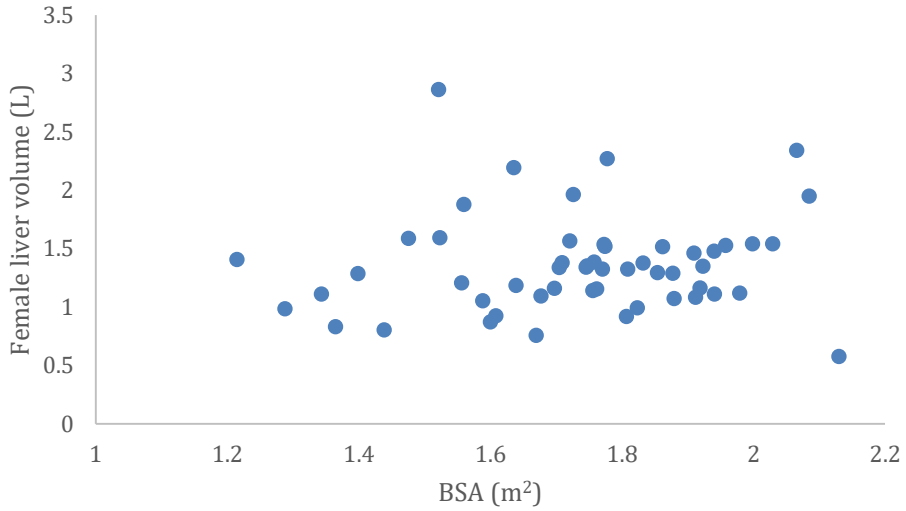

Figure 33: Female Liver Volume against BSA

Table 16: Model Summary of Graph of Female Liver Volume against BSA using SPSS

Model	R	R Square	Adjusted R Square	P-value
1	0.094[a]	0.009	0.011	0.503

Model equation

Liver volume (female) = 1.031 + 0.191×BSA

Model relationship between Liver Volume and BSI

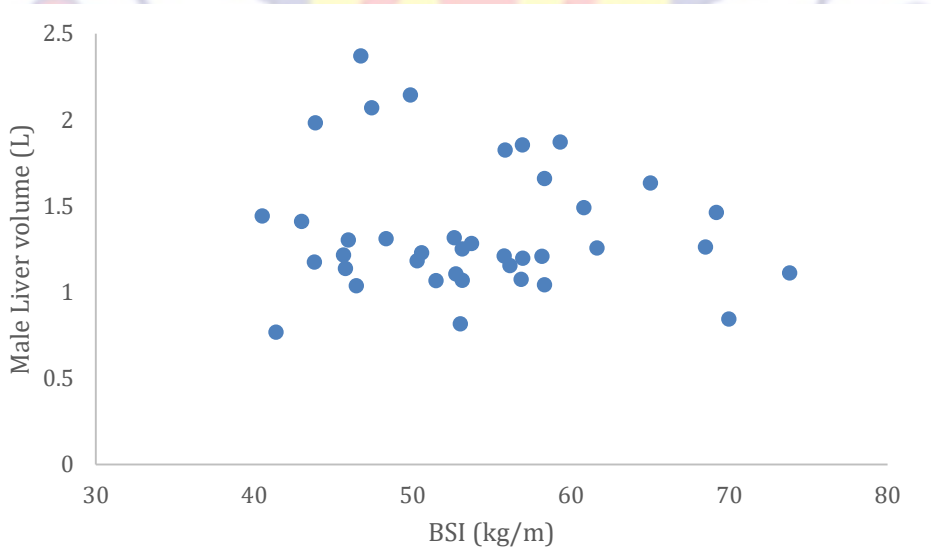

Figure 34: Male Liver Volume against BSI

Table 17: Model Summary of Graph of Male Liver volume against BSI using SPSS

Model	R	R Square	Adjusted R Square	P-value
1	0.105[a]	0.011	0.016	0.525

Model equation
Liver volume (male) = 1.613 - 0.005 × BSI

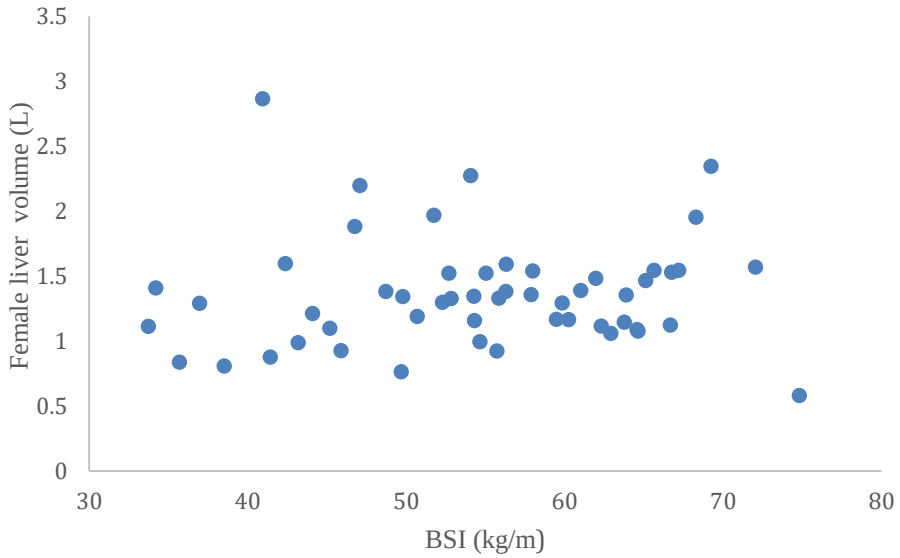

Figure 35: Female Liver Volume against BSI

Table 18: Model Summary of Graph of Female Liver Volume against BSI using SPSS

Model	R	R Square	Adjusted R Square	P-value
1	0.055[a]	0.003	-0.016	0.694

Model equation
Liver volume (female) = 1.238 + 0.002 × BSI

Figures 30 to 35 represent the scatter graphs of liver volume against body parameters. It was observed that none of the graphs represented any particular pattern and had no correlation, this might be as a result of the same sample size used which really did not bring out a correlation or a particular pattern

Tables 13 to 18 give the summary of the graphs. It was observed that there exist a weak correlation coefficient (R) for all the graphs with the highest being 0.2. It

was also observed that the values of the coefficient of determination (adjusted R^2) was 0.003 which is very low. The highest adjusted R^2 value recorded was 0.02 % and this was the graph between male liver volume and BMI, this value is very low, a good adjusted R^2 should have a value of 60 % and above. This means that for this study the calculated body parameters could not be used to predict the volume of the liver in adult Ghanaians. This could be attributed to the fact that most of the patients used were obese and hence did not have a regular liver volume as described in studies by Grante et al (Grante et al., 2020).

It was also observed that all the P-values from the regressions tables (tables 13 to 18) exceeded 0.05. This indicates it failed to reject the null hypothesis. The results were not significant and there existed no relationship between the liver volume and the calculated body parameters.

Dose Assessment

Tables 19-21, represent the measured $CTDI_{vol}$, DLP, AP and Lat lengths obtained from the various health facilities. $CTDI_{vol}$ and DLP values were obtained from the image information section of each image series, while the AP and Lat dimensions were measured from the axial CT images. The SSDE and ED were calculated from their respective equations.

Table 19: Dose and Body Parameters Measured and Calculated from the KBTH

AP (cm)	Lat (cm)	DLP (mGy.cm)	$CTDI_{vol}$ (mGy)	SSDE (mGy)	ED (mSv)
21.39	28.69	597.60	5.50	8.20	9.14
21.68	32.74	1065.60	7.10	9.88	16.30
23.53	34.22	852.90	6.20	8.10	13.05
26.46	35.02	1215.90	8.10	9.81	18.60
21.63	30.18	987.00	5.70	8.26	15.10
33.86	31.12	1331.10	7.70	8.66	20.37
25.33	31.00	1026.30	5.70	7.54	15.70
18.00	26.28	754.80	4.80	7.99	11.55
15.51	25.52	910.80	4.90	8.74	13.94
19.19	29.32	859.20	5.30	8.21	13.15
25.16	31.22	294.90	5.50	7.28	4.51
29.27	36.49	2634.90	16.00	17.84	40.31
21.10	34.42	825.90	5.70	7.84	12.64
20.83	36.07	364.80	13.50	18.27	5.58
25.30	31.51	286.30	6.20	8.14	4.38
21.58	31.11	825.90	5.60	8.01	12.64
25.95	37.84	2794.40	12.30	14.41	42.75
20.74	24.21	703.40	4.70	7.64	10.76
25.25	33.89	942.60	5.30	6.70	14.42
20.39	33.98	850.20	5.60	7.89	13.01
15.08	33.11	1311.50	4.70	7.66	20.07
29.23	34.58	1538.40	7.70	8.87	23.54
15.41	26.17	694.30	4.70	8.32	10.62
17.01	27.06	794.10	4.70	7.91	12.15
18.28	24.03	937.60	4.70	8.06	14.35
19.26	28.76	1174.40	5.10	7.96	17.97
17.38	25.95	759.00	4.70	7.98	11.61

Table 19 continued

24.60	35.34	1389.00	9.20	11.54	21.25
26.30	31.46	855.30	5.50	7.08	13.09
21.86	33.69	314.20	5.60	7.65	4.81
14.78	22.94	246.00	4.70	8.85	3.76
16.08	27.20	744.00	4.90	8.42	11.38
20.16	27.13	912.40	5.00	7.84	13.96
28.32	30.53	1431.90	8.70	10.94	21.91
19.73	31.49	745.20	4.90	7.26	11.40
25.47	32.82	1128.00	6.70	8.58	17.26
20.93	34.68	1283.20	5.20	7.16	19.63
17.38	27.2	793.80	4.90	8.16	12.15
25.56	37.7	2127.20	9.70	11.49	32.55
17.51	27.26	682.80	3.00	4.98	10.45
28.94	32.19	1275.80	7.10	8.57	19.52
15.47	25.93	911.40	4.70	8.34	13.94
24.38	28.07	549.60	5.30	7.51	8.41
20.43	29.01	913.50	5.20	7.71	13.98
23.79	34.93	1233.60	7.10	9.12	18.87
19.92	26.48	757.20	4.90	7.80	11.59
16.42	23.73	808.50	4.90	8.79	12.37
28.37	34.95	1537.50	9.20	10.72	23.52
18.90	25.62	269.50	4.90	9.75	4.12
21.21	28.62	682.80	9.20	8.87	15.08

Source: Field Data, 2020

Table 20: Dose and Body Parameters Measured and Calculated from the SSC

AP (cm)	Lat (cm)	DLP (mGy.cm)	$CTDI_{vol}$ (mGy)	SSDE (mGy)	ED (mSv)
18.48	25.58	817.20	7.60	37.98	12.50
32.58	34.91	2514.90	20.70	66.64	38.48
19.59	30.98	1135.30	14.80	66.52	17.37
23.59	31.39	1261.90	11.80	48.25	19.31
22.73	29.76	1201.50	13.10	55.98	18.38
31.22	38.54	2470.50	19.00	59.05	37.80
20.58	30.65	1007.70	12.07	53.29	15.42
22.95	36.68	1234.00	12.47	47.71	18.88
17.70	28.44	757.80	6.90	33.62	11.59
29.02	37.96	1886.80	20.70	67.97	28.87
28.27	38.61	2714.80	20.70	68.35	41.54
23.12	31.94	463.20	4.60	18.83	7.09
18.48	25.58	1072.20	9.00	12.72	16.40
32.58	34.91	1009.80	6.90	29.59	15.45
19.59	30.98	2452.50	20.70	77.01	37.52
23.59	31.39	1440.60	4.13	18.18	22.04
26.00	37.66	3291.60	27.60	97.16	50.36
28.85	38.50	1563.00	13.80	45.08	23.91
19.78	33.68	1256.40	10.40	44.77	19.22
18.82	26.16	848.10	6.20	30.48	12.98
22.46	35.51	922.40	9.20	36.22	14.11
21.67	35.82	1616.40	12.40	49.51	24.73
30.98	36.99	3233.20	27.60	88.45	49.47
21.28	26.82	827.10	7.60	35.10	12.65
22.78	34.24	1237.20	12.40	49.39	18.93
27.29	37.59	3144.00	20.70	70.93	48.10
26.61	37.97	693.20	18.43	63.72	10.61

Table 20 continued

20.92	25.96	299.00	9.70	15.26	4.57
22.22	31.39	1204.50	9.00	37.90	18.43
21.43	44.13	2550.90	19.00	68.22	39.03
24.64	30.76	1239.70	15.90	64.26	18.97
17.35	26.15	706.80	5.50	27.94	10.81
19.80	29.04	884.40	7.60	34.99	13.53
23.04	38.03	3027.90	20.70	77.53	46.33
27.70	38.68	2476.20	20.70	69.12	37.89
17.55	26.14	986.10	9.00	45.52	15.09
24.61	39.02	2559.70	19.00	67.63	39.16
19.24	29.82	3176.40	20.70	95.39	48.60
19.67	31.52	2209.20	20.70	92.14	33.80
21.22	38.91	3851.20	27.60	106.72	58.92
22.98	30.75	998.40	9.70	40.59	15.28
21.55	32.65	2416.50	17.30	72.54	36.97
21.59	37.21	1359.60	13.10	51.38	20.80
19.56	33.17	1446.50	13.80	60.15	22.13
28.29	35.92	3238.80	20.70	71.32	49.55
24.61	33.87	2342.70	20.70	79.64	35.84
29.22	35.91	2525.10	20.70	69.98	38.63
23.98	36.21	2665.20	20.70	77.92	40.78
19.84	35.39	926.70	8.30	34.84	14.18

Source: Field Data, 2020

Table 21: Dose Parameters Measured and Calculated from the CCTH

AP (cm)	Lateral (cm)	DLP (mGy.cm)	$CTDI_{vol}$ (mGy)	SSDE (mGy)	ED (mSv)
29.11	28.66	2776.30	26.6	34.10	41.64
18.73	29.70	2395.80	26.6	41.42	35.94
18.01	27.90	6522.00	26.6	43.23	97.83
19.63	27.47	2635.40	26.6	41.97	39.53
21.37	28.16	10292.20	24.5	36.84	154.38
24.66	31.77	5245.00	25.6	33.91	78.68
18.07	28.42	3327.50	26.6	42.84	49.91
17.86	26.04	5009.40	24.5	41.08	75.14
24.34	33.40	5914.40	24.5	31.84	88.72
18.43	27.83	3433.90	79.8	128.60	52.54
20.81	28.32	2395.80	53.2	80.76	36.66
24.55	30.28	2662.00	53.2	72.37	40.73
22.88	33.18	3673.50	79.8	107.41	56.20
21.80	28.07	2608.80	53.2	79.40	39.91
15.67	25.33	2422.40	53.2	94.75	37.06
14.65	24.45	3256.60	53.8	99.39	49.83
25.6	31.10	2894.30	55.6	73.04	44.28
28.45	32.14	5753.70	212.4	259.06	88.03
26.17	30.47	3156.40	54.3	71.27	48.29
21.03	31.48	3833.30	79.8	114.84	58.65
17.29	25.55	2395.80	53.20	91.02	36.66
21.00	27.53	2532.40	54.01	82.69	38.75
22.68	32.86	2941.60	56.84	77.22	45.01
15.76	27.93	2223.80	54.25	92.94	34.02
28.76	32.31	3186.98	56.35	68.11	48.76
19.87	25.90	2608.49	54.81	88.20	39.91
26.89	35.91	3589.52	51.41	60.81	54.92
18.66	27.90	2587.90	52.55	84.16	39.59

Table 21 continued

28.90	32.74	2189.70	54.99	65.80	33.50
26.77	32.74	3637.70	53.85	67.22	55.66
28.84	34.74	3186.20	54.76	63.41	48.75
29.64	35.96	2753.10	50.62	56.52	42.12
29.21	28.33	3527.30	53.67	69.09	53.97
19.58	27.42	2285.90	51.88	82.01	34.97
17.91	27.47	2686.40	53.85	88.28	41.10
24.66	31.77	5245.30	54.32	71.95	80.25
18.07	28.42	3327.50	52.85	85.12	50.91

Source: Field Data, 2020

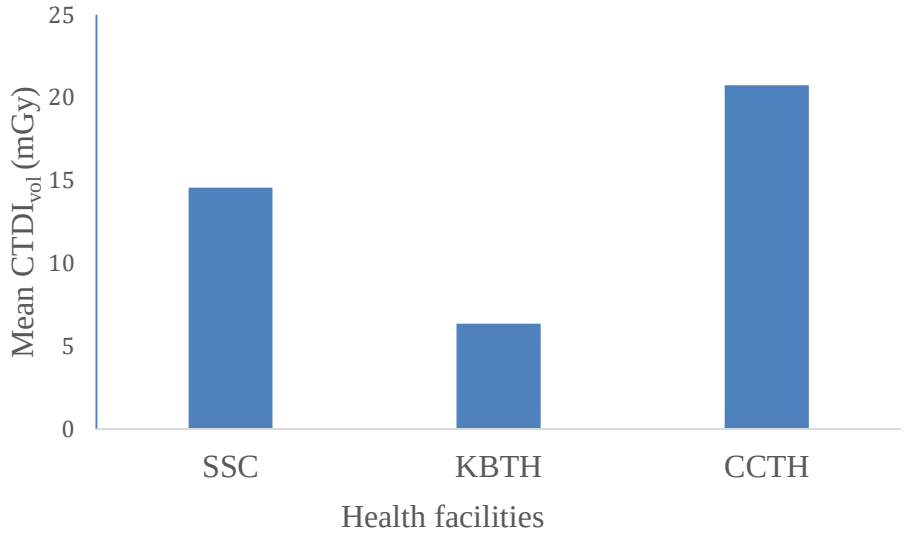

Figure 36: Mean $CTDI_{vol}$ for the three Health Facilities

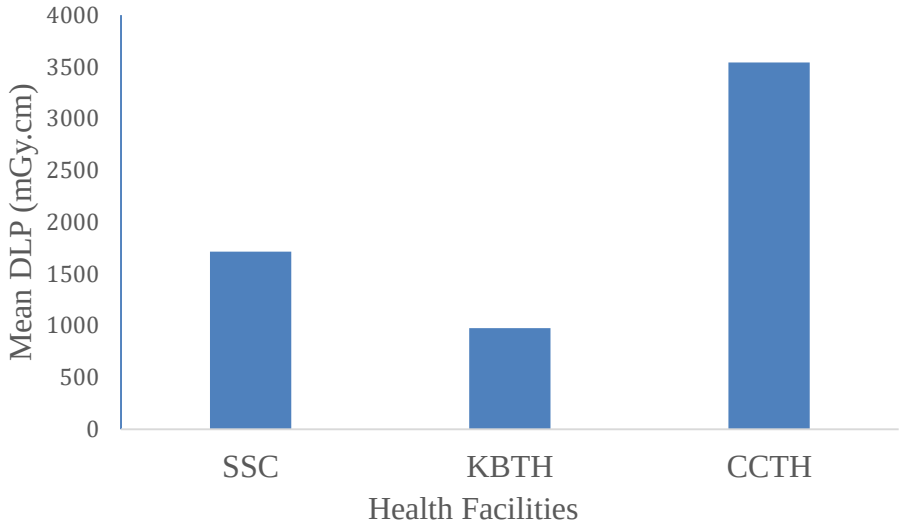

Figure 37: Mean DLP for the three Health Facilities

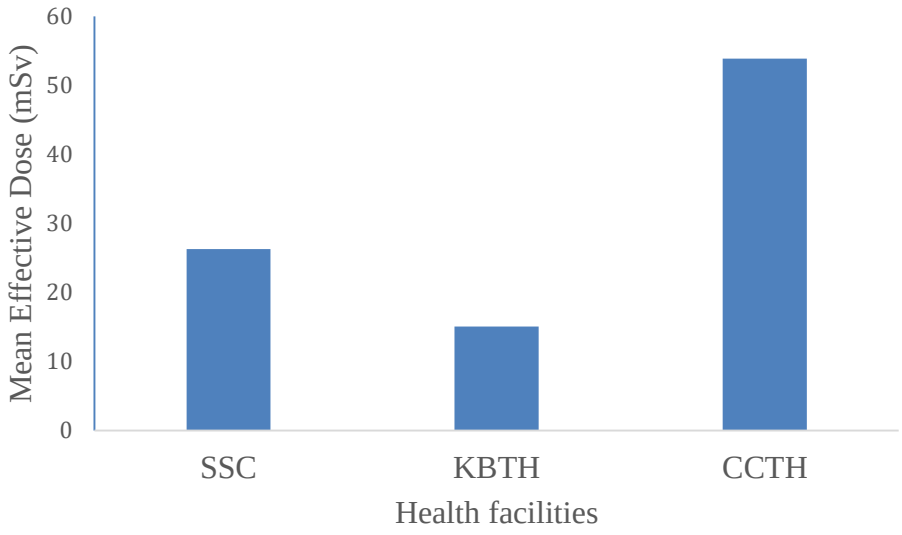

Figure 38: Mean Effective Dose (ED) for the three Health Facilities

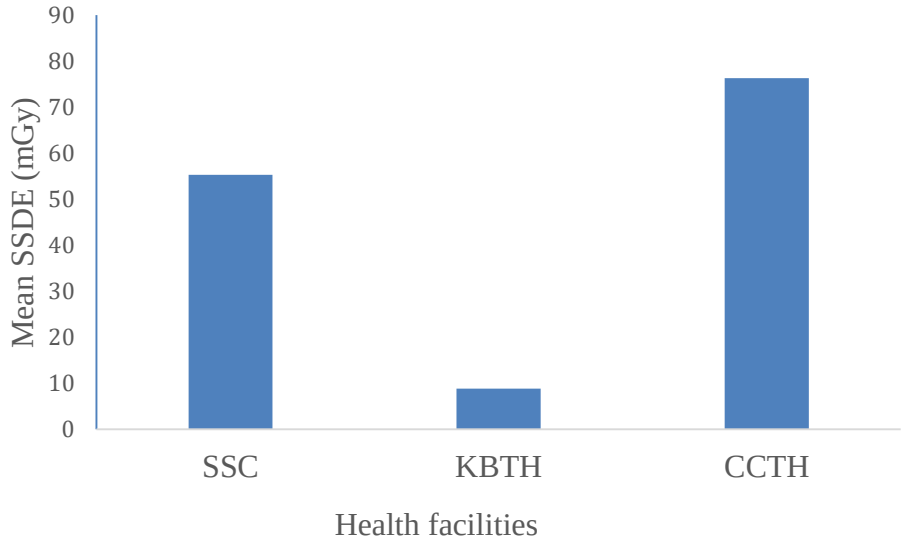

Figure 39: Mean SSDE for the three Health Facilities

Figures 36 to 39 show histograms which represent the mean dose parameters measured and calculated from the various health facilities. The measured parameters were AP, lateral, $CTDI_{vol,}$ and DLP. The calculated parameters were SSDE and ED. These graphs indicate that patients from the Korle-Bu Teaching Hospital were less exposed to radiation than all the other two (2) health facilities. This means the patients from SSC and CCTH were exposed by an extra radiation of 11.21 mSv and 38.8 mSv respectively.

Appendices E to P show charts which represent the variations in dose parameters measured and calculated from the various health facilities. Table 22 represents a statistical summary of the dose parameters measured and calculated from the various health facilities in terms of minimum (min), maximum (max) and mean values.

Table 22: Statistical Summary of the Dose Parameters Measured and Calculated

	Statistics	$CTDI_{vol}$ (mGy)	DLP mGy.cm	ED (mSv)	SSDE (mGy)
Supreme Specialist Center (SSC)	Min	4.13	299.00	4.57	12.71
	Max	27.60	3851.2	58.92	106.72
	Mean	14.56	1717.16	26.27	55.29
Korle Bu Teaching Hospital (KBTH)	Min	3.00	246.00	3.76	4.98
	Max	16.00	2794.40	42.75	18.26
	Mean	6.36	978.52	15.06	8.87
Cape Coast Teaching hospital (CCTH)	Min	16.87	2189.70	33.50	31.84
	Max	70.80	10292.90	154.38	259.06
	Mean	20.74	3543.63	53.86	76.29

Source: Field Data, 2020

Table 23: A Comparison of the Mean $CTDI_{vol}$ results with other Studies.

Studies		Abdomen
This study $CTDI_{vol}$ (mGy)	SSC (2020)	14.56
	KBTH (2020)	6.36
	CCTH (2020)	20.74
Other studies $CTDI_{vol}$ (mGy)	Inkoom et al (2014)	14.50
	European MDCT DRL-Bongartz et al., 2004	12.80
	Brix et al., 2003	14.00
	UK MDCT DRL-Shrimpton et al., 2003	10.90
	IAEA study-Tsapaki et al., 2006	25.00
	ACR 2008	14.50

Source: Field Data, 2020;

Table 23 shows that KBTH had the least $CTDI_{vol}$ compared to the other DRLs studies. CCTH and SSC recorded higher $CTDI_{vol}$ values compared to the other DRLs except that of the IAEA. This could be due to the high mAs used by CCTH and SSC. Also KBTH used a constant slice thickness of 5 cm while CCTH and SSC used a variation of 5 and 10 cm for patients.

Table 24: A Comparison of the Mean DLP results with other Studies.

Studies		Abdomen
This study DLP (mGy.cm)	SSC	1717.52
	KBTH	978.52
	CCTH	3543.63
Other studies DLP (mGy.cm)	Inkoom et al., (2014)	620
	European MDCT DRL-Bongartz et al., (2004)	724
	Brix et al., (2003)	552
	UK MDCT DRL-Shrimpton et al., (2003)	560
	IAEA study-Tsapaki et al., (2006)	696

Source: Field Data, 2020;

The results from Table 24 show that none of the mean DLP obtained for this study was lower than other international DLPs. This means the three (3) health facilities did not meet any of the compared international DLPs. CCTH had the highest mean DLP. DLP is the product of the scan length and CTDI and since CTDI is already high it is also expected that DLP will also be high. The higher values could also be as a result of higher scan length.

Table 25: A Cof the mean Effective Dose (ED) results with Other Studies.

Studies		Abdomen
This study Effective Dose (ED) (mSv)	SSC	26.27
	KBTH	15.06
	CCTH	53.86
Other studies Effective Dose (mSv)	Inkoom et al (2014)	9.50
	European MDCT DRL-Bongartz et al., 2004	12.10
	Brix et al., 2003	10.30
	UK MDCT DRL-Shrimpton et al., 2003	9.90
	IAEA study-Tsapaki et al., 2006	8.20
	UNSCEAR (2008)	12.00
	Olerud (2003)	12.80

Source: Field Data, 2020

As seen from Table 25, the ED from this study did not meet any of the international EDs. This was to be expected as the DLP for this research was higher than any of the compared DLPs. This means that the doses given to patients during these examinations are much higher from the known DRLs. CCTH had the highest ED which was also one hundred percent (100 %) higher than any of the compared international EDs.

Analysis of Dose Optimization and Image Quality

To establish a tradeoff between image quality and corresponding dose for the patients' dose optimization procedure, a numerical method was used to calculate the SNR of CT image. That is, the ratio of the Signal (process average) over the Noise (standard deviation). Mean measurements of signals and noises values from axial CT images were recorded (Appendix E). These were used to assess the image quality used for this study.

SNR values above 5 indicate that the image quality was good enough for medical diagnosis. For this study, 90 images which was 97.83 % of the entire images had SNR value above 5 (Shiraz, 2018). This means most of the images used for this study had good image quality hence good enough for medical diagnosis. Table 26 gives a statistical summary of the measured signal, noise and their corresponding SNR in terms of mean, maximum and minimum.

Table 26: Summarized Signal to Noise (SNR) Ratio data

Statistics	Signal	Noise	SNR
Liver			
Min	41.38	5.78	4.57
Max	93.74	15.97	14.34
Mean	67.56	10.29	6.83

Source: (Field Data, 2018)

Establishing a relationship between SNR, mAs and Peak Voltage (kVp)

During scanning, the two basic inputs are normally mAs and peak tube voltage (kVp). Knowing which combination of these two (2) inputs that results in SNR values above 5 enables radiographers during scanning to obtain images good enough for medical diagnosis with the least radiation exposure. Appendix F shows mAs, kVp, SNR and ED values for this study.

Minitab software was used to develop a model that estimated the SNR from both mAs and peak tube voltage.

Regression Analysis for SNR versus Exposure and Peak Voltage

Table 27: Model Summary of SNR versus mAs and kVp

R	R-sq	R-sq(adj)	P-value
0.963252	15.91	13.70	0.001

Source: SPSS analysis

The model summary shows the strength of the association between SNR, mAs and kVp. From Table 27, the correlation coefficient (R) between SNR, Exposure and peak voltage is 0.963, which implies that there existed a good relation between SNR, Exposure and peak voltage.

In addition, adjusted R Square shows the coefficient of determination is 13.70 %. This means that the total variation in SNR was explained by 13.70 % of exposure and peak tube voltage thus, Exposure and Peak voltage do not have a good impact on SNR.

Regression Equation

$$SNR = 1.80 + 0.0404 \times kVp + 0.00066 \times mAs \quad 4.1$$

The regression equations are generated by the SPSS software

The p-value was 0.001, it shows that there exists a significant relationship between SNR, kVp and mAs. Therefore, model is a best fit.

Establishing a relationship between ED, mAs and kVp

In order to protect patients during CT examinations, knowing the effective dose to a patient even before scan would enable Radiographer put in the appropriate parameters. Since mAs and peak tube voltage are the main inputs during CT scans, a model equation to predict a good SNR and its corresponding ED before scan would help Radiographers and patients. This model was done using SPSS software.

In order to estimate the ED, a regression of ED versus mAs and kVp was performed. Table 28 gives the ANOVA results.

The regression generates an equation and this equation is the model equation.

Regression Analysis of Effective Dose versus Exposure and Peak Voltage

Table 28: Model Summary of ED versus mAs and kVp

R	R-square	Adjusted R-square	P-value
0.88	64.90	64.01	0.000

Source: SPSS analysis

The R value was 0.88 which indicates a strong linear relationship between ED, mAs and kVp. The p-value of 0.000 shows that there exists a significant relation between ED, mAs and kVp at 5 % level of significance, since p-value was less than 0.05, model was a best fit.

Regression Equation

$$Effective\ Dose = 36.1 - 0.325 \times kVp + 0.2522 \times mAs \qquad (4.2)$$

The regression equations are generated by the SPSS software

In addition, adjusted R Square shows the coefficient of determination, which takes into consideration the sample size. From table 28, it shows that the total variation in ED was explained by 64.01 % of exposure and peak tube voltage, thus, mAs and kVp do have a good impact on ED.

Graphic User Interface (GUI) for Dose Optimization

In order to use equation 4.2 to be user friendly, a Graphic User Interface (GUI) was developed with C# codes for immediate visual feedback. The GUI is shown in Figure 40 and it is divided into input and output sections.

The input section is where the user keys in the dose input parameters such as the kVp, mAs, $CTDI_{vol}$, Lateral (Lat) and AP dimensions.

The output section consists of SNR, ED and SSDE. The right side of SNR displays the words “Good” or “Bad” for values of SNR greater than or equal to 5 and values less than 5, respectively as shown in Figures 41 and 42.

There is a ‘clear’ button that clears the entire display to allow for a new set of inputs.

The developed C# code is presented in Appendix S.

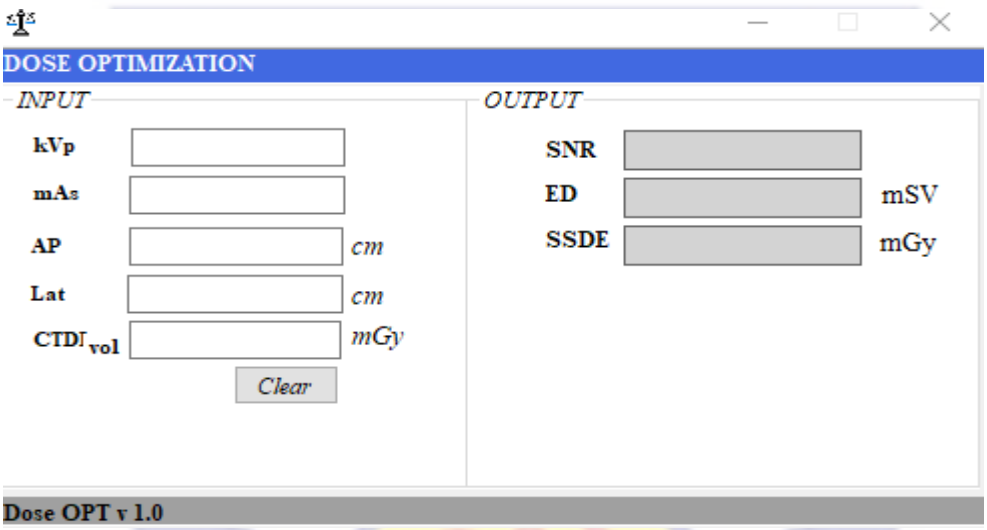

Figure 40: Graphic User Interface (GUI) for Dose Optimization

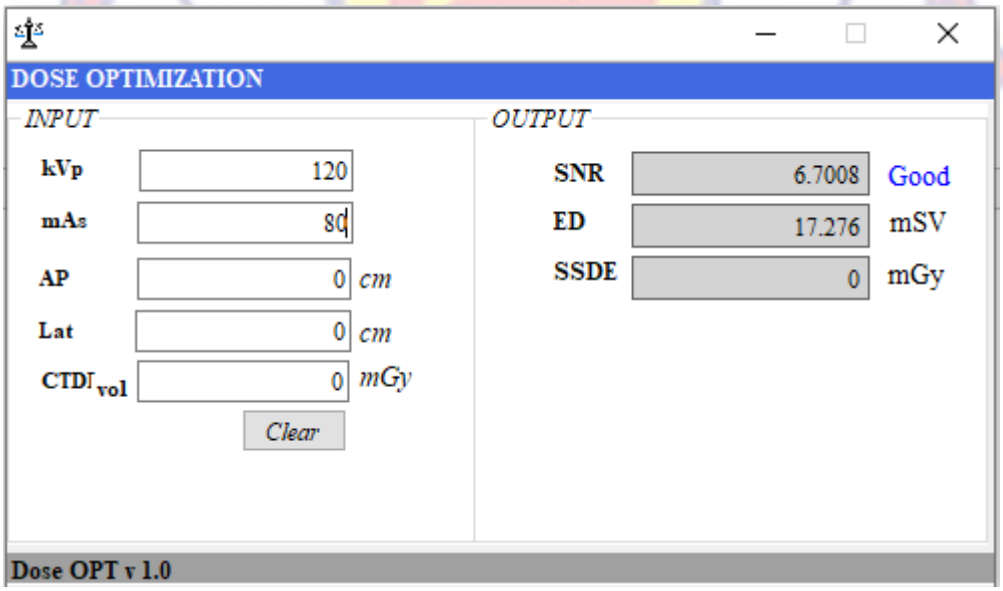

Figure 41: Graphic User Interface (GUI) displaying a Good SNR

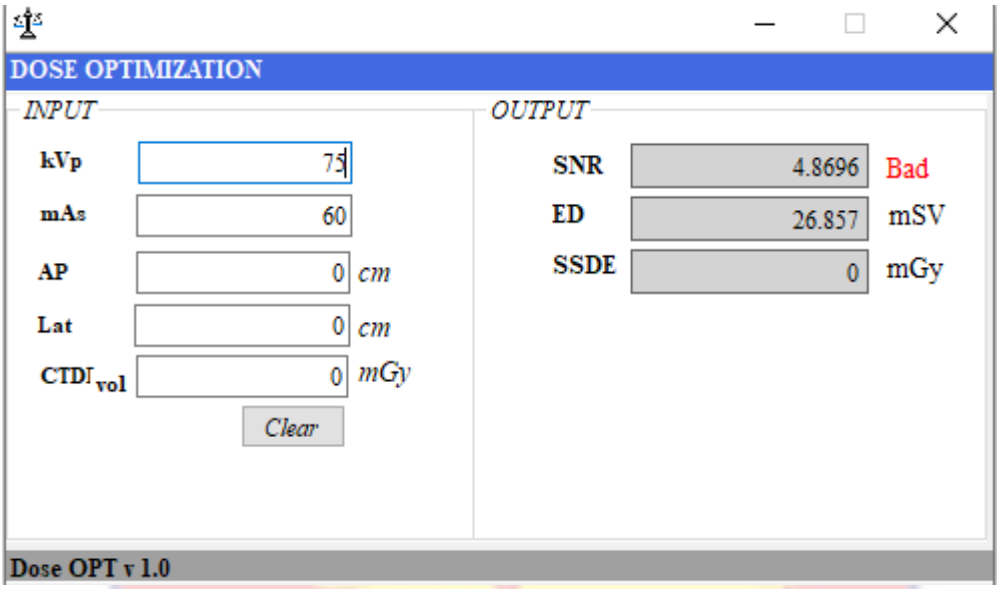

Figure 42: Graphic User Interface (GUI) displaying a Bad SNR

Chapter Summary

In summary, this chapter discussed the various results of the measured parameters in tables and graphical representation. It was established in this study that, the relationship between the liver volume (L) and body parameters such BMI, BSA and BSI were insignificant, as such, no model equation was established for this study. Since the relationship is not significant, a GUI wasn't designed for it. The BMI, BSA and BSI for this study was also compared to other international studies (since the same parameters were used) and found to be different due to demography of subjects used. The female liver volume for this study was also found to be larger than that of the male patients and this was due to the fact that most of the female patients used had higher BMI values and were obese. The SNR, SSDE, ED for each patient was calculated. In all, SSDE and ED were found to be highest with CCTH and least being KBTH. A model equation between SNR, mAs and kVp was also established to know the best combination of mAs and kVp to obtain a SNR value good enough for medical diagnosis. Another model equation were also established between ED, Exposure and peak voltage. The Exposure (mAs) and peak voltage (kVp) values used to establish a

good SNR is placed into the model equation to estimate the ED before the actual scan is performed. A GUI was developed with C# codes for the SNR and ED model equations to help Radiographers and Radiologists use this model easily.

CHAPTER FIVE

SUMMARY, CONCLUSIONS AND RECOMMENDATIONS

Introduction

The framework of this chapter is a summary of the major findings in relation to the measured liver volume to body parameters (BMI, BSA and BSI), the length of the liver in the midclavicular line, SSDE and ED to patients during abdominal CT scan. The chapter draws meaningful conclusions on the various findings.

Summary

This study had some specific aims to be achieved.

The first aim was to determine the length of the liver in the midclavicular line. With this, the average lengths recorded were 15.70 ± 2.31 and 15.90 ± 2.53 cm for male and female respectively.

The next aim of this study was to predict the liver volume of an average Ghanaian adult with standard reference body parameters like, BMI, BSI and BSA. This aim could not be achieved since all the model equations had p-values greater than 0.05 indicating that there exists no relationship between the calculated body parameters and the liver size. The mean liver volumes for the male and female adult for this study were 1.356 and 1.363 L, respectively. It shows that the measured female liver volume for this study was larger than that of the male. This was compared with the ICRP reference for liver volume which were 1.714 and 1.333 L for male and female, respectively.

The third aim of this study was to compare the measured parameters with international reference values and to make appropriate recommendations. The mean $CTDI_{vol}$ recorded for this study from the three health facilities SSC, KBTH and CCTH were 14.56, 6.36 and 20.74 mGy respectfully. These were compared

to other international studies as shown in Table 11 and it showed that all the recorded values were lower than the results of the study done by IAEA. It also shows that Center KBTH had the least $CTDI_{vol.}$.

The mean DLPs recorded from centers SSC, KBTH and CCTH were 1717.52, 978.52 and 3543.63 mGy.cm, respectively. These values were higher than other international studies and recommendations.

The mean ED to patients from SSC, KBTH and CCTH were 26.27, 15.06 and 53.86 mSv, respectively. These values were also compared to other international values. The values from these studies were higher than the recommended range of 8 – 14 mSv.

The mean SSDEs measured was 55.29, 8.87 and 76.29 mSv for SSC, KBTH and CCTH, respectively. These were the mean doses received by the patients due to their sizes.

A SNR equation was modelled with peak voltage (kVp) and exposure (mAs) as the predictors to help radiographers ascertain the quality of image before a scan to enhance dose optimization. The modelled equation was

$$SNR = 1.80 + 0.0404 \times kVp + 0.00066 \times mAs$$

A model equation for ED was also established with peak tube voltage (kVp) and mAs as the predictors. This equation would help Radiographers and Radiologists estimate the doses to patients before they are scanned. The equation is

$$Effective\ Dose\ (ED) = 36.1 - 0.325 \times kVp + 0.2522 \times mAs$$

In order to make these equations user friendly, a computer program was written in C# with a GUI to make it easy for Radiographers and Radiologists to use.

Conclusions

In conclusion, the results showed that the female liver volume was larger than the male liver. The length of the liver in the midclavicular line was also longer in female than in male. The DLP value recorded for this study was higher than the recommended value range. Since the effective dose was a function of DLP, the effective dose for this study was also higher than the recommended values.

A GUI has also been developed to help Radiographers and Radiologists to ascertain the quality of images and doses to patients before scanning.

Recommendations

Based on the study results, the following recommendations are addressed to stakeholders in order to help improve health care delivery in Ghana:

Imaging facilities should acquire the needed quality control (QC) equipment so that daily, quarterly and yearly QCs are performed regularly to ensure adequate patient protection.

It is recommended that Radiographers go through regular training to enable them ensure adequate patient protection. The Radiologists and Radiographers should use the results obtained from this study to estimate patient dose and SNR before scanning.

It is recommended that Medical Physicists should adopt the method used in this study to develop other organ models to be used as standard reference values for clinical applications and research in Ghana.

The DLP and abdominal effective dose exceeded the recommended ICRP values. This was an indication that effective regulatory oversight was needed from the Nuclear Regulatory Authority (NRA). NRA needs to perform

regular inspections to keep imaging centers to comply with regulatory requirements.

This study was based on gender variation because of the number of sample size. It is recommended that in future a larger sample size be used so that age variation could also be factored into the model equations.

REFERENCES

AAPM. (2008). AAPM Report Nº 96 - The Measurement, Reporting, and Management of Radiation Dose in CT. In *American Association of Physicists in Medicine*.

Andrew Murphy et al. (2020). Signal-to-noise ratio (CT) | Radiology Reference Article | Radiopaedia.org. Retrieved July 22, 2020, from https://radiopaedia.org/articles/signal-to-noise-ratio-ct

Applications and Clinical Benefits of CT Imaging | CT Scan | Imaginis - The Women's Health & Wellness Resource Network. (n.d.). Retrieved July 22, 2020, from https://www.imaginis.com/ct-scan/applications-and-clinical-benefits-of-ct-imaging

Brenner, D. J., & Hall, E. J. (2007). Computed tomography - An increasing source of radiation exposure. *New England Journal of Medicine*. https://doi.org/10.1056/NEJMra072149

Bushberg, J. T., Seibert, J. A., Leidholdt, E. M., Boone, J. M., & Goldschmidt, E. J. (2003). The Essential Physics of Medical Imaging. *Medical Physics*. https://doi.org/10.1118/1.1585033

Caldwell, S. H., De Lange, E. E., Gaffey, M. J., Sue, M., Boyd, J. C., Dickson, R. C., … Pruett, T. L. (1996). Accuracy and significance of pretransplant liver volume measured by magnetic resonance imaging. *Liver Transplantation and Surgery*. https://doi.org/10.1002/lt.500020606.

Cantlie, J. (1897). On a new arrangement of the right and left lobes of the liver. *Proceedings – Anatomical Society of Great Britain and Ireland*, *32*, 4–9.

Caon, M. (2004). Voxel-based computational models of real human anatomy: A review. *Radiation and Environmental Biophysics*, *42*(4), 229–235. https://doi.org/10.1007/s00411-003-0221-8

Chen, X. L., Chen, T. W., Zhang, X. M., Li, Z. L., Zeng, N. L., Li, T., … Li, C. P. (2014). Quantitative assessment of the presence and severity of cirrhosis in patients with hepatitis B using right liver lobe volume and spleen size measured at magnetic resonance imaging. *PLoS ONE*. https://doi.org/10.1371/journal.pone.0089973

Choukèr, A., Martignoni, A., Dugas, M., Eisenmenger, W., Schauer, R., Kaufmann, I., … Thiel, M. (2004). Estimation of liver size for liver transplantation: The impact of age and gender. *Liver Transplantation*. https://doi.org/10.1002/lt.20113

Cierniak, R. (2011). X-ray computed tomography in biomedical engineering. In *X-Ray Computed Tomography in Biomedical Engineering*. https://doi.org/10.1007/978-0-85729-027-4

Commission, I. E. (2010). Medical electrical equipment—Part 2-44: Particular requirements for the basic safety and essential performance of X-ray equipment for computed tomography. *International Standard IEC*.

Cormack, A. M. (1973). Reconstruction of densities from their projections, with applications in radiological physics. *Physics in Medicine and Biology*. https://doi.org/10.1088/0031-9155/18/2/003

De González, A. B., & Darby, S. (2004). Risk of cancer from diagnostic X-rays: Estimates for the UK and 14 other countries. *Lancet*. https://doi.org/10.1016/S0140-6736(04)15433-0

Du Bois, D., & Du Bois, E. F. (1989). A formula to estimate the approximate surface area if height and weight be known. 1916. *Nutrition (Burbank, Los Angeles County, Calif.)*.

Ferreira, F., Ferreira, F., & Ja, D. (2014). Accuracy of body mass index, waist circumference and body surface index to characterize overweight and obesity in adolescents. *Arch Exerc Health Dis*. https://doi.org/10.5628/aehd.v4i3.141

Frempong, G. (University of G. (2013). University Of Ghana. *Annals of Tropical Paediatrics*, *7*(3), 154–154. https://doi.org/10.1080/02724936.1987.11748497

Gao, L., Heath, D. G., Kuszyk, B. S., & Fishman, E. K. (1996). Automatic liver segmentation technique for three-dimensional visualization of CT data. *Radiology*. https://doi.org/10.1148/radiology.201.2.8888223

Glover, G. H. (1982). Compton scatter effects in CT reconstructions. *Medical Physics*. https://doi.org/10.1118/1.595197

Goo, H. W. (2010). State-of-the-art CT imaging techniques for congenital heart disease. *Korean Journal of Radiology*. https://doi.org/10.3348/kjr.2010.11.1.4

Govender, S., Lazarus, L., De Gama, B. Z., & Satyapal, K. S. (2017). Post-Mortem Organ Weights at a Medico-Legal State Facility in the eThekwini Region. *International Journal of Morphology*. https://doi.org/10.4067/s0717-95022017000401209

Grant, H., Zhang, Y., Li, L., Wang, Y., Kawamoto, S., Pénisson, S., … Elliot, K. (2020). *Organ size increases with obesity and correlates with cancer risk . Keywords*. 1–23.

Gurakar, A., & Dogan, S. (2015). Liver Transplantation Update: 2014. *Euroasian Journal of Hepato-Gastroenterology*, *5*(2), 98–106. https://doi.org/10.5005/jp-journals-10018-1144

Heckel, F., Schwier, M., & Peitgen, H. O. (2009). Object-oriented application development with mevislab and python. *INFORMATIK 2009 - Im Focus Das Leben, Beitrage Der 39. Jahrestagung Der Gesellschaft Fur Informatik e.V. (GI)*.

Henderson, J. M., Heymsfield, S. B., Horowitz, J., & Kutner, M. H. (1981). Measurement of liver and spleen volume by computed tomography. Assessment of reproducibility and changes found following a selective distal splenorenal shunt. *Radiology*. https://doi.org/10.1148/radiology.141.2.6974875

Heymsfield, S. B., Fulenwider, T., Nordlinger, B., Barlow, R., Sones, P., & Kutner, M. (1979). Accurate measurement of liver, kidney, and spleen volume and mass by computerized axial tomography. *Annals of Internal Medicine*. https://doi.org/10.7326/0003-4819-90-2-185

History of computed tomography - Wikipedia. (n.d.). Retrieved November 19, 2021, from https://en.wikipedia.org/wiki/History_of_computed_tomography

Hounsfield, G. N. (1973). Computerized transverse axial scanning (tomography): I. Description of system. *British Journal of Radiology*. https://doi.org/10.1259/0007-1285-46-552-1016

Hricak, H., Brenner, D. J., Adelstein, S. J., Frush, D. P., Hall, E. J., Howell, R. W., … Wagner, L. K. (2011). Managing radiation use in medical imaging: A multifaceted challenge. *Radiology*. https://doi.org/10.1148/radiol .10 101157

Huda, W., Ogden, K. M., & Khorasani, M. R. (2008). Converting dose-length product to effective dose at CT. *Radiology*, *248*(3), 995–1003. https://doi.org/10.1148/radiol.2483071964

I, C. on the A. of C. R. in P. near N. F.-P., Board, N. and R. S., Studies, D. on E. and L., & Council, N. R. (2012). *Radiation as a Carcinogen*. Retrieved from https://www.ncbi.nlm.nih.gov/books/NBK202000/

IAEA. (1993). *anatomical, physiological and. 1*.

ICRP. (2012). Basic Anatomical and Physiological Data for Use in Radiological Protection: Reference Values. *The International Commission on Radiological Protection*. https://doi.org/10.1016/j.icrp.2006.06.001

Imaging Principles in Computed Tomography | Radiology Key. (2021). Retrieved July 23, 2020, from https://radiologykey.com/imaging-principles-in-computed-tomography/

Johnson, T. R. C., Krauß, B., Sedlmair, M., Grasruck, M., Bruder, H., Morhard, D., … Becker, C. R. (2007). Material differentiation by dual energy CT: Initial experience. *European Radiology*. https://doi.org/10.1007/s00330-

006-0517-6

Kalra, M. K., Maher, M. M., Toth, T. L., Hamberg, L. M., Blake, M. A., Shepard, J. A., & Saini, S. (2004). Strategies for CT Radiation Dose Optimization. *Radiology*. https://doi.org/10.1148/radiol.2303021726

Kapoor, V. (MedCape). (2017). Liver Anatomy: Overview, Gross Anatomy, Microscopic Anatomy. Retrieved July 23, 2020, from https://emedicine.medscape.com/article/1900159-overview

Kawasaki, S., Makuuchi, M., Matsunami, H., Hashikura, Y., Ikegami, T., Chisuwa, H., … Kawarazaki, H. (1993). Preoperative measurement of segmental liver volume of donors for living related liver transplantation. *Hepatology*. https://doi.org/10.1002/hep.1840180516

Kokudo, T., Hasegawa, K., Uldry, E., Matsuyama, Y., Kaneko, J., Akamatsu, N., … Halkic, N. (2015). A new formula for calculating standard liver volume for living donor liver transplantation without using body weight. *Journal of Hepatology*. https://doi.org/10.1016/j.jhep.2015.05.026

Leitz, W., Axelsson, B., & Szendrö, G. (1995). Computed Tomography Dose Assessment - A Practical Approach. *Radiation Protection Dosimetry*. https://doi.org/10.1093/rpd/57.1-4.377

Mahesh, M. (2013). The Essential Physics of Medical Imaging, Third Edition. *Medical Physics*. https://doi.org/10.1118/1.4811156

Mahnken, A. H., Mühlenbruch, G., Günther, R. W., & Wildberger, J. E. (2007). Cardiac CT: Coronary arteries and beyond. *European Radiology*. https://doi.org/10.1007/s00330-006-0433-9

McCollough, C. H., Leng, S., Yu, L., Cody, D. D., Boone, J. M., & McNitt-Gray, M. F. (2011). CT dose index and patient dose : They are not the same thing. *Radiology*. https://doi.org/10.1148/radiol.11101800

McCollough, C. H., & Schueler, B. A. (2000). Calculation of effective dose. *Medical Physics*. https://doi.org/10.1118/1.598948

Mettler, F. A., Bhargavan, M., Faulkner, K., Gilley, D. B., Gray, J. E., Ibbott, G. S., … Yoshizumi, T. T. (2009). Radiologic and nuclear medicine studies in the United States and worldwide: Frequency, radiation dose, and comparison with other radiation sources - 1950-2007. *Radiology*. https://doi.org/10.1148/radiol.2532082010

MeVisLab - Wikipedia. (n.d.). Retrieved July 23, 2020, from https://en.wikipedia.org/wiki/MeVisLab

Murphy, A., & Morgan, M. (2016). Dose length product | Radiology Reference Article | Radiopaedia.org. Retrieved June 10, 2020, from https://radiopaedia.org/articles/dose-length-product

Overview | New generation cardiac CT scanners (Aquilion ONE, Brilliance iCT, Discovery CT750 HD and Somatom Definition Flash) for cardiac imaging in people with suspected or known coronary artery disease in whom imaging is difficult with earlier generation CT scanners | Guidance | NICE. (n.d.).

Paper, C., Children, S. C., & Angeles, L. (2011). *Size-specific Dose Estimates in CT : Presentation of AAPM Report 204*. (November).

Pourjabbar, S. (2014). Size-specific dose estimates: Localizer or transverse abdominal computed tomography images? *World Journal of Radiology*.

https://doi.org/10.4329/wjr.v6.i5.210

Pulitano, C., Ho, P., Verran, D., Sandroussi, C., Joseph, D., Bowen, D. G., … Shackel, N. (2018). Molecular profiling of postreperfusion milieu determines acute kidney injury after liver transplantation: A prospective study. *Liver Transplantation*, *24*(7), 922–931. https://doi.org/10.1002/lt.25178

Saygili, O. B., Tarhan, N. C., Yildirim, T., Serin, E., Ozer, B., & Agildere, A. M. (2005). Value of computed tomography and magnetic resonance imaging for assessing severity of liver cirrhosis secondary to viral hepatitis. *European Journal of Radiology*. https://doi.org/10.1016/j.ejrad.2004.08. 001

Schindl, M. J., Redhead, D. N., Fearon, K. C. H., Garden, O. J., & Wigmore, S. J. (2005). The value of residual liver volume as a predictor of hepatic dysfunction and infection after major liver resection. *Gut*. https://doi.org/10.1136/gut.2004.046524

Shimamoto, D., Nishie, A., Asayama, Y., Ushijima, Y., Takayama, Y., Fujita, N., … Honda, H. (2015). MR prediction of liver function and pathology using gd-eob-dtpa: Effect of liver volume consideration. *BioMed Research International*. https://doi.org/10.1155/2015/141853

Shiraz, I. (2018). Determination Of Standard Reference Renal Volume Model And Dose Optimisation Procedures For Clinical Applications.

Shrimpton, P. C. (2004). Assessment of Patient Dose in CT. *National Radiological Protection Board*.

Shuter, B., & Aslani, A. (2000). Body surface area: Du Bois and Du Bois

revisited. *European Journal of Applied Physiology*. https://doi.org/10.1007/s004210050679

Small, R., Surujpaul, P. P., & Chakraborty, S. (2019). *Patient Dose Audit in Computed Tomography at Cancer Institute of Guyana Journal of Medical Diagnostic Methods*. *8*(1), 1–13. https://doi.org/10.4172/2168-9784.1000282

Smith-Bindman, R., Lipson, J., Marcus, R., Kim, K. P., Mahesh, M., Gould, R., … Miglioretti, D. L. (2009). Radiation dose associated with common computed tomography examinations and the associated lifetime attributable risk of cancer. *Archives of Internal Medicine*. https://doi.org/10.1001/archinternmed.2009.427

Strunk, H., Stuckmann, G., Textor, J., & Willinek, W. (2003). Limitations and pitfalls of Couinaud's segmentation of the liver in transaxial imaging. *European Radiology*. https://doi.org/10.1007/s00330-003-1885-9

Task Group on Control of Radiation Dose in Computed Tomography. (2000). Managing patient dose in computed tomography. A report of the International Commission on Radiological Protection. *Annals of the ICRP*. https://doi.org/10.1016/s0146-6453(01)00049-5

Urata, K., Kawasaki, S., Matsunami, H., Hashikura, Y., Ikegami, T., Ishizone, S., … Makuuchi, M. (1995). Calculation of child and adult standard liver volume for liver transplantation. *Hepatology*. https://doi.org/10.1016/ 0270-9139(95)90053-5

WHO. (2004). Changing history. *Drapers*, (21-APRIL-2012), 18–20. https://doi.org/10.7765/9781526125149.00006

Wolf, D. C. (n.d.). Evaluation of the Size, Shape, and Consistency of the Liver - PubMed. Retrieved July 23, 2020, from https://pubmed.ncbi. nlm.nih. gov/21250261/

Yang, X., Yang, J. Do, Lee, S., Hwang, H. P., Ahn, S., Yu, H. C., & You, H. (2018). Estimation of standard liver volume using CT volume, body composition, and abdominal geometry measurements. *Yonsei Medical Journal*, *59*(4), 546–553. https://doi.org/10.3349/ymj.2018.59.4.546

Yu, H. C., You, H., Lee, H., Jin, Z. W., Moon, J. Il, & Cho, B. H. (2004). Estimation of standard liver volume for liver transplantation in the Korean population. *Liver Transplantation*. https://doi.org/10.1002/lt.20188

Zoli, M., Cordiani, M. R., Marchesini, G., Abbati, S., Bianchi, G., & Pisi, E. (1990). Ultrasonographic follow-up of liver cirrhosis. *J.Clin.Ultrasound*.

APPENDICES

APPENDIX A

ETHICAL CLEARANCE

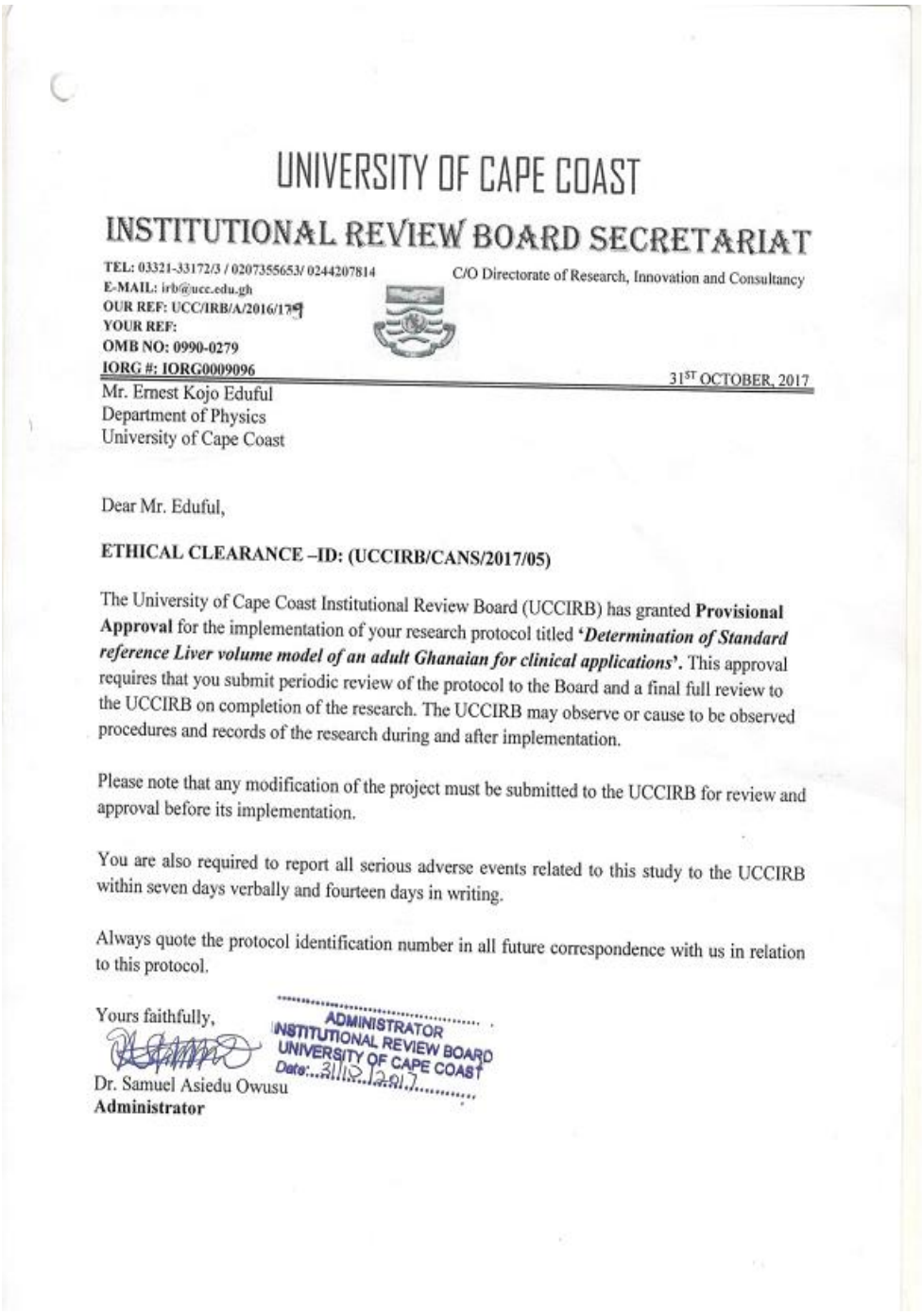

UNIVERSITY OF CAPE COAST

INSTITUTIONAL REVIEW BOARD SECRETARIAT

TEL: 03321-33172/3 / 0207355653/ 0244207814
E-MAIL: irb@ucc.edu.gh
OUR REF: UCC/IRB/A/2016/179
YOUR REF:
OMB NO: 0990-0279
IORG #: IORG0009096

C/O Directorate of Research, Innovation and Consultancy

31ST OCTOBER, 2017

Mr. Ernest Kojo Eduful
Department of Physics
University of Cape Coast

Dear Mr. Eduful,

ETHICAL CLEARANCE –ID: (UCCIRB/CANS/2017/05)

The University of Cape Coast Institutional Review Board (UCCIRB) has granted **Provisional Approval** for the implementation of your research protocol titled '***Determination of Standard reference Liver volume model of an adult Ghanaian for clinical applications***'. This approval requires that you submit periodic review of the protocol to the Board and a final full review to the UCCIRB on completion of the research. The UCCIRB may observe or cause to be observed procedures and records of the research during and after implementation.

Please note that any modification of the project must be submitted to the UCCIRB for review and approval before its implementation.

You are also required to report all serious adverse events related to this study to the UCCIRB within seven days verbally and fourteen days in writing.

Always quote the protocol identification number in all future correspondence with us in relation to this protocol.

Yours faithfully,

ADMINISTRATOR
INSTITUTIONAL REVIEW BOARD
UNIVERSITY OF CAPE COAST
Date: 31/10/2017

Dr. Samuel Asiedu Owusu
Administrator

APPENDIX B

WEIGHT CALIBRATION CERTIFICATE 1

GHANA STANDARDS AUTHORITY
METROLOGY DIRECTORATE
CALIBRATION CERTIFICATE

CERTIFICATE NO.: GSA/MED/114.14 (A)/BL/1248

ITEM CALIBRATED : TOP LOADING SCALE

AMBIENT CONDITIONS: Temperature: (24.0 to 24.5) ^{O}C
Humidity : (50 to 55) %

CALIBRATION RESULTS

A. ***REPEATABILITY TEST***

Applied Load (L): 140 kg Standard deviation: 0.000 g

No.	1	2	3	4	5
Indication/kg	139.9	139.9	139.9	139.9	139.9

B. ***TEST OF ERRORS OF INDICATION***

Nominal Mass /kg	Mean Scale Reading /kg	Mean Deviation /g	Coverage Factor (k)	Expanded Uncertainty /g
20	19.9	-100	2.00	97.9797
60	59.9	-100	2.00	97.9807
100	100.0	0	2.00	97.9827
140	140.0	0	2.00	97.9858
160	159.9	-100	2.00	97.9876

C ***ECCENTRICITY TEST***

Applied Load (L): 40 kg

Load position	Scale Reading /kg	Deviation referring to centre/g
CENTRE	39.90	0
FRONT LEFT	39.90	0
BACK LEFT	39.90	0
BACK RIGHT	39.90	0
FRONT RIGHT	39.90	0

Traceability: *Reference mass pieces OIML class F1 Set is traceable to DAkkS, through Certificate No.: DKD-K-15209/ML-0054/2020-07*

Measurement uncertainty*: The expanded uncertainty reported on the certificate is based on combined uncertainty multiplied by coverage factor k=2 providing a confidence level of approximately 95%.*

APPENDIX C

WEIGHT CALIBRATION CERTIFICATE 2

GHANA STANDARDS AUTHORITY
METROLOGY DIRECTORATE
CALIBRATION CERTIFICATE

CERTIFICATE NO.: GSA/MED/114.14 (A)/BL/1247

ITEM CALIBRATED : TOP LOADING SCALE

AMBIENT CONDITIONS: Temperature: (24.0 to 24.5) ^{O}C
Humidity : (50 to 55) %

CALIBRATION RESULTS

A. ***REPEATABILITY TEST***

Applied Load (L): 140 kg Standard deviation: 0.000 g

No.	1	2	3	4	5
Indication/kg	140.0	140.00	140.00	140.00	140.00

B. ***TEST OF ERRORS OF INDICATION***

Nominal Mass /kg	Mean Scale Reading /kg	Mean Deviation /g	Coverage Factor (k)	Expanded Uncertainty /g
20	20.00	0	2.00	97.9797
60	60.05	50	2.00	97.9807
100	100.00	0	2.00	97.9827
140	140.00	0	2.00	97.9858
160	159.90	-100	2.00	97.9876

C *ECCENTRICITY TEST*

Applied Load (L): 40 kg

Load position	Scale Reading /kg	Deviation referring to centre/g
CENTRE	40.10	0
FRONT LEFT	40.10	0
BACK LEFT	40.10	0
BACK RIGHT	40.10	0
FRONT RIGHT	40.10	0

Traceability: *Reference mass pieces OIML class F1 Set is traceable to DAkkS, through Certificate No.: DKD-K-15209/ML-0054/2020-07*

Measurement uncertainty*: The expanded uncertainty reported on the certificate is based on combined uncertainty multiplied by coverage factor k=2 providing a confidence level of approximately 95%.*

APPENDIX D

PRIMARY PATIENT DATA COLLECTED AT THE SSC AND CCTH FOR LIVER VOLUME ANALYSIS

ID	Gender	Age (yrs)	Height (cm)	Weight (kg)	Centre
1	F	44	162.0	50.5	SSC
2	F	44	168.0	93.5	SSC
3	F	64	159.0	52.3	SSC
4	M	45	176.0	77.8	SSC
5	F	41	166.0	63.7	SSC
6	F	49	164.0	109.2	SSC
7	F	56	160.0	64.2	SSC
8	F	69	156.0	77.2	SSC
9	M	42	172.0	61.4	SSC
10	F	81	155.0	64.9	SSC
11	F	48	166.0	99.5	SSC
12	M	62	179.0	82.9	SSC
13	F	65	130.0	68.4	SSC
14	F	49	158.0	46.2	SSC
15	F	49	156.0	88.6	SSC
16	M	32	139.0	71.4	SSC
17	F	55	165.0	86.8	SSC
18	F	66	159.0	89.3	SSC
19	M	50	172.0	72.3	SSC
20	M	55	174.0	51.5	SSC
21	F	85	174.0	71.9	SSC
22	M	37	105.0	81.7	SSC
23	F	60	146.0	84.5	SSC
24	M	58	167.0	54.5	SSC
25	M	57	161.0	69.9	SSC
26	M	29	176.0	110.9	SSC

APPENDIX D continued

27	M	43	162.0	84.9	SSC
28	F	50	161.0	58.2	SSC
29	F	55	170.0	58.5	SSC
30	M	66	171.0	62.4	SSC
31	F	44	162.0	93.8	SSC
33	F	35	156.0	41.7	SSC
34	M	56	161.0	58.0	SSC
35	F	38	163.0	95.0	SSC
36	F	68	161.0	88.6	SSC
37	F	42	170.0	52.4	SSC
38	F	53	160.0	93.4	SSC
39	M	61	169.0	56.1	SSC
40	F	60	161.0	73.3	SSC
41	F	56	158.0	90	SSC
42	M	68	167.0	68.5	SSC
43	F	45	163.0	82	SSC
44	F	45	163.0	72.1	SSC
45	F	73	163.0	74.9	SSC
46	F	52	150.0	80.9	SSC
47	F	49	169.0	98.6	SSC
48	M	72	162.0	98.3	SSC
49	M	53	174.0	93.9	SSC
50	M	34	169.0	76.9	SSC
51	F	33	161.0	72.1	SSC
52	F	85	159.0	55	SSC
53	M	51	154.0	79	SSC
54	M	42	162.0	55.1	SSC
55	F	18	141.0	37.7	SSC
56	M	45	170.0	71.2	SSC

APPENDIX D continued

57	M	73	174.0	81.8	SSC
58	M	42	175.0	86.5	SSC
59	F	55	131.0	49.0	SSC
60	F	67	132.0	79.3	SSC
61	F	75	133.0	94.5	SSC
62	F	79	163.0	75.1	SSC
63	F	27	157.0	43.7	SSC
64	M	24	174.0	59.9	SSC
65	M	79	159.5	50.8	CCTH
66	M	73	156.0	64.9	CCTH
67	M	43	160.5	64.6	CCTH
68	M	40	166.5	66.4	CCTH
69	F	24	145.5	78.5	CCTH
70	F	38	164.5	70.3	CCTH
71	F	56	154.0	58.4	CCTH
72	F	22	166.5	73.8	CCTH
73	F	78	159.5	71.7	CCTH
74	F	54	161.5	60.2	CCTH
75	M	39	172.0	73.3	CCTH
76	M	19	170.5	60.7	CCTH
77	M	25	180.5	80.7	CCTH
78	M	39	159.5	61.9	CCTH
79	F	34	174.0	71.2	CCTH
80	M	48	160.5	58.2	CCTH
81	F	42	163.5	65	CCTH
82	M	44	192.5	85.4	CCTH
83	F	40	167.5	82.4	CCTH
84	M	44	176.5	79.9	CCTH
85	F	70	158.5	39.1	CCTH

APPENDIX D continued

87	F	62	165.5	86.3	CCTH
88	M	36	182.5	73.4	CCTH
89	M	37	173.5	77.2	CCTH
90	M	74	167.0	71.3	CCTH
91	F	35	153.7	76.5	CCTH
92	M	32	135.1	89.3	CCTH

APPENDIX E

PATIENTS AT SSC AND THEIR CORRESPONDING $CTDI_{vol}$ DURING CT SCAN

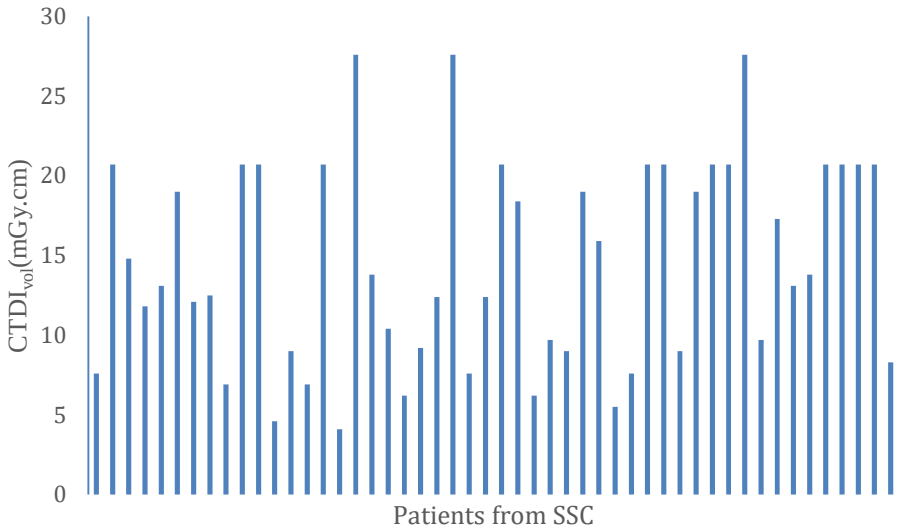

APPENDIX F

PATIENTS AT KBTH AND THEIR CORRESPONDING $CTDI_{vol}$ DURING CT SCAN

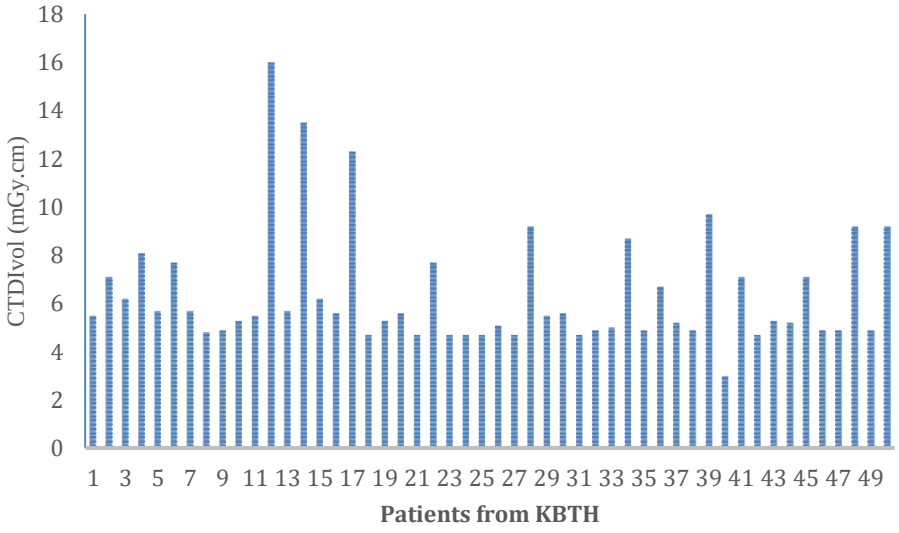

APPENDIX G

PATIENTS AT CCTH AND THEIR CORRESPONDING $CTDI_{vol}$ DURING CT SCAN

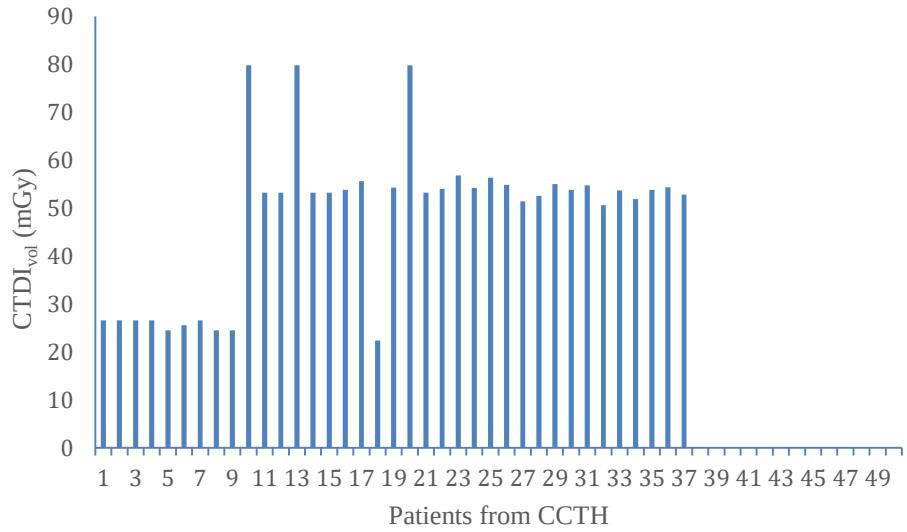

APPENDIX H

PATIENTS AT SSC AND THEIR CORRESPONDING DLP DURING CT SCAN

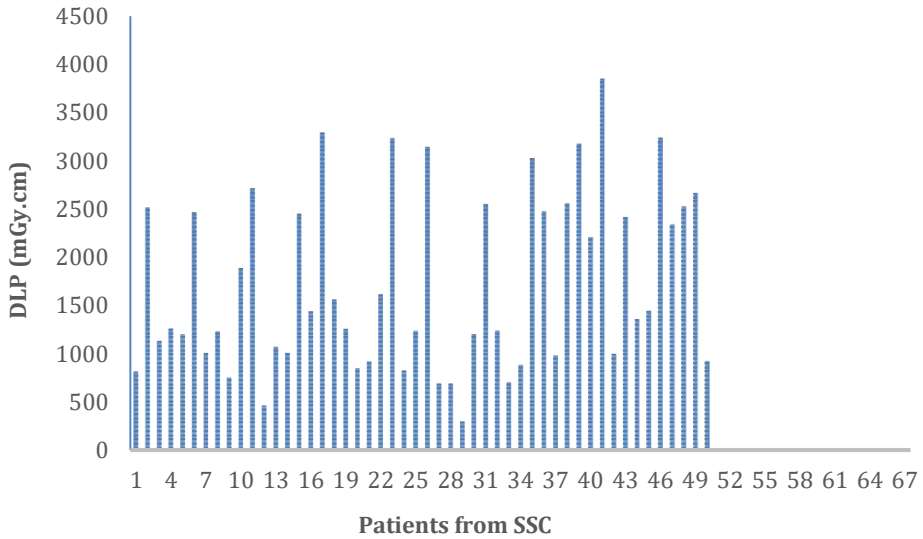

APPENDIX I

PATIENTS AT KBTH AND THEIR CORRESPONDING DLP DURING CT SCAN

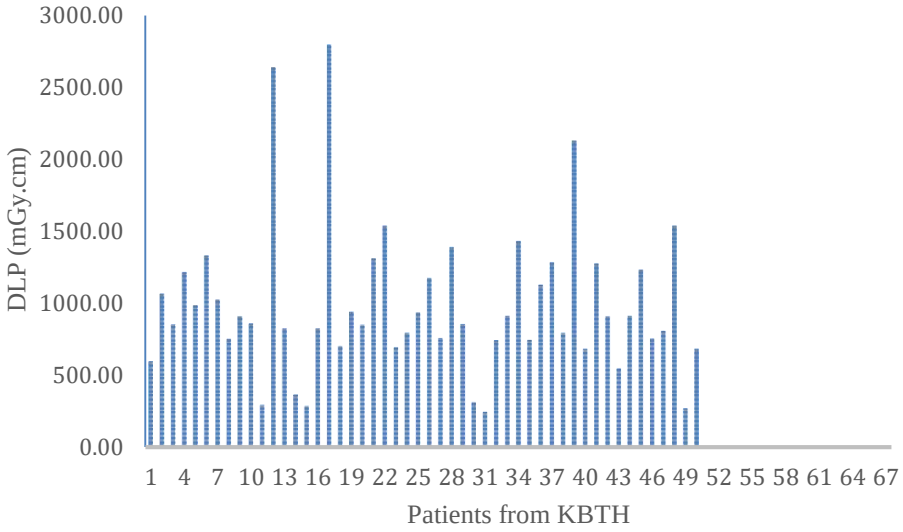

APPENDIX J

PATIENTS AT CCTH AND THEIR CORRESPONDING DLP DURING CT SCAN

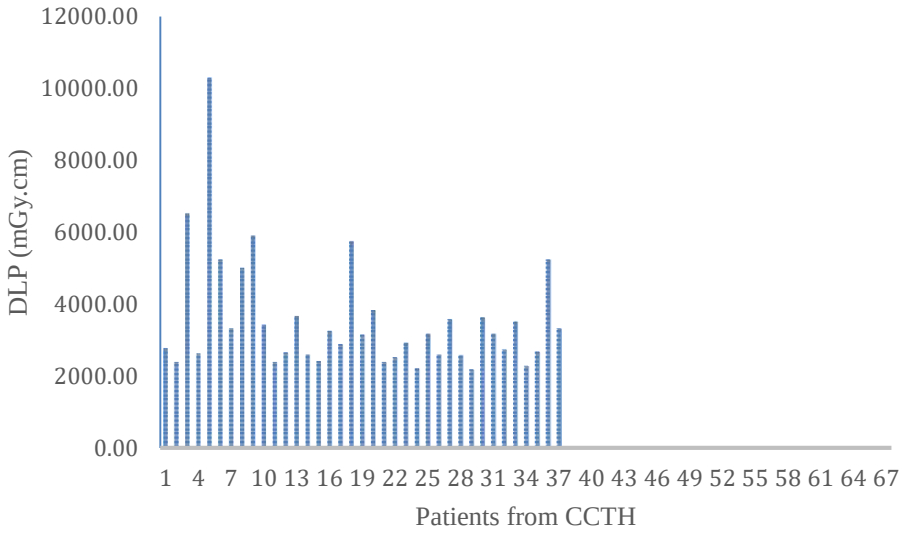

APPENDIX K

PATIENTS AT SSC AND THEIR CORRESPONDING EFFECTIVE DOSE DURING CT SCAN

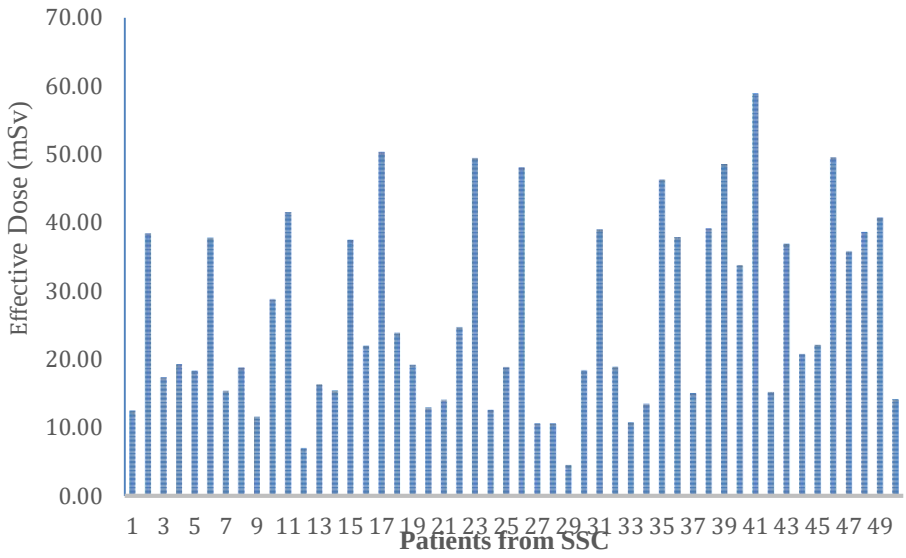

APPENDIX L

PATIENTS AT KBTH AND THEIR CORRESPONDING EFFECTIVE DOSE DURING CT SCAN

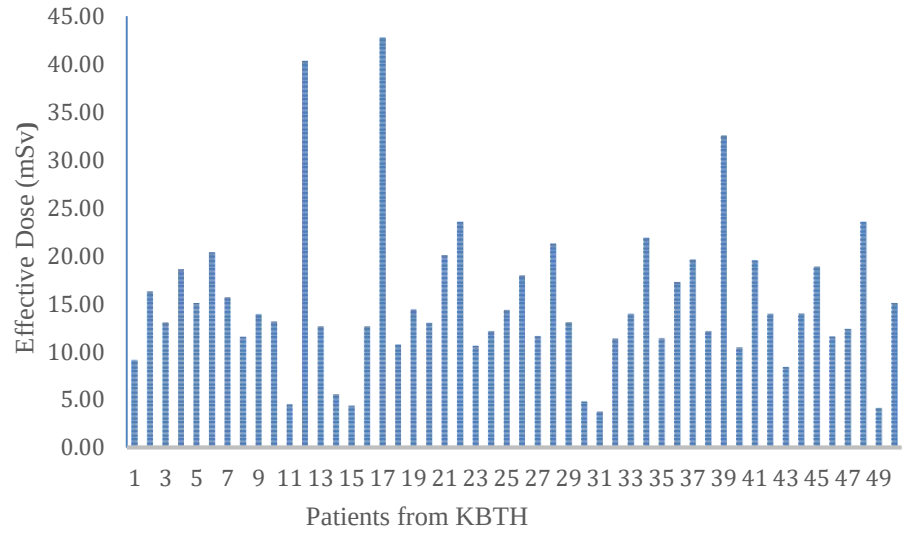

APPENDIX M

PATIENTS AT CCTH AND THEIR CORRESPONDING EFFECTIVE DOSE DURING CT SCAN

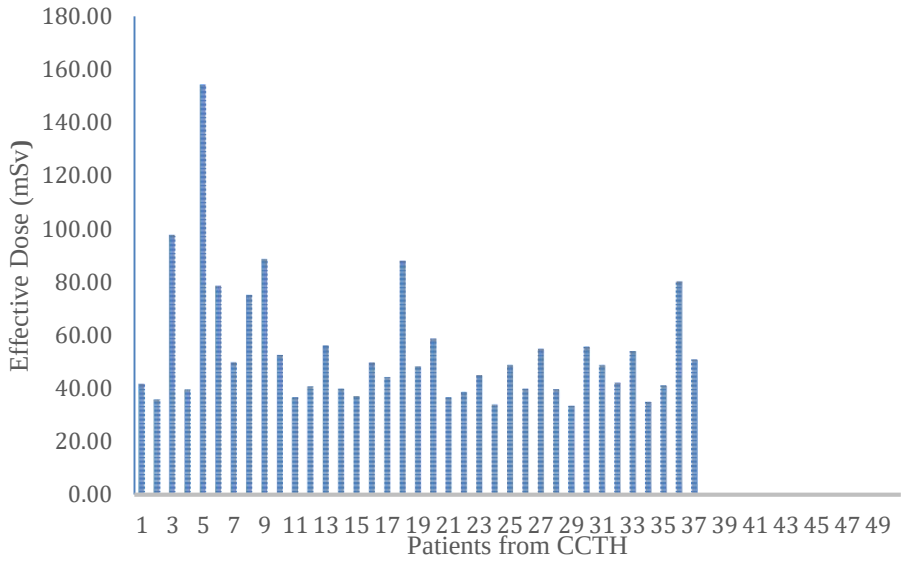

APPENDIX N

PATIENTS AT SSC AND THEIR CORRESPONDING SSDE DURING CT SCAN

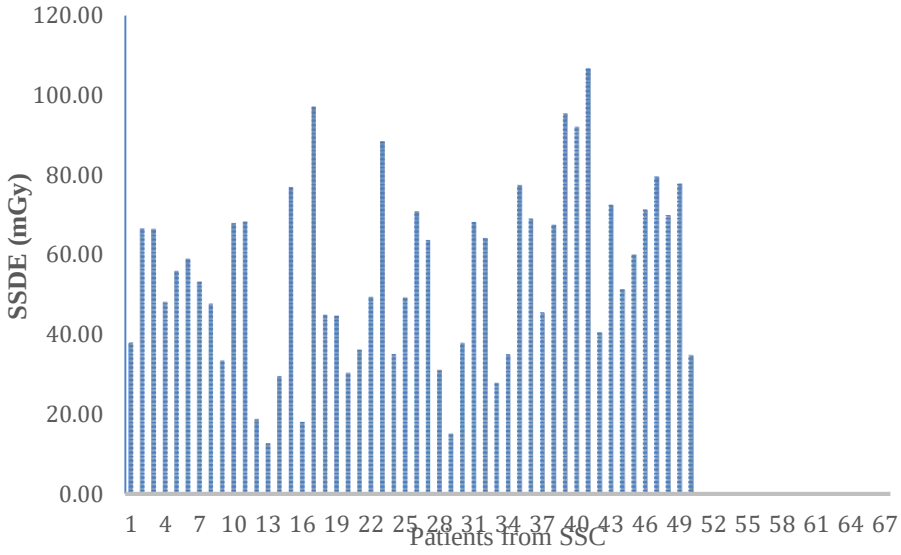

APPENDIX O

PATIENTS AT KBTH AND THEIR CORRESPONDING SSDE DURING CT SCAN

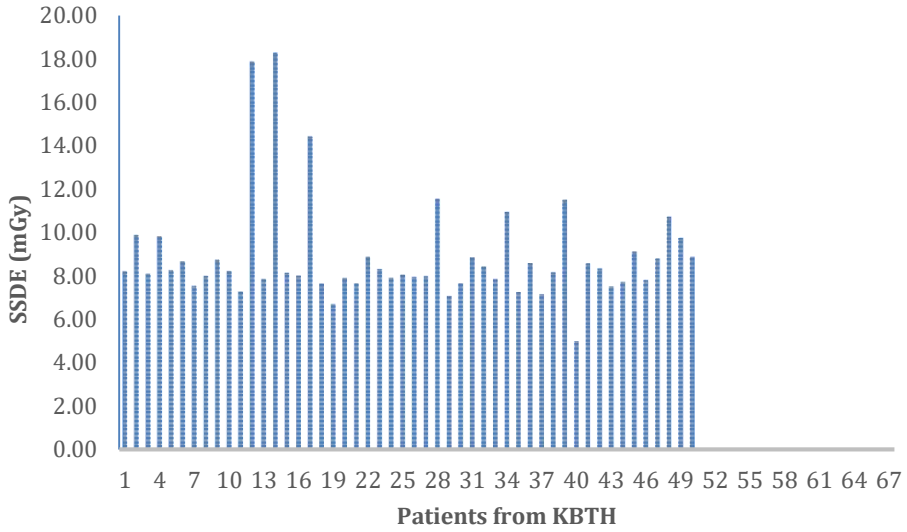

APPENDIX P

PATIENTS AT CCTH AND THEIR CORRESPONDING SSDE DURING CT SCAN

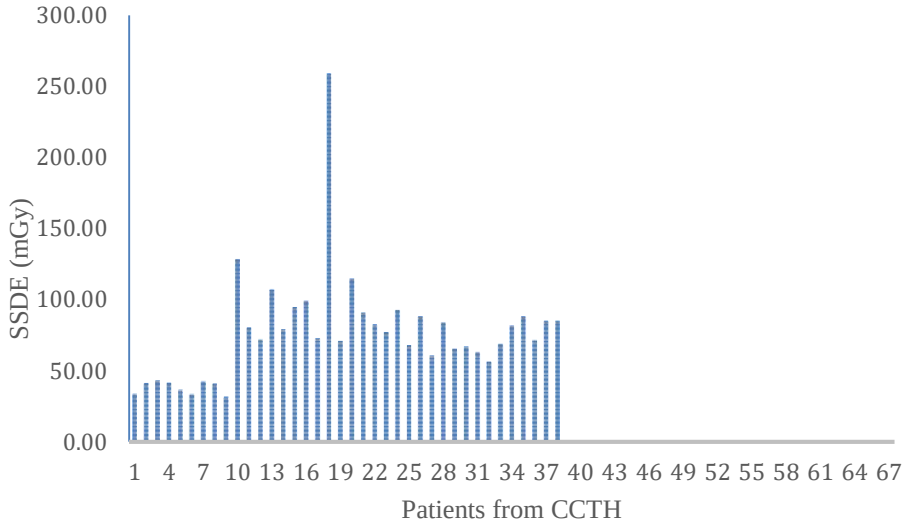

APPENDIX Q

SIGNAL TO NOISE (SNR) RATIO OF IMAGES FOR STUDY

Signal	Noise	SNR
88.97	12.93	6.88
76.43	12.44	6.14
89.21	15.08	5.92
69.04	11.64	5.93
59.04	10.86	5.44
70.59	12.52	5.64
77.30	7.98	9.69
76.77	12.63	6.08
53.89	9.46	5.70
83.42	12.06	6.92
56.87	6.09	9.34
65.45	11.54	5.67
59.90	7.65	7.83
67.80	12.53	5.41
66.50	8.56	7.77
59.80	8.34	7.17
83.46	14.50	5.76
65.33	8.93	7.32
59.45	7.44	7.99
65.45	11.92	5.49
56.78	7.17	7.92
68.89	7.61	9.05
68.92	8.99	7.67
56.89	8.12	7.01
63.41	8.02	7.91
67.44	12.06	5.59
55.62	7.95	7.00

APPENDIX Q continued

67.35	9.76	6.90
80.05	12.07	6.63
63.45	12.31	5.15
70.87	14.21	4.99
65.19	12.8	5.09
50.33	8.56	5.88
63.17	9.382	6.73
54.12	9.12	5.93
41.38	7.47	5.54
72.11	5.78	12.48
64.07	11.70	5.48
74.21	9.28	8.00
69.53	10.88	6.39
67.09	9.11	7.36
74.90	12.69	5.90
55.57	9.17	6.06
71.23	13.41	5.31
60.15	10.59	5.68
63.29	7.44	8.51
60.89	11.32	5.38
58.57	8.06	7.27
70.27	10.93	6.43
72.73	15.92	4.57
85.14	13.77	6.18
65.92	9.48	6.95
62.39	10.12	6.17
60.92	10.35	5.89
52.52	10.25	5.12
66.77	9.83	6.79

APPENDIX Q continued

52.50	9.92	5.29
73.08	12.04	6.07
55.72	9.54	5.84
62.61	10.03	6.24
58.79	10.73	5.48
55.19	9.81	5.63
67.43	8.18	8.24
66.92	5.964	11.22
83.89	10.15	8.27
78.53	9.57	8.21
68.65	8.08	8.50
57.97	7.03	8.25
57.64	7.17	8.04
63.88	12.06	5.30
65.18	11.75	5.55
74.08	9.18	8.07
67.18	7.90	8.50
83.42	15.05	5.54
63.05	8.04	7.84
93.74	15.97	5.87
76.09	11.85	6.42
86.09	12.52	6.88
85.75	13.44	6.38
76.91	9.05	8.50
65.92	8.44	7.81
60.34	11.07	5.45
67.09	12.05	5.57
85.35	5.95	14.34
69.08	6.89	10.03

APPENDIX Q continued

76.03	12.61	6.03
67.14	12.01	5.59
77.04	12.46	6.18
56.87	10.42	5.46
66.48	10.51	6.33
65.05	10.59	6.14
68.04	7.84	8.68

APPENDIX R

KVP, MAS, SNR AND EFFECTIVE DOSE (ED) FOR THIS STUDY

Peak voltage (kVp)	Exposure (mAs)	SNR	Effective Dose (ED)
120.00	80.00	6.88	12.50
120.00	90.00	6.14	38.48
120.00	82.00	5.92	17.37
120.00	90.00	5.93	19.31
120.00	94.00	5.44	18.38
120.00	80.00	5.64	37.80
120.00	85.00	9.69	15.42
120.00	80.00	6.08	18.88
120.00	80.00	5.70	11.59
120.00	84.00	6.92	28.87
120.00	97.00	9.34	41.54
120.00	141.00	5.67	7.09
120.00	82.00	7.83	16.40
120.00	154.00	5.41	15.45
120.00	109.00	7.77	37.52
120.00	85.00	7.17	22.04
120.00	128.00	5.76	50.36
120.00	80.00	7.32	23.91
120.00	117.00	7.99	19.22
120.00	100.00	5.49	12.98
120.00	80.00	7.92	14.11
120.00	84.00	9.05	24.73
120.00	20.00	7.67	49.47
120.00	80.00	7.01	12.65
120.00	152.00	7.91	18.93
120.00	80.00	5.59	48.10
120.00	80.00	7.00	10.61

APPENDIX R continued

100.00	60.00	6.63	4.57
100.00	75.00	5.15	18.43
100.00	112.00	4.99	39.03
100.00	60.00	5.09	18.97
100.00	60.00	5.88	10.81
100.00	60.00	6.73	13.53
100.00	150.00	5.93	46.33
100.00	142.00	5.54	37.89
100.00	60.00	12.48	15.09
100.00	182.00	5.48	39.16
100.00	60.00	8.00	48.60
100.00	60.00	6.39	33.80
100.00	135.00	7.36	58.92
100.00	60.00	5.90	15.28
100.00	96.00	6.06	36.97
100.00	97.00	5.31	20.80
100.00	96.00	5.68	22.13
100.00	187.00	8.51	49.55
100.00	127.00	5.38	35.84
100.00	80.00	7.27	38.63
100.00	90.00	6.43	40.78
100.00	60.00	4.57	14.18
100.00	60.00	6.18	24.73
100.00	60.00	6.95	15.32
100.00	85.00	6.17	31.02
100.00	60.00	5.89	13.30
100.00	60.00	5.12	10.36
100.00	75.00	6.79	19.83
100.00	97.00	5.29	28.91

APPENDIX R continued

100.00	112.00	6.07	30.51
100.00	60.00	5.84	12.88
100.00	82.00	6.24	33.16
100.00	191.00	5.48	39.61
100.00	62.00	5.63	22.36
100.00	60.00	8.24	15.31
100.00	60.00	11.22	13.73
120.00	187.00	8.27	52.54
120.00	187.00	8.21	36.66
120.00	187.00	8.50	40.73
120.00	187.00	8.25	56.20
120.00	187.00	8.04	39.91
120.00	187.00	5.30	37.06
120.00	187.00	5.55	49.83
120.00	187.00	8.07	44.28
120.00	187.00	8.50	88.03
120.00	187.00	5.54	48.29
120.00	187.00	7.84	58.65
120.00	187.00	5.87	36.66
120.00	187.00	6.42	38.75
120.00	187.00	6.88	45.01
120.00	187.00	6.38	34.02
120.00	187.00	8.50	48.76
120.00	187.00	7.81	39.91
120.00	187.00	5.45	54.92
120.00	187.00	5.57	39.59
120.00	187.00	14.34	33.50
120.00	187.00	10.03	55.66
120.00	187.00	6.03	48.75

APPENDIX R continued

120.00	187.00	5.59	42.12
120.00	187.00	6.18	53.97
120.00	187.00	5.46	34.97
100.00	146.00	6.33	41.10
120.00	187.00	6.14	80.25
120.00	187.00	8.68	50.91

APPENDIX S

C# CODE FOR GUI

```
using System;
using System.Collections.Generic;
using System.ComponentModel;
using System.Data;
using System.Drawing;
using System.Linq;
using System.Text;
using System.Windows.Forms;
namespace bodyordganmeasurement
{
   public partial class frmbodyandorganmeasurement : Form
   {
      public frmbodyandorganmeasurement()
      {
         InitializeComponent();
      }
      private void txtheight_TextChanged(object sender, EventArgs e)
      {
      }
      private void txtweight_TextChanged(object sender, EventArgs e)
      {


      }
      private void cbosex_SelectedIndexChanged(object sender, EventArgs e)
      {
```

```
        }
    private void txtheight_KeyPress(object sender, KeyPressEventArgs e)
    {
    }
    private void txtweight_KeyPress(object sender, KeyPressEventArgs e)
    {
    }
    private void frmbodyandorganmeasurement_Load(object sender,
EventArgs e)
    {
    }
    private void cmdclear_Click(object sender, EventArgs e)
    {
       txtkvp.Text = "";
       txtlat.Text = "";
       txtctdivol.Text = "";
       txtap.Text = "";
       txtmas.Text = "";
       lblssde.Text = "";
       lblsnr.Text = "";
       lbled.Text = "";
       lblssde.Text = "";
       lbled.Text = "";
       lblsnr.Text = "";
    }
    private void txtkvp_TextChanged(object sender, EventArgs e)
```

```
{
    double fb;
    double effd;
    //string sex;
    double ctdivol;
    double ap;
    double lat;
    double kvp;
    double snr;
    double ed;
    double ssde;
    double masvalue;
    if (txtkvp.Text == "" || txtmas.Text == "" || txtap.Text == "" || txtlat.Text
== "" || txtap.Text == "" || txtctdivol.Text == "")
    {
        //do nothing
    }
    else
    {
        kvp = double.Parse(txtkvp.Text);
        masvalue = double.Parse(txtmas.Text);
        ap = double.Parse(txtap.Text);
        lat = double.Parse(txtlat.Text);
        ctdivol = double.Parse(txtctdivol.Text);

        effd = Math.Sqrt(ap * lat);
```

```
        fb = 3.704369 * Math.Exp(-0.03671937 * effd);
        ssde = fb * ctdivol;
        snr = 1.80 + (0.0404 * kvp) + (0.00066 * masvalue);
        ed = 36.1 - (0.325 * kvp) + (0.2522 * masvalue);
        lblssde.Text = Convert.ToDouble(ssde).ToString();
        lblsnr.Text = Convert.ToDouble(snr).ToString();
        lbled.Text = Convert.ToDouble(ed).ToString();
        if (snr >= 5)
        {
            lblindicator.Text = "Good";
            //do nothing
            lblindicator.ForeColor = System.Drawing.Color.Blue;
        }
        else
            if (snr < 5)
            {
                lblindicator.Text = "Bad";
                lblindicator.ForeColor = System.Drawing.Color.Red;
            }
    }
}
private void txtmas_TextChanged(object sender, EventArgs e)
{
    double fb;
    double effd;
    //string sex;
```

```
double ctdivol;
double ap;
double lat;
double kvp;
double snr;
double ed;
double ssde;
double masvalue;
if (txtkvp.Text == "" || txtmas.Text == "" || txtap.Text == "" || txtlat.Text
== "" || txtap.Text == "" || txtctdivol.Text == "")
{
  //do nothing
}
else
{
  kvp = double.Parse(txtkvp.Text);
  masvalue = double.Parse(txtmas.Text);
  ap = double.Parse(txtap.Text);
  lat = double.Parse(txtlat.Text);
  ctdivol = double.Parse(txtctdivol.Text);
  effd = Math.Sqrt(ap * lat);
  fb = 3.704369 * Math.Exp(-0.03671937 * effd);
  ssde = fb * ctdivol;
  snr = 1.80 + (0.0404 * kvp) + (0.00066 * masvalue);
  ed = 36.1 - (0.325 * kvp) + (0.2522 * masvalue);
  lblssde.Text = Convert.ToDouble(ssde).ToString();
```

```
            lblsnr.Text = Convert.ToDouble(snr).ToString();
            lbled.Text = Convert.ToDouble(ed).ToString();
            if (snr >= 5)
            {
                lblindicator.Text = "Good";
                //do nothing
                lblindicator.ForeColor = System.Drawing.Color.Blue;
            }
            else
                if (snr < 5)
                {
                    lblindicator.Text = "Bad";
                    lblindicator.ForeColor = System.Drawing.Color.Red;
                }
        }
    }
    private void txtap_TextChanged(object sender, EventArgs e)
    {
        double fb;
        double effd;
        //string sex;
        double ctdivol;
        double ap;
        double lat;
        double kvp;
        double snr;
```

```
        double ed;
        double ssde;
        double masvalue;
        if (txtkvp.Text == "" || txtmas.Text == "" || txtap.Text == "" || txtlat.Text
== "" || txtap.Text == "" || txtctdivol.Text == "" )
        {
            //do nothing
        }
        else
        {
            kvp = double.Parse(txtkvp.Text);
            masvalue = double.Parse(txtmas.Text);
            ap = double.Parse(txtap.Text);
            lat = double.Parse(txtlat.Text);
            ctdivol = double.Parse(txtctdivol.Text);
            effd = Math.Sqrt(ap * lat);
            fb = 3.704369 * Math.Exp(-0.03671937 * effd);
            ssde = fb * ctdivol;
            snr = 1.80 + (0.0404 * kvp) + (0.00066 * masvalue);
            ed = 36.1 - (0.325 * kvp) + (0.2522 * masvalue);
            lblssde.Text = Convert.ToDouble(ssde).ToString();
            lblsnr.Text = Convert.ToDouble(snr).ToString();
            lbled.Text = Convert.ToDouble(ed).ToString();
            if (snr >= 5)
            {
```

```
            lblindicator.Text = "Good";
            //do nothing
            lblindicator.ForeColor = System.Drawing.Color.Blue;
        }
        else
            if (snr < 5)
            {
                lblindicator.Text = "Bad";
                lblindicator.ForeColor = System.Drawing.Color.Red;
            }
    }
}
private void txtlat_TextChanged(object sender, EventArgs e)
{
    double fb;
    double effd;
    //string sex;
    double ctdivol;
    double ap;
    double lat;
    double kvp;
    double snr;
    double ed;
    double ssde;
    double masvalue;
```

```
if (txtkvp.Text == "" || txtmas.Text == "" || txtap.Text == "" || txtlat.Text
== "" || txtap.Text == "" || txtctdivol.Text == "")
{
   //do nothing
}
else
{
   kvp = double.Parse(txtkvp.Text);
   masvalue = double.Parse(txtmas.Text);
   ap = double.Parse(txtap.Text);
   lat = double.Parse(txtlat.Text);
   ctdivol = double.Parse(txtctdivol.Text);

   effd = Math.Sqrt(ap * lat);
   fb = 3.704369 * Math.Exp(-0.03671937 * effd);
   ssde = fb * ctdivol;
   snr = 1.80 + (0.0404 * kvp) + (0.00066 * masvalue);
   ed = 36.1 - (0.325 * kvp) + (0.2522 * masvalue);
   lblssde.Text = Convert.ToDouble(ssde).ToString();
   lblsnr.Text = Convert.ToDouble(snr).ToString();
   lbled.Text = Convert.ToDouble(ed).ToString();

   if (snr >= 5)
   {
      lblindicator.Text = "Good";
      //do nothing
```

```
                lblindicator.ForeColor = System.Drawing.Color.Blue;
            }
            else
                if (snr < 5)
                {
                    lblindicator.Text = "Bad";
                    lblindicator.ForeColor = System.Drawing.Color.Red;
                }
        }
    }
    private void txtctdivol_TextChanged(object sender, EventArgs e)
    {
        double fb;
        double effd;
        //string sex;
        double ctdivol;
        double ap;
        double lat;
        double kvp;
        double snr;
        double ed;
        double ssde;
        double masvalue;
        if (txtkvp.Text == "" || txtmas.Text == "" || txtap.Text == "" || txtlat.Text
== "" || txtap.Text == "" || txtctdivol.Text == "")
        {
```

```
    //do nothing
}
else
{
    kvp = double.Parse(txtkvp.Text);
    masvalue = double.Parse(txtmas.Text);
    ap = double.Parse(txtap.Text);
    lat = double.Parse(txtlat.Text);
    ctdivol = double.Parse(txtctdivol.Text);
    effd = Math.Sqrt(ap * lat);
    fb = 3.704369 * Math.Exp(-0.03671937 * effd);
    ssde = fb * ctdivol;
    snr = 1.80 + (0.0404 * kvp) + (0.00066 * masvalue);
    ed = 36.1 - (0.325 * kvp) + (0.2522 * masvalue);
    lblssde.Text = Convert.ToDouble(ssde).ToString();
    lblsnr.Text = Convert.ToDouble(snr).ToString();
    lbled.Text = Convert.ToDouble(ed).ToString();
    if (snr >= 5)
    {
        lblindicator.Text = "Good";
        //do nothing
        lblindicator.ForeColor = System.Drawing.Color.Blue;
    }
    else
        if (snr < 5)
        {
```

```
                lblindicator.Text = "Bad";
                lblindicator.ForeColor = System.Drawing.Color.Red;
            }
        }
    }
    private void txtkvp_KeyPress(object sender, KeyPressEventArgs e)
    {
        if (!char.IsControl(e.KeyChar) && !char.IsDigit(e.KeyChar) &&
(e.KeyChar != '.'))
        {
            e.Handled = true;
        }
        // If you want, you can allow decimal (float) numbers
        if ((e.KeyChar == '.') && ((sender as TextBox).Text.IndexOf('.') > -1))
        {
            e.Handled = true;
        }
    }
    private void txtmas_KeyPress(object sender, KeyPressEventArgs e)
    {
        if (!char.IsControl(e.KeyChar) && !char.IsDigit(e.KeyChar) &&
(e.KeyChar != '.'))
        {
            e.Handled = true;
        }
        // If you want, you can allow decimal (float) numbers
```

```
        if ((e.KeyChar == '.') && ((sender as TextBox).Text.IndexOf('.') > -1))
        {
            e.Handled = true;
        }
    }
    private void txtap_KeyPress(object sender, KeyPressEventArgs e)
    {
        if (!char.IsControl(e.KeyChar) && !char.IsDigit(e.KeyChar) &&
(e.KeyChar != '.'))
        {
            e.Handled = true;
        }
        // If you want, you can allow decimal (float) numbers
        if ((e.KeyChar == '.') && ((sender as TextBox).Text.IndexOf('.') > -1))
        {
            e.Handled = true;
        }
    }
    private void txtlat_KeyPress(object sender, KeyPressEventArgs e)
    {
        if (!char.IsControl(e.KeyChar) && !char.IsDigit(e.KeyChar) &&
(e.KeyChar != '.'))
        {
            e.Handled = true;
        }
        // If you want, you can allow decimal (float) numbers
```

```
            if ((e.KeyChar == '.') && ((sender as TextBox).Text.IndexOf('.') > -1))
            {
                e.Handled = true;
            }
        }
        private void txtctdivol_KeyPress(object sender, KeyPressEventArgs e)
        {
            if (!char.IsControl(e.KeyChar) && !char.IsDigit(e.KeyChar) &&
(e.KeyChar != '.'))
            {
                e.Handled = true;
            }
            // If you want, you can allow decimal (float) numbers
            if ((e.KeyChar == '.') && ((sender as TextBox).Text.IndexOf('.') > -1))
            {
                e.Handled = true;
            }
        }
    }
}
```